Sediment Accumulation Rates in Waimapu, Waikareao and Tuapiro Estuaries, Tauranga Harbour

Prepared for Bay of Plenty Regional Council

August 2021

Prepared by:
Manawa Huirama,
Andrew Swales,
Greg Olsen,
Ron Ovenden

For any information regarding this report please contact:

Andrew Swales
Programme Leader - Catchments to Estuaries
Coastal and Estuarine Physical Processes Group
+64-7-856 7026
andrew.swales@niwa.co.nz

National Institute of Water & Atmospheric Research Ltd
PO Box 11115
Hamilton 3251

Phone +64 7 856 7026

Quality Assurance Statement		
Alan Orpin [signature]	Reviewed by:	Alan Orpin
[signature]	Formatting checked by:	Alex Quigley
M. P. Bruce [signature]	Approved for release by:	Michael Bruce

Sediment coring in Waikareao Estuary (Tauranga Moana), September 2020.

Contents

Tables

Figures

Executive summary

Bay of Plenty Regional Council (BoPRC) commissioned a study to determine historical sediment accumulation rates (SAR) in three sub-estuaries fringing the western shore of Tauranga Harbour. These sub-estuaries are Tuapiro, Waikareao and Waimapu. The objectives of this study are:

- Determine long-term SAR within three Tauranga Harbour sub-estuaries and measure vertical changes in texture (particle sizes) through time.

- Determine background SAR within selected sub-estuaries prior to the arrival of people in Aotearoa – New Zealand, about 700 years ago (Wilmshurst et al. 2008).

- Extend BoPRC's existing sediment-accretion record (2013–2020) measured in the sub-estuaries at ~seasonal intervals using buried plates. Compare sediment accretion plate and sediment core SAR data.

Sediment cores were collected in September and October 2020 at three key locations in each sub-estuary. The core locations were selected to be adjacent (i.e., within several tens of metres) to BoPRC sediment-accretion monitoring stations plate sites. This co-location enables comparison of relatively short-term sediment accretion measurements (buried plates – several years of data) with long term SAR measurements (i.e., decades to millennia). The monitoring sites are Tuapiro (P54, P55, P56), Waikareao (P16, P17, P21) and Waimapu (P12, P13, P14). Sediment composition was determined from x-ray imaging, sediment bulk density and particle-size analysis. Sediment accumulation rates over the last several decades to century were determined by from lead-210 (^{210}Pb) dating. Pre-human SAR going back ~7,000 years was determined by radiocarbon (^{14}C) dating of cockle-shell valves preserved as layers in cores P55 (Tuapiro) and P12 (Waimapu).

The key findings of this study are:

- ^{210}Pb SAR in the Tuapiro, Waikareao and Waimapu sub-estuaries have averaged **2.6** to **15.1 mm yr^{-1}** since the early-1900s.

- These apparent ^{210}Pb SAR are at least **fifty-fold higher** than time-average SAR over the previous ~7,000 years (i.e. ^{14}C dates give **0.05 mm yr^{-1}**). Typical ^{210}Pb SAR for New Zealand estuaries are typically an **order of magnitude higher** than background values.

- The overall time-weighted average SAR for the study estuaries is **5.2 mm yr^{-1}**. This average SAR is **at least five-fold higher** than measured for intertidal flats in Tauranga Harbour (i.e. 1 mm yr^{-1}, Figure 4-2) and model predictions that indicate no long-term accumulation of fine sediment in the main body of Tauranga Harbour (0 mm yr^{-1}, Figure 4.5, Green, 2010)..

- This estuary-average SAR of **5.2 mm yr^{-1}** for these three Tauranga Harbour estuaries is among the highest SAR measured across ~30 New Zealand estuaries studied by NIWA (i.e. **2 mm yr^{-1} higher than the average for all of these estuaries (3.2 mm yr^{-1}**, Figure 4-2).

- The spatial distribution of SAR in Tuapiro, Waikareao and Waimapu (Figure 4-1) are primarily attributed to wave-driven resuspension, fine-sediment winnowing and sediment transport. In terms of sedimentary dynamics, these estuaries are typical shallow-fetch limited estuaries.

- The BoPRC **sediment-accretion plate data display considerable variability** (i.e., accretion and erosion) between ~seasonal surveys; from -14 to +13 mm (Tuapiro), -16 to +18 mm (Waikareao) and -13 to +16 mm (Waimapu). Two of the nine sites had significant positive correlations, i.e. measured accretion and sediment accumulation. The strongest example was Tuapiro Estuary with a regression coefficient of 0.65, SAR of 2.3 mm yr^{-1} (P-55) and accretion of 3.1 mm yr^{-1} (P-56) respectively.

- The high variability and low accretion and erosion rates in the BoPRC plate data suggests that **seasonal sedimentation rates in the sub-estuaries are driven by episodic storm events** (i.e., wind and rainfall). These sediment-accretion plate data are seemingly at odds with the long-term SAR determined from the dated cores. These differences occur because sediment cores are more likely to capture the high-magnitude and low-frequency storm events (i.e., accretion and erosion) over longer time scales (i.e., 10–1000 years).

An overarching finding of our study is that these Tauranga Harbour sub-estuaries have been **impacted by substantial increases in sedimentation** over the last century. Fine sediment is most likely derived from catchment erosion and partly derived from other sub-catchments (i.e., transported by tidal currents, Green, 2010). Once in the estuaries, a substantial fraction of this fine sediment deposited on the intertidal flats is likely to be re-suspended by waves and transported by tidal currents (Green, 2010). This interpretation is supported by the sediment composition information, BoPRC sediment-accretion SOE data and what we know about sediment transport and deposition processes in sediment infilled/ intertidal dominated estuaries (e.g., Swales et al., 2004; Green and Coco, 2014), such as Tauranga Harbour's estuaries. The transported sediment will eventually accumulate in long-term sinks, such as accreting fringing coastal wetlands, or will be exported to the sea. In contrast, event-driven deposition is temporary, and these Tauranga Harbour estuaries are being continually impacted by the adverse effects of fine sediment. Effects include increased turbidity and reduced water clarity, resulting in the loss of biodiversity of benthic ecosystems and kaimoana. Identifying the major sources of sediment and loci for erosion within the study catchments may help inform catchment managers to ultimately restore the freshwater and estuarine environment.

1   Introduction

1.1   Background to study

Estuaries have been increasingly degraded by excessive land-derived contaminants, in particular sediment, nutrients and urban-derived stormwater contaminants. This degradation has been exacerbated by land-use intensification, urban expansion and coastal development (Schiel and Howard-Williams, 2016). Excessive sedimentation resulting from catchment land-use activities and associated soil erosion is one of the key stressors causing degradation of NZ estuaries and coastal system (MacDiarmid et al. 2012; Parliamentary Commissioner for the Environment 2020). Although soil erosion and deposition in New Zealand estuaries and coastal marine receiving environments is a natural process, the rate at which sedimentation is now occurring is an order of magnitude higher than before human activities disturbed the natural land cover (e.g., Swales et al. 2002a, b; Thrush et al. 2004; Hunt, 2019). In New Zealand, increases in sediment loads to estuaries and coastal ecosystems coincided with large-scale deforestation, which followed the arrival of people about 700 years ago (Wilmshurst et al. 2008).

Soil erosion rates in New Zealand are naturally high by global standards due to steep terrain, weathered, friable and easily erodible rocks, generally high rainfall and the frequent occurrence of high-intensity rainstorms (Basher, 2013). Historical catchment deforestation, large-scale conversion to pastoral agriculture and land-use intensification and catchment disturbance have increased landscape yields and net erosion rates. Important erosion processes include rainfall-triggered shallow landslides, earthflows and slumps, gully and surface erosion (i.e., sheet, rill) and streambank erosion (Basher, 2013; Hughes, 2016).

Timber extraction, mining and land conversion to pastoral agriculture after European settlement triggered large increases in fine sediment yields from catchments. During the peak period of deforestation from the mid-1800s to early 1900s, sediment accumulation rates (SAR) in many New Zealand estuaries increased by a factor of ten or more. This influx of fine sediment resulted in a shift from sandy and relatively clear to more turbid, intertidal and muddy environments and degradation of ecosystems (Thrush et al. 2004). Studies mainly in North Island estuaries indicate that in pre-Polynesian times (i.e., before 1300 A.D.) SAR averaged 0.1–1 millimetre per year (mm yr^{-1}). Sedimentation rates over the last century have averaged 2–5 mm yr^{-1} in these same ecosystems (e.g., Bentley et al. 2014; Handley et al. 2017; Hume and McGlone, 1986; Sheffield et al. 1995; Swales et al. 1997; 2002a, 2002b, 2012, 2016). Previous studies have also documented the environmental changes that have resulted from increased catchment sediment yields following large-scale catchment deforestation that began in the mid-1800s. Effects include accelerated sedimentation, shifts in substrate from sand to mud, aggradation and shoreline progradation (building seaward) and former subtidal habitats shoaling to become intertidal.

ANZECC guidance for sedimentation in estuaries recommends: (1) a default guideline value (DGV) of **2 mm yr^{-1} above the natural annual sedimentation rates** (i.e., for a native-forest catchment) ; and (2) "*estuarine sedimentation and its effects should be better linked to catchment processes*"…. to…" *facilitate a clearer understanding of erosion pathways and thereby improved targeted management responses*" (Townsend and Lohrer, 2015). The DGV is based on knowledge of event-scale effects adapted for annual sedimentation rates.

The National Policy Statement for Freshwater Management (NPS-FM) has recently been updated, with new policies introduced in the "*Essential Freshwater*" policy document (Ministry for the

Environment, 2020). This updated NPS-FM signals a new direction for freshwater management with the key objectives of:

1. stopping further degradation of New Zealand's freshwater resources and start making immediate improvements so that water quality is materially improving within five years

2. reverse past damage to bring New Zealand's freshwater resources, waterways and ecosystems to a healthy state within a generation.

The NPS-FM (2020) recognises that land-use intensification has contributed to major degradation of estuaries and that sediment is one of the most prominent environmental stressors in New Zealand freshwater and estuarine environments. Councils will be required to develop plans that address degradation of freshwater and estuaries (enact by 2026) and shifts the emphasis from effects- to limits-based management. The ANZECC guidelines and NPS-FM recognise sediment as a threat to the estuarine environment and the need to manage and mitigate sediment inputs from the land. Regional Councils must also give effect to both these policies through their regional and coastal plans.

1.2   Evolution of New Zealand estuaries – overview

At the last glacial maximum (LGM, c. 21,000 years ago), sea levels were about 134 m lower than they are today (Lambeck et al., 2014). At the end of the LGM, rising sea-levels gradually flooded the continental shelf, which formed extensive plains with lowland forest, and ultimately the river valleys that had cut into the emergent landmass. This process created the estuaries along the shore margins that we see today that slowly accumulated sediment, over millennia, eroded from the land and marine sediment carried into them by the tide. New Zealand's estuaries formed between 7,000–12,000 years ago as sea-level rise slowed then peaked at the end of last ice age, the Ōtira Glaciation (King et al., 2021).

How our estuaries have evolved since their creation is largely determined by three key factors:

- sediment supply rate

- original volume of the ancestral river valley; and

- mix of estuarine processes that control sediment trapping. These processes include tidal current asymmetry (i.e., ebb- vs flood-dominated currents, wave driven sediment resuspension, estuary geomorphology and sediment accommodation volume. The modern sediment accommodation volume of an estuary reflects a number of factors, including: the original volume of the ancestral river valley, catchment sediment load, estuary high tide area and tidal-prism volume (i.e., intertidal volume) the spatial proportion of intertidal flat. The importance of sediment resuspension by fetch-limited waves increases with estuary size and reducing water depth (e.g., Swales et al., 2020a).

The estuaries of Aotearoa-New Zealand are classified into several common types, with distinctive features or coastal hydrosystems (Hume and Hart, 2020). These types include tidal lagoons (e.g., Ohiwa Harbour), shallow (e.g., Whangamata) and deep drowned river valleys (e.g., Pelorus Sound), Hapua (e.g., Rakaia) tidal river mouths (e.g., Hokitika), and Fjords (e.g., Milford Sound).

Catchment characteristics are an important determinate of sediment supply to estuaries. New Zealand catchments are highly erodible with high sediment yields, in comparison to global erosion rates, due to our steep and dissected topography, friable and easily erodible rock and high frequency rainfall events (Basher 2013). Further, although sediment delivery to estuaries is a natural process (e.g. Swales et al. 2002a; Thrush et al. 2004; Hunt 2019), human activities have accelerated soil erosion rates and therefore increased sediment supply to estuaries (e.g. Swales et al. 2002b; Thrush et al. 2004; Hunt 2019).

The average rate at which sediment infills estuaries over time is termed the **sediment accumulation rate** (SAR). Estimations of SAR pre-Polynesian arrival (i.e. before 1300 A.D.) were 0.1–1 mm yr^{-1} (e.g., Hume and McGlone 1986; Sheffield et al. 1995; Swales et al. 1997; Swales et al. 2002b; Bentley et al. 2014; Handley et al. 2017). Increases in SAR peaked with large-scale deforestation (i.e. mid-1800s to early 1900's) following European arrival. Over the last century, average SAR rates have typically been an order of magnitude higher than long-term background rates (e.g. Swales et al. 2002; Thrush et al. 2004; Hunt 2019) to 2–5 mm yr^{-1} (Hume and McGlone 1986; Sheffield et al. 1995; Swales et al. 1997; Swales et al. 2002a,b; Bentley et al. 2014; Handley et al. 2017). As SAR increased, estuarine ecosystems became degraded and have transformed previously sandy estuaries to more turbid, intertidal and muddy estuaries (Thrush et al. 2004; Swales et al., 2020a).

Estuaries with large catchments, and/or catchments with features that make them susceptible to high sediment yields, receive high sediment loads relative to their tidal volume and have largely infilled and have reached old age (Figure 1-1). Conversely, estuaries with small catchments and/or small sediment loads relative to their sediment accommodation volume (inherited from their ancestral river valleys) remain subtidal with large expanses of water even at low tide. In these relatively "youthful" estuaries (e.g., Te Kouma Harbour, Coromandel; Waitemata, Auckland; Pelorus Sound, Marlborough), substantial areas of subtidal habitat remain, with relatively small areas of intertidal flat fringing the shoreline.
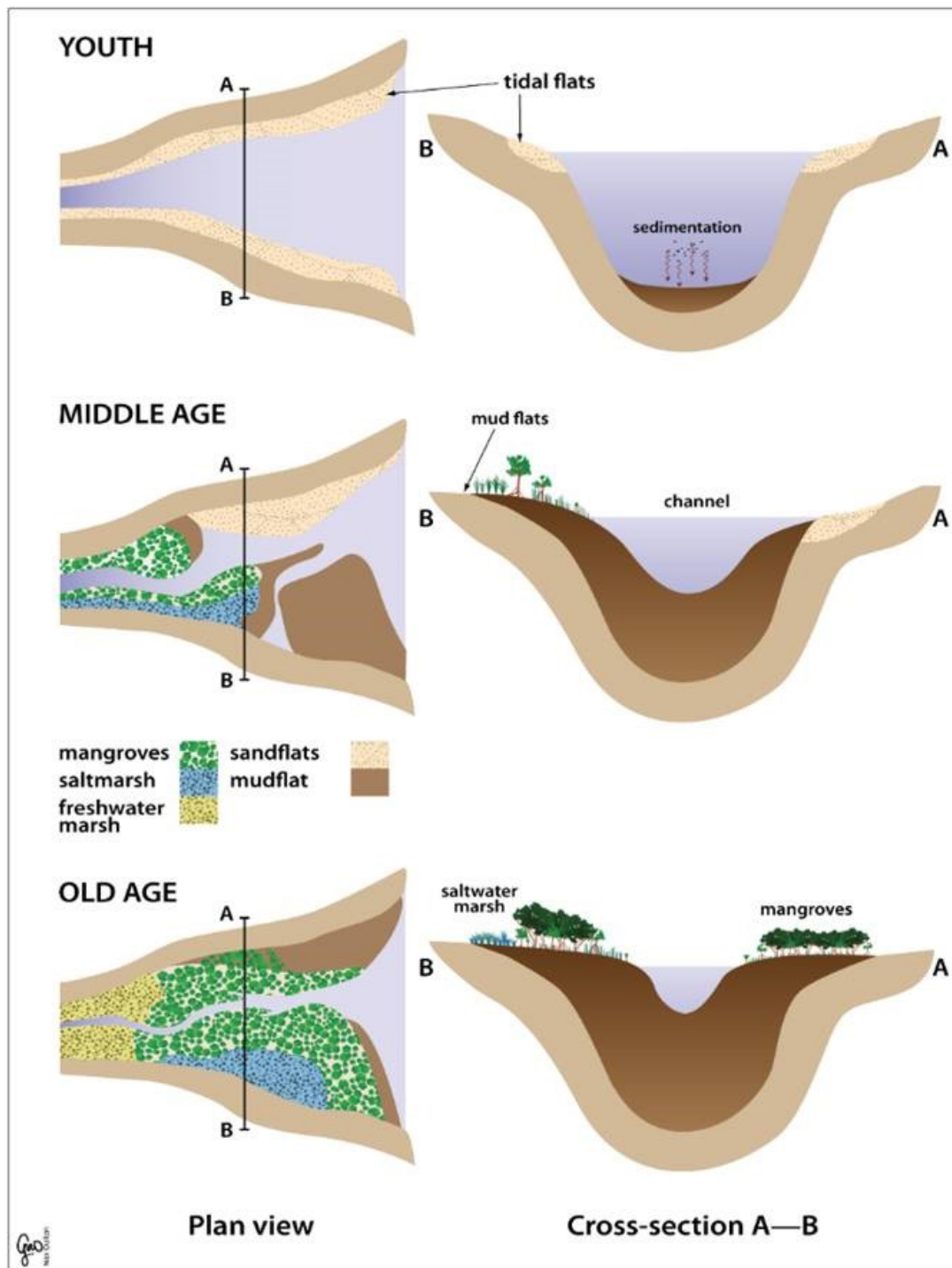
Figure 1-1:   Simplified illustration of the natural life cycle of estuaries, from youth, middle age to old age.
Youth: Estuaries are basins with open water and tidal flats are formed at river outlets. **Middle age**: Intertidal
flats become more extensive and are colonised by new communities of plants and animals. Sediment
accumulation rates (SAR) in Aotearoa-New Zealand have increased ten-fold and have buried sand flats in mud
over the last ~170 years. This is due to accelerated erosion associated with land use activities such as
deforestation. **Old age**: Sediment infills most of the estuary's available accommodation space for sediment
deposition. A narrow tidal channel is flanked by extensive intertidal flats exposed at low tide. These tidal flats
are colonised by coastal wetlands, such as saltmarsh and mangroves (in northern estuaries) and seagrass
meadow, unless otherwise smothered by mud. Freshwater marshes eventually replace saltmarshes in the
upper estuary as the marine influence wanes due to sedimentation and vertical aggradation and shoreline
progradation. **Source**: Swales et. al. (2011).

1.3   Long-term sedimentation vs sediment accretion

Studies of sedimentation in estuaries employed a range of methods, largely depending on the time scale of interest. Radionuclide geochronology and palynological analysis of cores has provided estimates of **sediment accumulation rates** (SAR) typically over annual-to-centennial or longer time scales (e.g., Swales et al., 2002a, 2015). These measurements integrate the long-term effects of erosion and deposition cycles, producing variable sediment accumulation rates so that time-averaged SAR typically reduce with increasing time scale (Sadler, 1981; Parkinson et al., 1994). Sedimentation also encompasses processes associated with early diagenesis (e.g., compaction, bioturbation), which can alter the vertical distribution of tracers (e.g., ^{210}Pb) thereby influencing apparent SAR inferred from sedimentary records (e.g., Christensen, 1982; Bentley et al., 2014). Sediment accumulation or deposition describes sedimentation over shorter time scales (i.e., minutes to months) and is usually measured in units of mass deposited per unit area and/or time (Thomas and Ridd, 2004; Nolte et al., 2013). Short-term sediment accumulation is commonly referred to as **sediment accretion**, which is defined as the vertical accumulation (e.g., mm yr^{-1}) of sediment deposited on the substrate surface (e.g., Callaway et al., 2013; Nolte et al., 2013), over characteristic time scales of months to years.

Sediment accretion rates have been measured using sedimentary marker horizons (e.g., layers of iron filings, sand, brick dust, feldspar, clay or distinctive chemical profiles such as DDT or radionuclides), with vertical accretion over time determined relative to the upper surface of the marker layer (e.g., Chapman and Ronaldson, 1958; Cahoon and Turner, 1989; French and Spencer, 1993; Nolte et al., 2013). Sediment accretion has also been measured using buried plates (Pasternack and Brush, 1998; Neubauer et al., 2002; Watson, 2008) and pre-weighed filters (Reed, 1989) placed on the substrate to sample net sediment deposition over discrete time intervals. **Sediment accretion plates**, typically buried in the substrate are widely employed by Regional Councils in New Zealand, including BoPRC to provide a reference surface to measure sediment accretion, primarily on intertidal flats. Plastic-mesh plates have been demonstrated to provide comparable data to impervious ceramic plates and can be employed in coastal wetlands were aerial roots, steams and trunks pose difficulties for sediment accretion measurement (Swales et al., 2020b). BoPRC measured sediment accretion at ~seasonal intervals in the study estuaries using buried plates from late-2013 until late-2020.

1.4   Purpose of the report

Bay of Plenty Regional Council (BoPRC) have identified sedimentation as one of the key issues impacting Tauranga Harbour (Lawton and Conroy 2019), traditionally known to iwi as Te Awanui (Ellis et al. 2013). Impacts of increased sedimentation in the harbour are numerous and include the degradation of saltmarsh and seagrass habitats and mangrove-habitat expansion onto intertidal flats. The iwi of Tauranga Moana are Ngāti Ranginui, Ngāi Te Rangi, and, Ngāti Pukenga. Sedimentation has impacted iwi and hapū values due to their intrinsic physical and spiritual connection to the harbour. As such, the decline of kaimoana in the harbour has been identified as a key issue by iwi and hapū members (Conroy et al. 2019; Lawton and Conroy 2019). In particular, the smothering of shellfish beds in the Waikareao and Waimapu Estuaries is a cause for concern (Crawshaw 2020b). Rapid population growth, urban development and land-use intensification over the last 20 years (~50%), within Tauranga City and townships, continued to exacerbate sediment inputs into the harbour (Lawton and Conroy 2019). The present project will assist BoPRC to set sedimentation limits for Tauranga Harbour within their regional plan as required under the NPS-FM.

BoPRC commissioned NIWA to determine long-term sediment accumulation rates in three sub-estuaries fringing Tauranga Harbour. These sub-estuaries are part of a larger long-term regional monitoring programme measuring sedimentation and estuarine benthic health in the Tauranga Harbour system. The three sub-estuaries are (from north to south, Figure 1-2):

- Tuapiro Estuary.

- Waikareao Estuary.

- Waimapu Estuary.

1.5   Study objectives

The objectives of the current study are to:

- Determine long-term sediment accumulation rates (SAR) within Tuapiro, Waikareao and Waimapu estuaries, and determine changes in sediment texture (particle size) over time.

- Determine background (i.e., pre-human) sediment accumulation rates (SAR) within Tuapiro, Waikareao and Waimapu estuaries.

- Identify any evidence of event sedimentation layers preserved in the sediment cores, that could be attributable to Cyclone Bola (March 1988) or the failure of the Ruahihi Power Station dam (1981).

- Extend the length of the sedimentation record by incorporating long-term SAR from cores at the BoPRC sediment accretion monitoring sites (as described above).

1.6   Study area

1.6.1   Tauranga Moana

Tauranga Moana is located in the western Bay of Plenty, with the City of Tauranga fringing its southern shoreline. The harbour is indented on its western shore by numerous estuaries, typically with high-tide areas less than several km^2. The harbour is sheltered from the open coast to the east by Matakana Island, a 25-km long sand barrier (Briggs et al. 1996). Tauranga Moana has a total high tide area of ~200 km^2 , and receives runoff from a 1,300 km^2 catchment , which consists of 27 major rivers and 46 minor streams (Lawton and Conroy 2019). The Harbour is generally shallow with extensive intertidal sandflats and mudflats (total intertidal: 154 km^2, NZ estuaries classification database [NZECD], NIWA) in sheltered areas with short wave fetch and/or near sub-catchment outlets (Briggs et al. 1996). The spring tidal-prism volume is some 211 million m^3 (0.211 km^3) with a mean water depth is 2.1 m (NZECD, Hicks and Hume 1997; Lawton and Conroy 2019). The Port of Tauranga, located near Tauranga City, is the largest commercial port in New Zealand (Lawton and Conroy, 2019). Although the harbour is generally shallow, tidal scour and artificial dredging at the port, maintains the southern harbour entrance (Briggs et al. 1996).

The BoPRC Coastal Environment Plan has identified Tauranga Moana as an outstanding natural feature and landscape, and an area of significant conservation value (excludes Port of Tauranga) (Lawton and Conroy 2019). The BoPRC measures sedimentation rates in Tauranga Moana at 69 intertidal sites, as part of the Estuarine Benthic Health Monitoring programme. Sediment accretion rates at these sites are measured seasonally using buried plates.

Several previous studies have obtained sediment accumulation rates (SAR) for Tauranga Harbour. Burggraaf et al. (1994) calculated a SAR of ~1 mm yr^{-1} (1950–1991) in the Waikareao, based on DDT contaminant profiles. Hancock et al. (2009) calculated SAR from the naturally occurring radionuclide ^{210}Pb in sediment cores for intertidal flats located in several estuaries in the vicinity of Tauranga City. The ^{210}Pb SAR varied from 1.3–7.2 mm yr^{-1} over the previous 70–90 years. Stokes (2010) also calculated a ^{210}Pb SAR of 2.3 mm yr^{-1} (1950–1990) for Waikaraka Estuary.
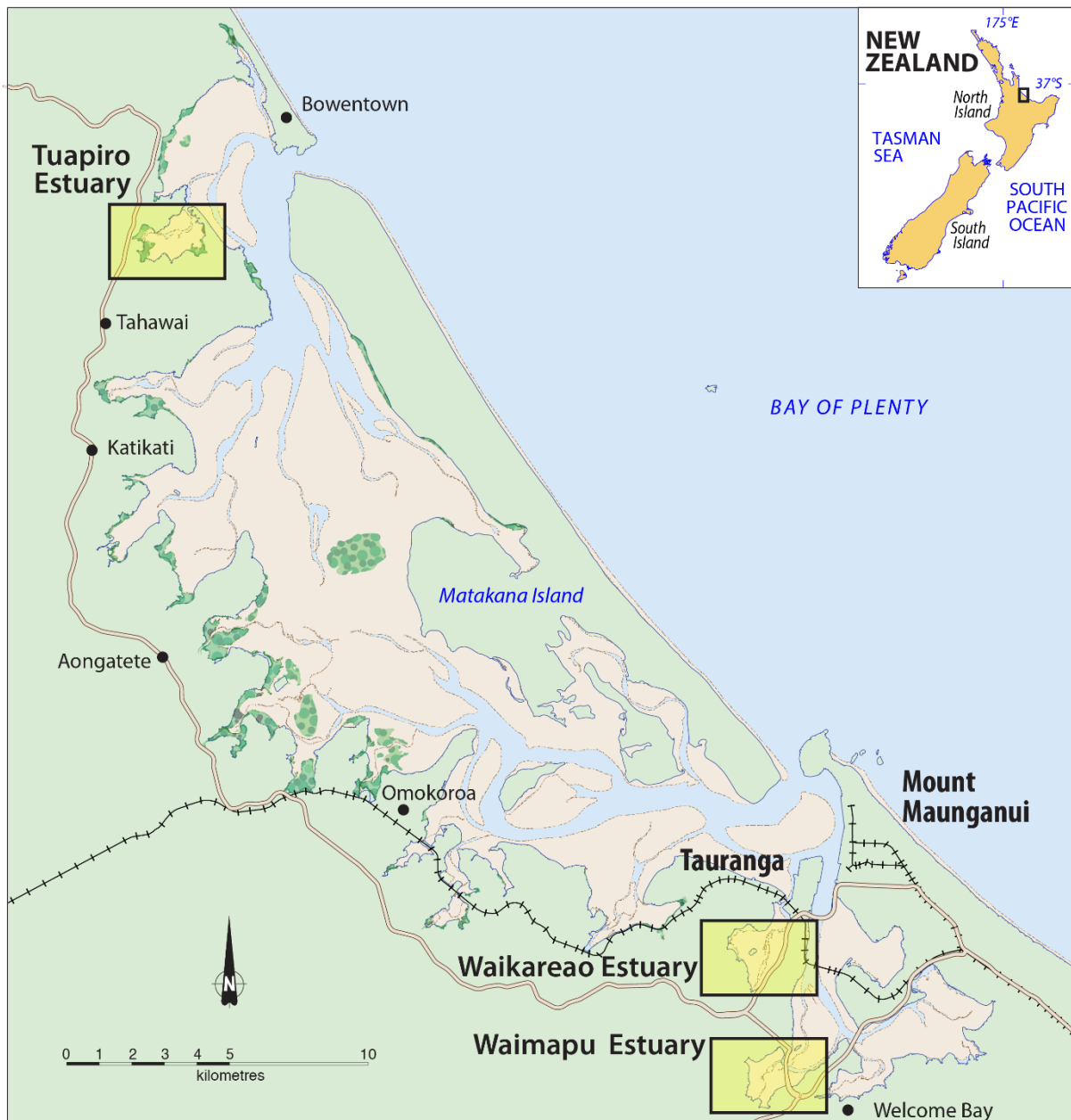

Figure 1-2: **Tauranga Harbour and sub-estuary study sites: Tuapiro Estuary, Waikareao Estuary and Waimapu Estuary.**

1.6.2 Climate, geology and land use

Tauranga Moana is largely sheltered from the prevailing south-west winds by the Kaimai and Mamaku ranges, so that a large proportion of rainfall is received during periods of north to north-

east (i.e., onshore) winds. When pressure gradients associated with weather systems are weak on fine summer days, northerly sea breezes of 20–30 km hr^{-1} develop and penetrate inland (Chappell, 2013). Mean annual wind speeds in Tauranga Moana are 14 km hr^{-1}. Median annual rainfall varies from 1,200–1,600 mm yr^{-1} (Tauranga Harbour) and can reach up to 2,200 mm yr^{-1} in the coastal ranges. The median annual temperature for Tauranga Moana is 9.6°C (Chappell, 2013).

The geology of Tauranga Moana and its catchment is composed of late Pliocene to Pleistocene volcanic rocks and volcanogenic sediment. The Tauranga Basin is one of the six principle physiographic units within Tauranga Moana. Basement rocks are composed of Waiteariki Ignimbrite (average 2.2 m thick) at 50 – 100 m depth below the seafloor. The sediment that has subsequently infilled the basin is composed of unconsolidated or weakly consolidated mud, sand and gravel of terrigenous, estuarine and shallow marine origin (Briggs et al. 1996; MacPherson et al. 2017).

Land cover in the Tauranga Moana's catchment is mainly comprised of mature bush (i.e. indigenous forest has 41% coverage and exotic forest 12%) and agricultural land (just over 40% coverage, comprising sheep, beef and dairy). Urban areas accounts for 9% of the total catchment area, although the proportion of urban land use has increased since 2012 (Lawton and Conroy, 2019). Recent historical events that may have impacted on sedimentation in the study estuaries are the 1981 failure of the Ruahihi Power Station dam and Cyclone Bola (1988). An estimated 1.5 million cubic metres of mud was discharged to the harbour by the dam failure. Cyclone Bola resulted in severe hillslope failure and soil erosion that would likely have delivered large quantities of fine sediment to the harbour and its fringing estuaries (Crawshaw 2020a).

1.6.3   Estuaries and catchments

The Tuapiro, Waikareao and Waimapu study estuaries fringe the western shore of the harbour. Salient features of each estuary are described in this section.

Tuapiro Estuary

Tuapiro Estuary receives freshwater runoff from the 77 km^2 Tuapiro Stream catchment. Land use includes indigenous vegetation (48%) in the upper catchment, pastoral land (32%), horticultural land (15%) and exotic forest (5%). Soils are generally derived from air-fall ash and most recently from the Kaharoa eruption that occurred 700 years ago (Bay of Plenty Regional Council 2012b). The soils are generally gritty sand and silt loams (i.e. Katikati series), and are naturally well-drained (Rjikse and Guinto 2010). Soils are susceptible to erosion and the catchment is classified as medium to high risk of erosion (Bay of Plenty Regional Council, 2012b). The annual catchment sediment yield averages at 46.3 ± 2.2 t km^2 yr^{-1} (i.e., catchment total sediment loss of ~3,570 t yr^{-1}) (Hicks, 2019).

Waikareao Estuary

Waikareao Estuary receives freshwater runoff from the Kopurererua Stream catchment (74 km^2). Land use is largely a mix of pastoral land (41%) and indigenous vegetation (41%). Horticulture (6%) and exotic forest (6%) account for small proportions of the catchment area. Soils are derived from volcanic tephra (Bay of Plenty Regional Council 2012a). The upper catchment is characterised by a sandy soil (i.e. Oropi series) and the middle to lower catchment by gritty sand and silt loam soils (i.e. Katikati series) (Rjikse and Guinto 2010; Bay of Plenty Regional Council 2012a). These soils are susceptible to erosion, particularly in areas where the Land Use Capability Class 6 occurs (25% of the catchment). There, soils are vulnerable to erosion, particularly in areas with a Land Use Capability class of six (25% of the catchment). BoPRC plan to mitigate erosion sources within this catchment which includes riparian fencing and stock exclusion (Bay of Plenty Regional Council 2012a). Hughes

and Hoyle (2014) found that the suspended sediment load within the Kopurererua catchment was dominated by bank erosion (95-99%), rather than hillslope erosion. Bank erosion in is generally seen in the upper and middle reaches of the catchment. The annual catchment sediment yield averages 36.4 ± 1.7 t km^2 yr^{-1} (i.e., catchment total sediment loss of ~2,690 t yr^{-1})(Hicks, 2019).

Waimapu Estuary

Waimapu Estuary is drained by the Waimapu Stream catchment (112 km^2). Catchment land use is divided into pastoral land (45%), indigenous vegetation (23%), horticultural land (5%) and exotic forestry (8%) with some areas converted to dairy land. Waimapu Estuary also has large areas of estuarine wetlands (Bay of Plenty Regional Council 2012c). Similar to Tuapiro Estuary, the catchment is dominated with air-fall ash, with mostly well-drained gritty sand and silt loam soils (i.e. Katikati series) (Rjikse and Guinto 2010; Bay of Plenty Regional Council 2012c).The soils are susceptible to erosion and a large portion (48%) of the catchment has a medium risk of erosion with a Land Use Capability of 6 (Bay of Plenty Regional Council, 2012c). The annual catchment sediment yield averages 63.3 ± 1.2 t km^2 yr^{-1} (i.e., catchment total sediment loss of ~7,090 t yr^{-1}) (Hicks, 2019).

BoPRC have prioritised riparian protecting, fencing and erosion control in all three catchments (BoPRC, 2012a, b and c).

1.6.4   Current and future sedimentation

The Tauranga Harbour Sediment Study (2007–2010) forecast potential changes in the southern half of Harbour over decadal timescales under a range of catchment development/land use change scenarios (Green, 2010 and references therein). Scenario modelling was undertaken using catchment and estuary computational models of hydrology and sediment loads (catchment), hydrodynamics and sediment transport (harbour), supported by measurements. Future sedimentation in the Harbour was considered under current (Green, 2010) land use and projected future land use, with and without predicted climate change effects.

For the three estuaries included in the present study, Waimapu and Waikareao estuaries were evaluated as sediment sinks, whereas fine sediment delivered to Waikareao Estuary may also be exported out of the harbour to the open ocean (Green, 2010). Wairoa River, the largest catchment discharging to Tauranga Harbour exports an estimated 95% of its sediment load to the ocean. The modelling also indicated that the Wairoa River is also likely to contribute to sedimentation in the adjacent Waikareao Estuary (Green, 2010). The results of the modelling showed that SAR in the sub-estuaries did not directly correspond to sediment loads from their immediate catchments. This was attributed to tidal import of fine sediment from other sub-catchment sources, and non-linear changes in sediment loads and resulting sediment-transport patterns in the Harbour (Green, 2010). For the sub-estuaries of interest included in the modelling, predicted SAR for current land use (2001) and future projected land use were:

- Waimapu Estuary: Current land use: 1.2 mm yr^{-1} (fine sediment, FS) and 3.6 mm yr^{-1} (coarse sediment, CS). Total SAR: **4.8 mm yr^{-1}**. Future land use scenario with climate change: 2.2 mm yr^{-1} (FS) and 4.2 mm yr^{-1} (CS). Total SAR: **6.4 mm yr^{-1}**, an increase of ~30%.

- Waikareao Estuary: Current land use: 1.0 mm yr^{-1} (fine sediment) and 0.95 mm yr^{-1} (course sediment). Total SAR: **2 mm yr^{-1}**. Future land use scenario with climate change: 1.7 mm yr^{-1} (FS) and 1.7 mm yr^{-1} (CS). Total SAR: **3.4 mm yr^{-1}**, an increase of ~70%.

2 Methods

2.1 Initial site visit

An initial site visit to the study estuaries was conducted on Monday 20th July 2020 to coincide with low tide ±3 hours (Figure 1-2). The purpose of the site visit was to inform planning for the sediment coring and to identify any site-specific logistical issues. NIWA staff were accompanied by BoPRC staff. The coring sites were co-located (i.e., within tens of metres) of the buried sediment accretion plates incorporated in the BoPRC Estuarine Health Monitoring programme. The sediment accretion plate sites were cores were collected are:

- Tuapiro Estuary (Tau P54, Tau P55, Tau P56),

- Waikareao Estuary (Tau P16, Tau P17, Tau P21)

- Waimapu Estuary (Tau P12, Tau P13 and Tau P14).

2.2 Estuarine sediment cores

Sediment cores were collected from the estuaries at low tide ±3 hours between 28–30 September 2020 and 16 October 2020 (Figure 2-1). The coring method employed was a rectangular Perspex tray corer (80 x 27 x 3 cm), with a cross-sectional area of 81 cm^2. In this method, under normal conditions the Perspex corer is eased into the tidal flat sediment without its front cover plate to avoid core disturbance due to surface friction on the inside faces of the corer. The cover plate (stainless steel or Perspex) is inserted once the corer has penetrated the sediment to the required depth. Through field trials, due to the compact substrate, and sand and buried shell layers at each site, a stainless steel spade was manufactured into which the Perspex tray was inserted (Figure 2-2). This allowed the tray-corer to be better driven through resistant layers. The tray was excavated from the substrate and the Perspex cover plate replaced the steel cover used for the field recovery.

The advantage of using the rectangular Perspex trays are ideal for x-ray imaging because they are have even thickness and are wide enough to capture decimetre-scale horizontal sedimentary structures. They can be used directly with NIWA's digital x-ray imaging system (i.e. no further preparation needed). However, the Perspex tray method was not suitable at site P-14 (Waikareao Estuary) due to a particular compact surface sand layer that made penetration of the Perspex tray difficult so that traditional cylindrical (pipe) cores were taken instead.
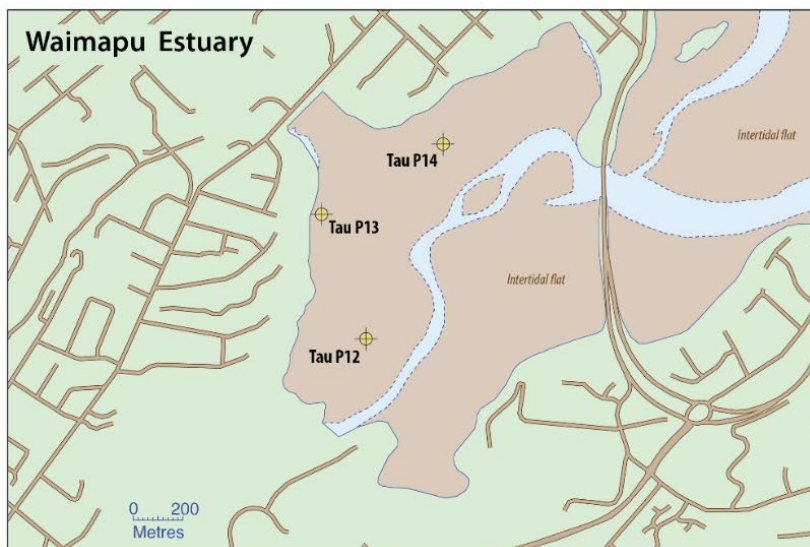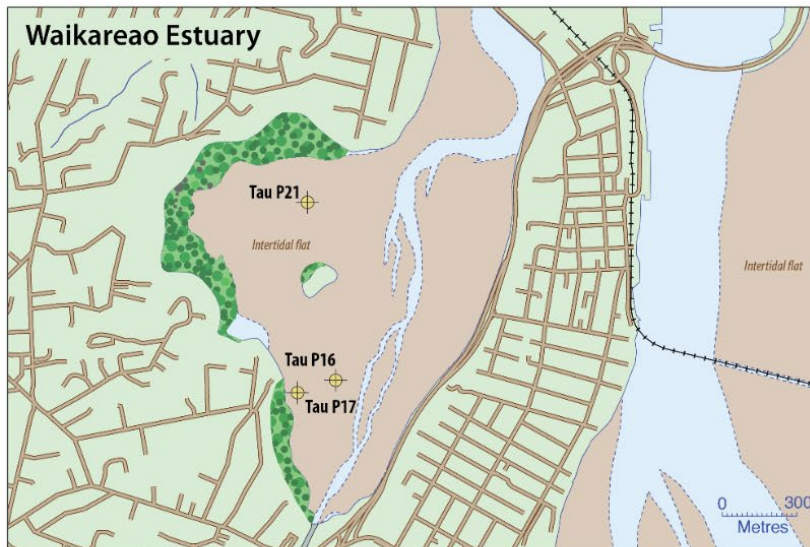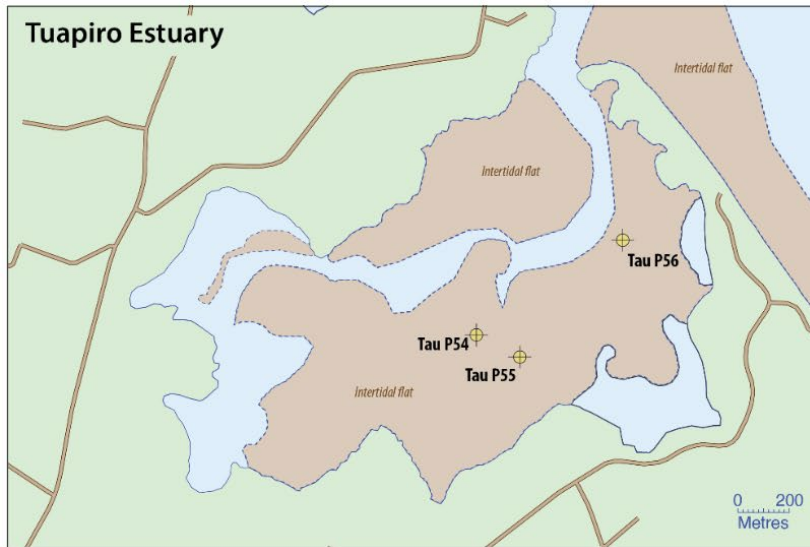
Figure 2-1: **Location of sediment core sites in study estuaries, Tauranga Harbour.** Cores collected 28–30 September and 16 October 2020.

Two pipe cores (10 cm internal diameter) were also collected at each site using an Aquatic Research Large Bore Sediment Corer. The corer includes a one-way check valve that creates suction inside the top of the core tube that reduces the risk of core loss during extraction. One core was available for x-ray imaging and dating, if required, and the remaining pipe core was withheld for archiving. Cores were inserted directly into the tidal flat substrate and then excavated carefully using a spade, with minimal disturbance. All cores were packed securely and transported back to the NIWA's Hamilton campus. Details of core sites, including locations, provided in Appendix A.

Figure 2-2:   Sediment coring in the study estuaries. Left: Intertidal sand flat in Tuapiro Estuary (site P54). Right: Perspex-tray trays being used to collect sediment cores in the Waikareao Estuary (site P16) Photos: Greg Olsen.

2.3   Sediment composition

Sediment cores were processed at NIWA's sediment laboratory. The sediment composition and stratigraphy preserved in the cores were determined by x-ray imaging and analyses of selected samples. X-radiographs reveal material density contrasts (due to particle size and composition, porosity) and provides information on fine-scale sedimentary fabric (i.e., structures and sediment textures formed by physical processes and animals living in the sediment) preserved in the cores. Density differences between layers of silt and sand or mud-infilled animal burrows are easily recognised the x-radiographs even though they may not be visible to the naked eye. These x-radiographs are negative images so that relatively high-density objects appear white (e.g., shell valves) and low-density materials such as muds or organic material appear as darker areas.

As well as documenting changes in sediment composition with depth, this x-radiographs are used to inform selection of samples for dating. Fine-scale (mm) differences in sediment density due to particle size, composition and/or water content are readily identified. For ground-truthing sediment

properties, dry-bulk sediment density (ρ_d, g cm^{-3}) profiles were also determined for each core from the net dry weight of samples of a known volume.

The sediment cores were x-ray imaged using a Varian PaxScan 4030E digital detector panel and an Ecotron EPX-F2800 portable x-ray generator. X-ray energy and exposure settings were typically 63–71 keV and 25 mAs (milli-Amp seconds).

Particle size distributions (PSD, 0.1–300, 10–2000 μm) of selected core samples were determined using an Eye-Tech stream-scanning laser system. Sediments were analysed from the following depth increments in each core: 0–1 cm; base of excess ^{210}Pb (dating) profile (i.e., variable age depending on SAR) and a buried mud deposit that could be attributable to the 1988 Cyclone Bola or the earlier 1981 failure of the Ruahihi Power Station dam. The Eye-Tech employs the time-of-transition (TOT) method to directly measure the diameters of individual particles (e.g. Jantschik et al. 1992). Samples were analysed using both the A-lens (size range: 0.6–300 μm) and B-lens (size range: 10–2000 μm) and PSD based on particle spherical volume were calculated (i.e., $V = 4/3\pi r^3$). The sediment displayed a wide size range, from mud (< 62.5 μm) to very coarse sand (2,000 μm) that included small shell fragments. The results for the B-lens are primarily presented herein as they provide the best representation of the overall PSD (volume %) of the typically poorly sorted silty sandy material. In addition, the contribution of the < 10 μm size fraction to volume PSD in these muddy sands was negligible, as described in the results for the fine A-lens. For comparison, a 100 μm diameter spherical sand particle has one thousand times the volume of a 10 μm sphere and one million times the volume of a 1 μm sphere.

2.4   Sediment accumulation rates

Sediment accumulation rates (SAR) were determined from radionuclide profiling of the sediment cores. The calculated SAR are time-averaged values expressed as millimetres per year (mm yr^{-1}). Radionuclides are strongly attracted to the surfaces of clays and silt particles, characteristic of fine-grained sediment deposits, which makes them particularly useful as "mud meters" to determine sediment accumulation rates (Sommerfield et al. 1999). In the present study, sediment accumulation rates over the last several decades to century were quantified using the depth profiles of naturally occurring excess lead-210 (^{210}Pb$_{ex}$, half-life 22 years). The basic principles of ^{210}Pb dating are described in (Appendix A). Caesium-137 (^{137}Cs, half-life 30 years) dating has also commonly used to determine SAR in aquatic receiving environments for sediment deposited since the early-1950s (Robbins and Edgington 1975; Wise 1977; Ritchie and McHenry 1990), when atmospheric deposition of nuclear bomb-produced ^{137}Cs was first detected in New Zealand. In the present study, ^{137}Cs was not detected in any of the sediment cores and is now at the limits of its usefulness due its short half-life (Miller and Kuehl, 2010).

Radiocarbon (^{14}C) dating was also employed to calculate long-term SAR over the last several thousand years prior to the early–mid 20th Century, defined by the maximum depth of ^{210}Pb$_{ex}$ in the cores. The surface-mixed layer (SML), where it occurs, can be identified from the vertical profile of radionuclide activity. Mixing occurs due to the burrowing and feeding activities of benthic animals and/or physical disturbance by processes such as sediment resuspension/deposition by wind waves. These radionuclide dating techniques are described in detail in Appendix A.

Sediment dating using two or more independent methods offsets the limitations of any one approach. This is important when interpreting sediment profiles from estuaries because of the potential confounding effects of sediment mixing by physical and biological processes (Smith, 2001).

This was not possible in the present study as only $^{210}Pb_{ex}$ occurred in measurably quantities in the sediment.

The activity of excess ^{210}Pb in each core was determined by gamma spectrometry of 40–60 g dry samples (1-cm slices) of sediment taken at increasing depths from each core. The radionuclide activity of a sediment sample is expressed as Becquerel (number of disintegrations per second) per kilogram (Bq kg^{-1}). The radioactivity of samples was counted at the ESR National Radiation Laboratory for 23 hours using a Canberra Model BE5030 hyper-pure germanium detector. Details of the calculation of sediment accumulation rates are presented in Appendix A.

Estimates of pre-historic SAR were determined at two core sites (Tuapiro [site P55], Waimapu [site P12]) using atomic mass spectrometry (AMS) radiocarbon (^{14}C) dating. Replicate shell valves of the common suspension-feeding bivalve *Austrovenus stutchburyi* (cockle) were selected for dating. The New Zealand cockle is particularly suitable for radiocarbon dating as they have ^{14}C concentrations in their carbonate that are similar to those found in marine shellfish (Hogg et al. 1998). This means that marine reservoir effects (i.e., "old" carbon in ocean waters mixing with coastal waters) can, in part, be modelled for using the marine ^{14}C calibration curve (Petchey et al. 2008). However, the reservoir age in New Zealand is relatively poorly constrained (Clark et al., 2019). All radiocarbon ages reported in the current study are in calibrated years before present (cal. yr BP) following laboratory calibration using OxCal 4.4.4 (Bronk Ramsey, 2021) r5, using marine data from Heaton et al. (2020) and a reservoir correction (ΔR -154 ± 38).

Shelly basal sediment layers were identified in the cores that occur well below the depth profile of excess ^{210}Pb. Samples from articulated values with intact surface ornamentation were favoured for dating. This indicates that the animals died in situ in the upper-most sediment column or were not transported far from their place of origin. In life, cockles typically occur in the upper several cm of the substrate. In the Tuapiro P55 core, three shell valves were taken from a shell layer at 63–65 cm depth. Three samples from a shell bed (59–64 cm) were selected from the Waimapu P16 core, with two of these samples from individual shellfish with articulated valves. Details of the dated samples are included in Table B-1.

2.5   Preservation of 1980s event deposition

One of the objectives of this study is to document evidence of preserved event-sedimentation layers in the cores that could be attributable to either the Ruahihi dam failure (September 1981) or Cyclone Bola (March 1988). An episodic or seasonal event deposition layer will characteristically be composed of mud with fine-scale laminations preserved. An example of what an event deposit looks like is captured in core P-55 (38–43-cm depth), composed of a discrete unit of laminated, millimetre- to centimetre-thick layers of mud and sand. This laminated sediment directly overlays a unit of abundant cockle shells in a muddy-sand matrix. The degree of preservation of the primary sedimentary fabric and the sharp contact with the underlying cockle shell also suggests that the laminated layer was deposited during a storm event when enhanced water motions drive sediment hydrodynamics (Figure 3-3).

Event layers will be deposited under conditions that vary from the average conditions in the depositional environment, such as elevated suspended sediment concentrations and different particle sizes. Preservation of event layer in the sedimentary record depends on a number of interdependent factors, including thickness of the event layer (L_s) in comparison to the thickness of the surface mixing layer (i.e., bioturbation, L_b), burial rate (SAR) and bioturbation rate (Bentley et al.,

2006). Preservation of an event layer is less likely when $L_s < L_b$ and SAR are low (i.e.,< cm yr^{-1}), but there is longstanding debate around how and when particular events are preserved and the representativeness of the geological record in general (e.g. Sommerfield, 2006).

The sedimentological information provided by the Tauranga Estuary cores (x-radiographs, particle size, bulk density) is used to evaluate if the Ruahihi and Cyclone Bola event layers are preserved in the sedimentary record. These two events delivered fine sediment (mud and fine sand) eroded from catchment soils that were readily transported in suspension to sites of deposition in the Tauranga estuaries.

3 Results

The following sections present the results of the x-ray imaging, ^{210}Pb and ^{14}C dating and sediment composition analysis for each core site.

3.1 Tuapiro Estuary

3.1.1 Core P-54

The x-radiographs for core P-54 show that sediment deposits are composed of bioturbated muddy and gravelly (shell) sands with abundant cockle shell valves throughout. A zone of organic-rich sediment (black) can also be observed at 20–30 cm depth (Figure 3-1). Dry bulk densities (ρ_d) of 1.1–1.4 g cm^{-3} also indicate that sediment depositing at this site is primarily composed of muddy sand. For comparison, a clay-rich, unconsolidated estuarine mud typically has a surficial ρ_d as low as ~0.5 g cm^{-3} (e.g., mudflats, southern Firth of Thames) (Figure 3-1). The sediment in core P-54 is composed of slightly-muddy fine sand (mean: 120–175 μm, D90: 181–280 μm) with a mud content of 4–10%. Mud content increases with depth from ~4% in the top 11-cm to 10% at 25–26-cm depth (Figure 3-5,Table 3-2). The laser particle sizer A-lens (0.6–300 μm) results show that the < 10 μm fraction (clay – very fine silt/fine silt) accounted for < 0.42% (mean: 0.24%) for that size range in the four core P-54 samples analysed. Consequently, the actual contribution of the < 10 μm fraction to the entire particle size distribution of the matrix (≤ 2000 μm, very-coarse sand) will be substantially lower. The ^{210}Pb SAR at this site has averaged 5.4 mm yr^{-1} (fit: r^2 = 0.70) over the last ~49 years (i.e., 1971–2020) in the top-most 25 cm of sediment column. No [210]Pb$_{ex}$ SML was observed at this site (Figure 3-2). Dry bulk sediment densities of the mud and sand matrix do not display an apparent trend with depth (Figure 3-2), possibly as a result of biological mixing and reworking from water motions.

These bioturbated sediments do not preserve any evidence of muddy event deposits that could be attributed to high fluxes of fine sediment associated with either the failure of the Ruahihi dam or Cyclone Bola during the 1980s.

Figure 3-1: **Core P-54 x-radiograph (intertidal: Tuapiro Estuary, 0-63 cm).** These x-radiographs have been inverted so that relatively high-density objects appear white (e.g., shell valves) and low-density materials such as muds or organic material appear as darker areas. The x-radiographs represent core sections up to 35-cm long, with the depth intervals indicated the top of each image. The coloured arrows indicate matching positions (i.e., depth in core) in each x-radiograph. The calculated depth range for sediment deposited in the 1980s (^{210}Pb dating) is indicated.

Figure 3-2: Core P-54 (Tuapiro Estuary) - ages of sediment layers, sediment accumulation rates (SAR), and sediment properties. (a) Excess ^{210}Pb activity profiles with 95% confidence intervals shown. Time-averaged SAR (mm yr^{-1}, black text) derived from regression fit ($r^2 = 0.70$) to natural log-transformed excess ^{210}Pb data. Calculated age at the base of activity profile is shown in red text. Surface mixed layer (SML), where indicated inferred from $^{210}Pb_{ex}$ (half-life = 22 yr) profiles; (b) Sediment dry bulk density profile (g cm^{-3}).

3.1.2 Core P-55

X-radiographs for core P-55 reveal a complex stratigraphy (Figure 3-3). Shelly gravelly sands characterise the top-most 20-cm of the core, with a distinct lithological change to muddy-sands below this layer. A distinctive and well-preserved layer of laminated, mm to cm-thick, layers mud and sand occurs at 38–43-cm depth. This laminated sediment directly overlays abundant cockle shells in a muddy-sand matrix. The degree of preservation of the sedimentary fabric in the muddy laminated layer and the sharp contact with the underlying cockle shell suggests that the laminated layer was deposited during a storm event. Dry bulk densities above the laminated sediment of 1–1.5 g cm^{-3} are consistent with a muddy-sand matrix. Within the event layer, ρ_d values as low as 0.5 g cm^{-3} are consistent with a clay-rich mud (Figure 3-4). The sediment in core P-55 is composed of muddy very-fine to fine sand (mean: 86–125 μm, D90: 141–218 μm) with a mud content of 11–31%. Mud content increases with depth from 11–14% in the top 16-cm to 31% at 62–63-cm depth in core basal sediment (Figure 3-5, Table 3-2). The laser particle sizer A-lens (0.6–300 μm) results show that the < 10 μm fraction (clay – very fine silt/fine silt) accounted for < 6.6% (mean: 3.1%) for that size range in the four core P-55 samples analysed. Consequently, the actual contribution of the < 10 μm fraction

to the entire particle size distribution of the matrix (≤ 2000 μm, very-coarse sand) will be lower. PSD size class and cumulative distribution plots for surficial and basal sediment are presented in Figure 3-6. The ^{210}Pb SAR at this site has averaged 4.5 mm yr^{-1} (fit: r^2 = 0.96) over the last ~80 years (i.e., 1940–2020) in the upper-most 35 cm of the sediment column (Figure 3-4). No $^{210}Pb_{ex}$ SML was observed at this core site. These bioturbated sediments do not preserve any evidence of muddy event deposits that could be attributed to high fluxes of fine-sediment loads associated with either the failure of the Ruahihi dam or Cyclone Bola during the 1980s, although older muddy deposits are evident deeper in the core.
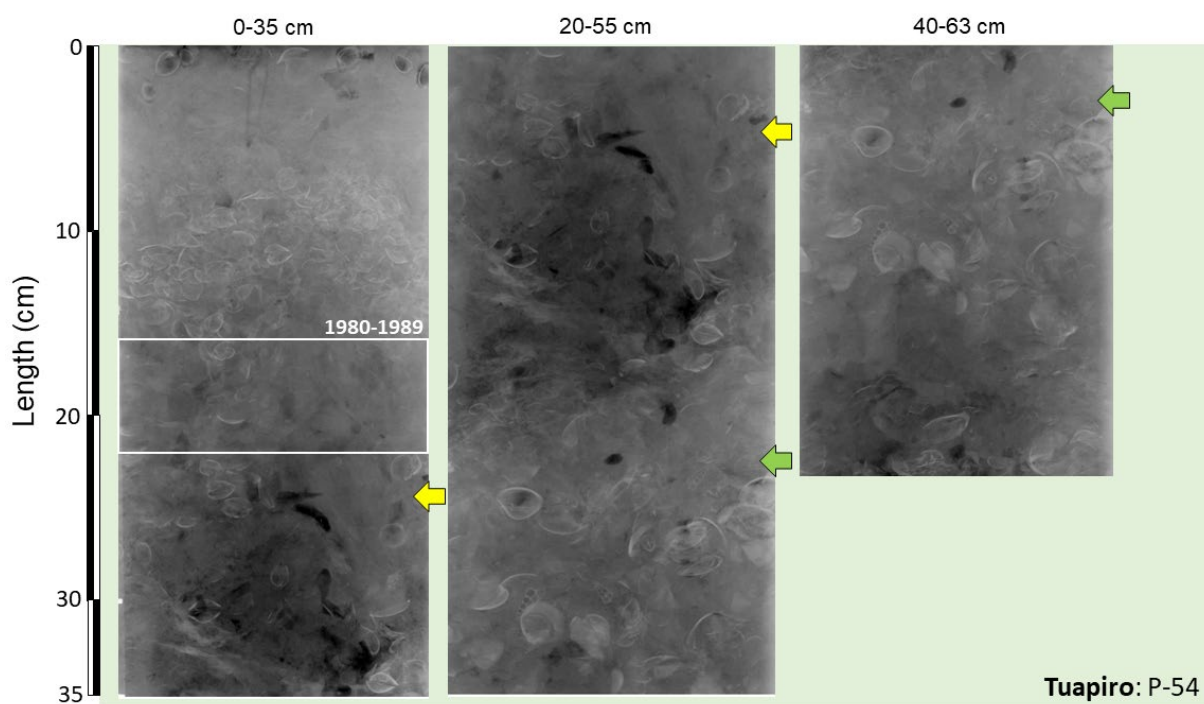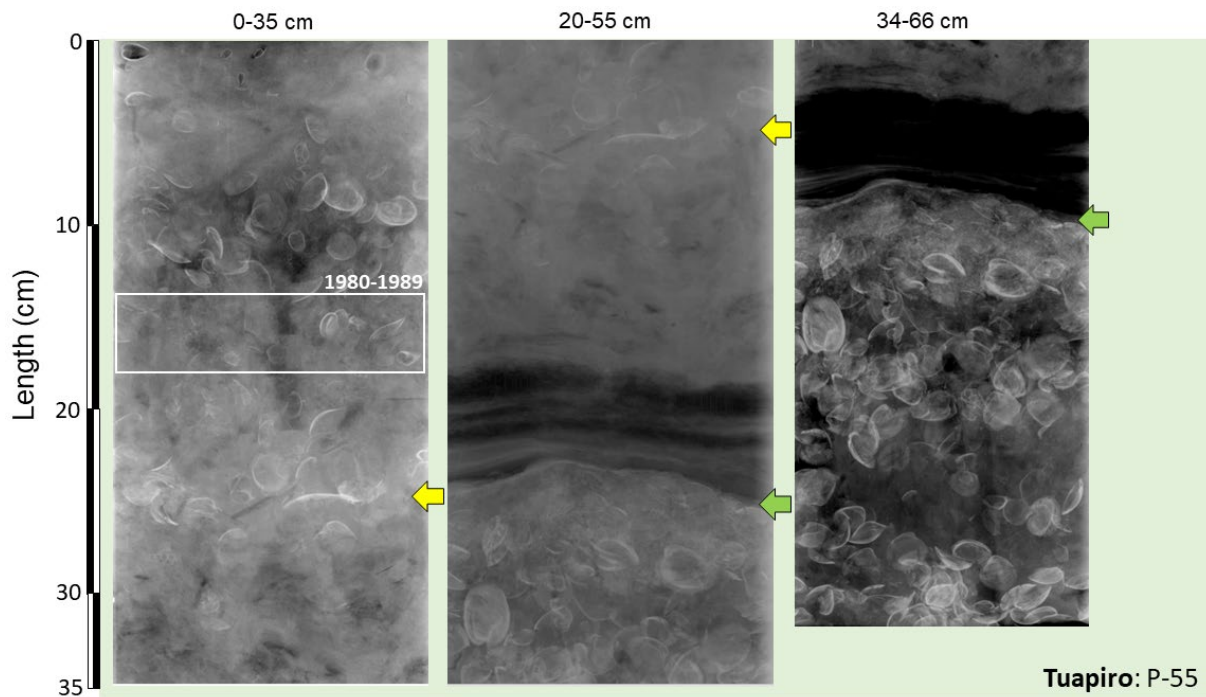

Figure 3-3:   Core P-55 (intertidal: Tuapiro Estuary): 0-66 cm.   The x-radiographs represent core sections up to 35-cm long, with the depth intervals indicated the top of each image. The coloured arrows indicate matching positions (i.e., depth in core) in each x-radiograph. The calculated depth range for sediment deposited in the 1980s (^{210}Pb dating) is indicated.
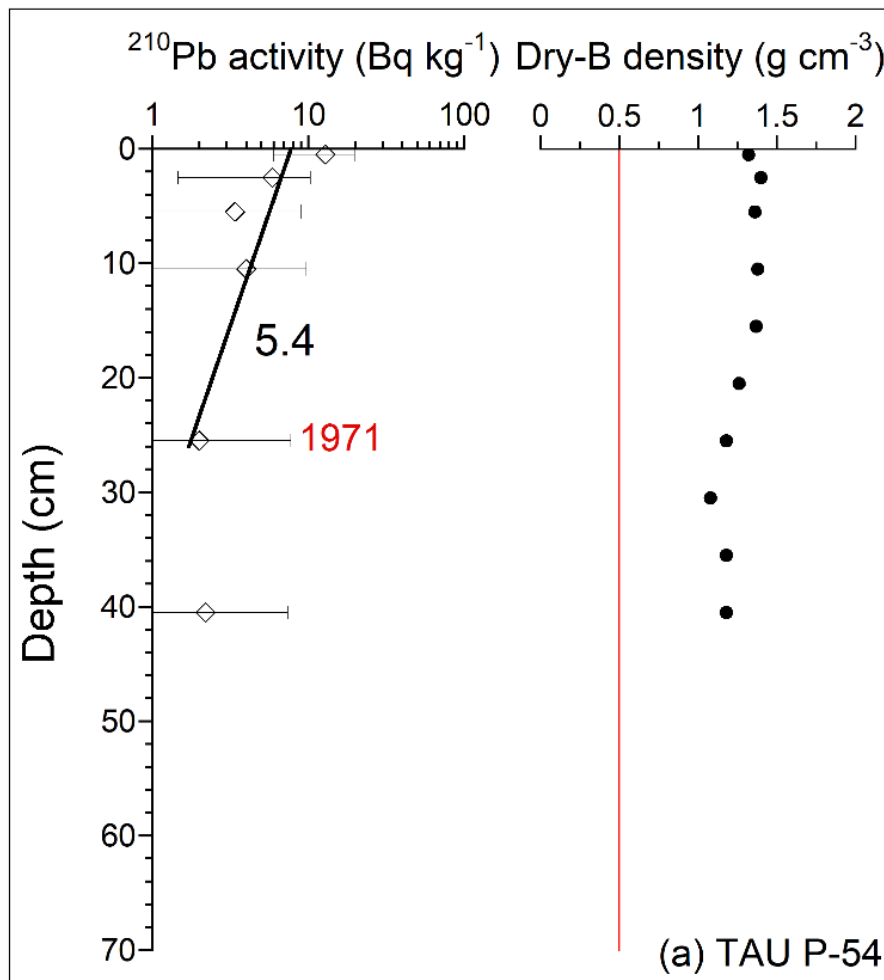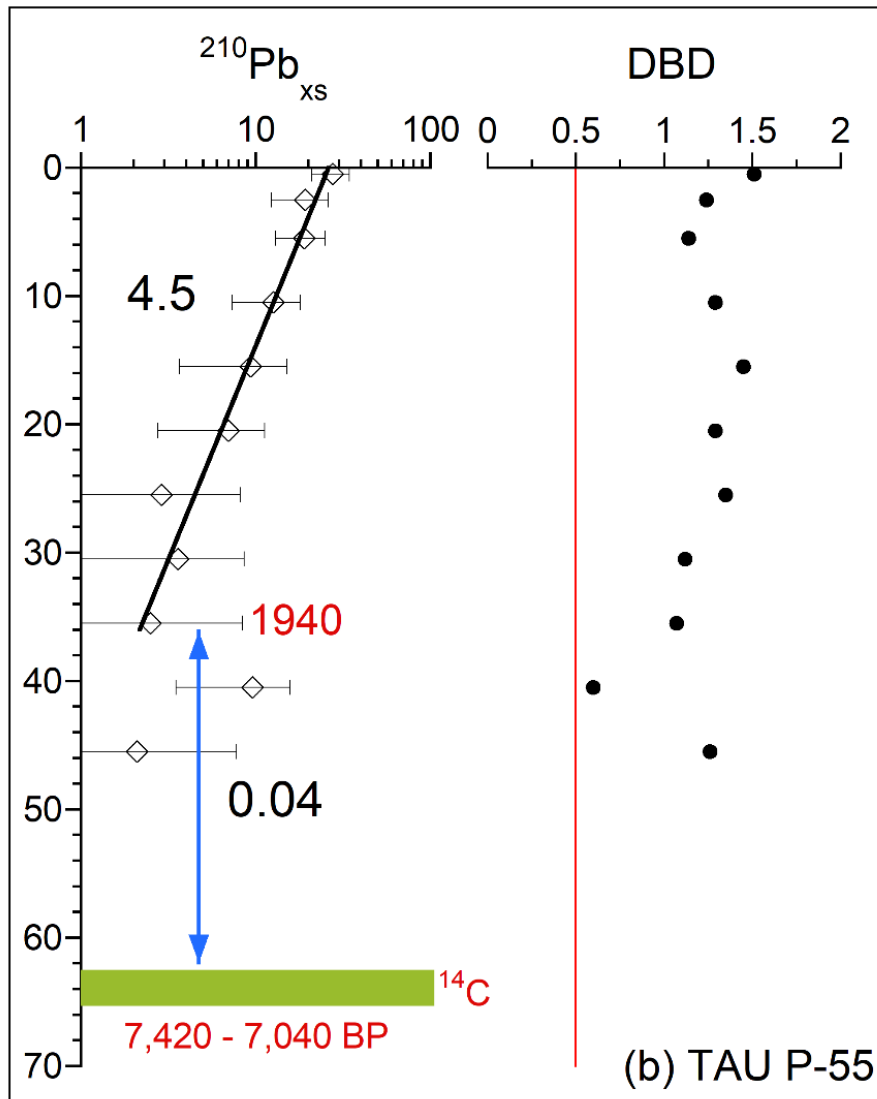
Figure 3-4: **Core P-55 (Tuapiro Estuary) - ages of sediment layers, sediment accumulation rates (SAR) and sediment properties.** (a) (a) Excess ^{210}Pb activity profiles with 95% confidence intervals shown. Time-averaged SAR (mm yr^{-1}, black text) derived from regression fit (r^2 = 0.96) to natural log-transformed excess ^{210}Pb data. Calculated age at the base of activity profile is shown in red text. Surface mixed layer (SML), where indicated, is inferred from ^{210}Pb$_{ex}$ (half-life = 22 yr) profiles; (b) Sediment dry bulk density profile (g cm^{-3}). Background SAR for ~7,000-year period (AMS ^{14}C dating of cockle shell valves) prior to the early-1900s shown.

Radiocarbon dating of three cockle shell valves (*Austrovenus stutchburyi*) from three different individuals (63–65 cm depth) from the deep shell layer provided consistent ages (Table 3-1): the 95% probability range of calibrated ^{14}C ages are 7,420-7,040 cal. yr BP and yielded a time-average SAR of 0.04 mm yr^{-1} below the excess ^{210}Pb layer (i.e., pre-1940).

Table 3-1:   **Summary of AMS ¹⁴C dating results.**   Radiocarbon dating results for cockle shell (*Austrovenus stutchburyi*) sampled from cores TUA P55 (Taupiro Estuary) and WMP P12 (Waimapu Estuary). The ¹⁴C age ± 1 standard deviation (Before Present, BP = 1950) is based on the Libby half-life (5,568 yr) with correction for isotopic fractionation. The laboratory calibration used OxCal 4.4.4 (Bronk and Ramsey, 2021) r5, using marine data from Heaton et al. (2020) and a reservoir correction (ΔR -154 ± 38).The 95% probability age range is used to calculate the time-average SAR value.

Core	Sample ID	Depth increment (cm)	¹⁴C (radiocarbon) age (Years Before Present)	Calibrated ¹⁴C age range (cal. yr BP, 95% Probability)
Tuapiro Estuary				
TUA P55	*Wk-52640*	63–65 (sample A)	6,790 ± 21	7,420–7,100
	Wk-52641	63–65 (sample B)	6,747 ± 21	7,390–7,040
	Wk-52642	63–65 (sample C)	6,767 ± 21	7,410–7,060
Waimapu Estuary				
WMP P12	*Wk-52643*	60–64 (sample A)	6,161 ± 21	6,740–6,380
	Wk-52644	63–65 (sample B)	6,200 ± 20	6,780–6,420
	Wk-52645	63–65 (sample C)	6,167 ± 25	6,760–6,380
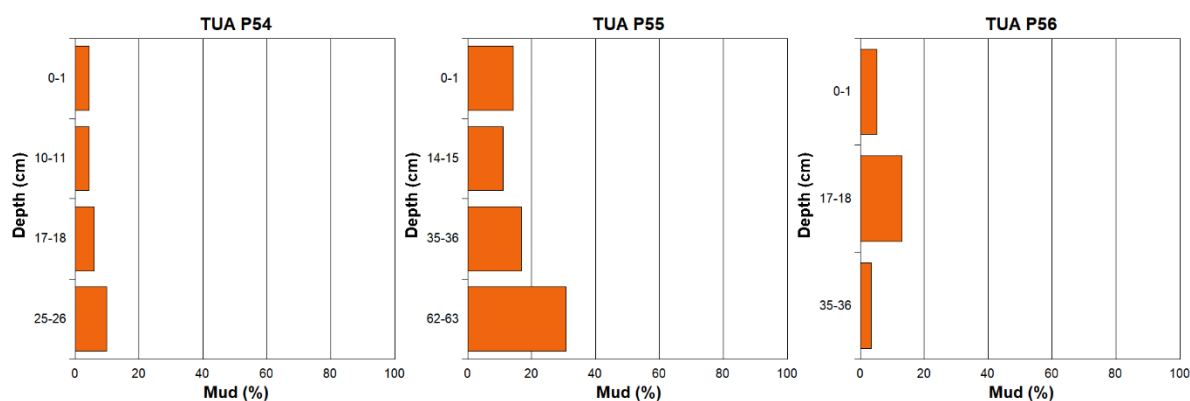
Figure 3-5:   **Mud content (% volume) for selected core samples, Tuapiro Estuary.**   Particle size summary statistics are presented in Table 3-2. Note that the depth axis varies as time periods and/or particular units were targeted (surface sample, ~1988 (Bola) and base of excess Pb-210 profile), so the depth of samples varies depending on SAR.
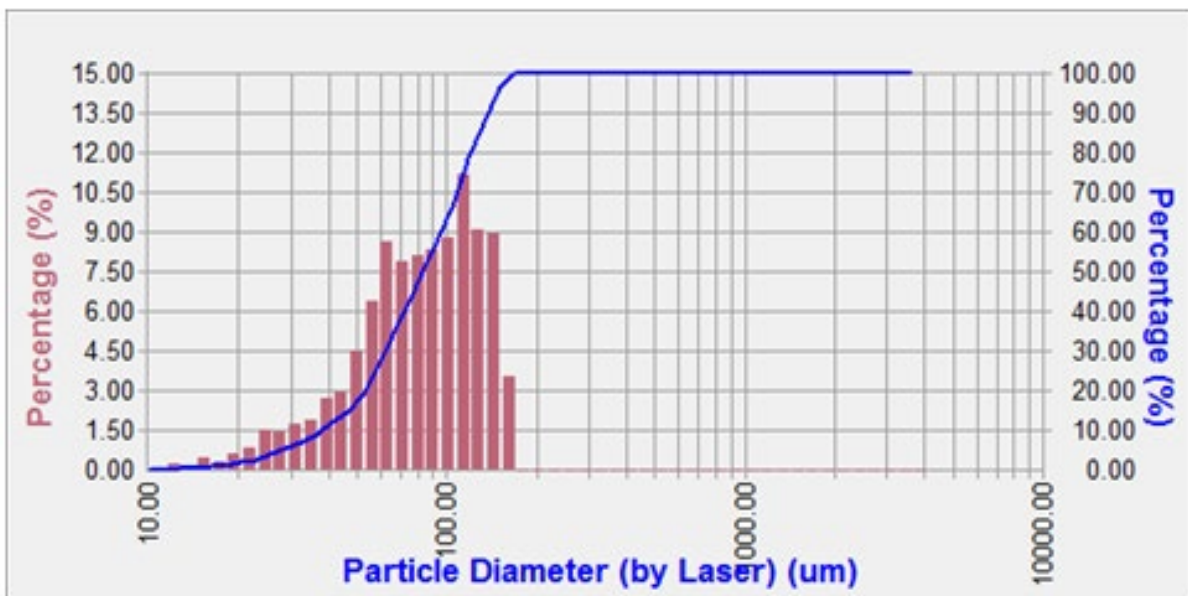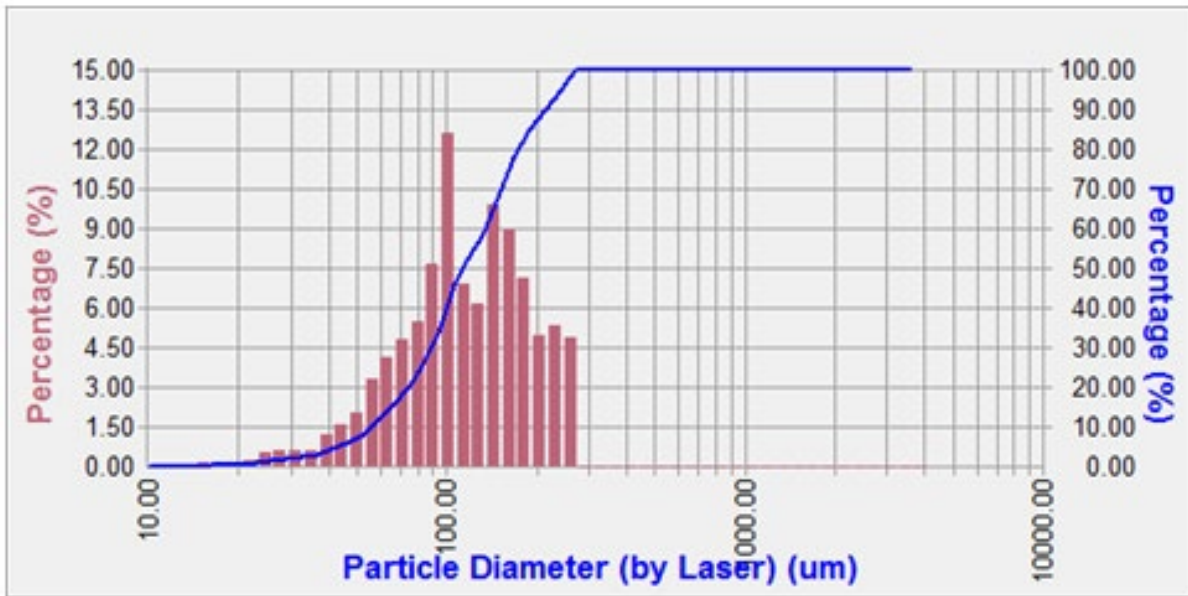
Figure 3-6:   Examples of Tuapiro Core P-55 particle-size frequency and cumulative percent distribution.
Data: Particle size (microns) frequency histogram by volume percent (red) cumulative percent (blue), assuming spherical particles. Top: 0–1-cm and bottom: 62–63-cm depth samples.

3.1.3   Core P-56

The x-radiographs for core P-56 indicate predominantly muddy-sand deposition at this site, with abundant cockle shell valves from 5 to 36 cm depth (Figure 3-7, Figure 3-8). An abrupt depth transition to organic- and/or mud-rich sediment with rare shells occurs below this surface shell layer. Dry bulk densities of 1.3–1.7 g cm^{-3} to the base of the cockle shell layer are consistent with a slightly-muddy sand-rich matrix. The sediment in core P-56 is composed of slightly-muddy fine sand (mean: 114–183 μm, D90: 186–277 μm) with a mud content of 4–13%. Mud content is highest at 17–18-cm depth (Figure 3-5,Table 3-2). The laser particle sizer A-lens (i.e., 0.6–300 μm) results show that the < 10 μm fraction (i.e., clay – very fine silt/fine silt) accounted for < 1.0% (mean: 0.66%) for that size

range in the three core P-56 samples analysed. Consequently, the actual contribution of the < 10 μm fraction to the entire particle size distribution (≤ 2000 μm, very-coarse sand) will be substantially lower. The ^{210}Pbex profile also extend to the base of the cockle shell hash layer (36-cm) with a time-averaged SAR of 5.6 mm yr^{-1} (fit: r^2 = 0.87) over the last ~64 years (i.e., 1956–2020) (Figure 3-8). No ^{210}Pb$_{ex}$ SML was observed at site P-56.

These bioturbated sediments do not preserve any evidence of muddy event deposits that could be attributed to high-fluxes of fine-sediment loads associated with either the failure of the Ruahihi dam or Cyclone Bola during the 1980s.

Figure 3-7:   Core P-56 (intertidal: Tuapiro Estuary): 0-65 cm.   The x-radiographs represent core sections up to 35-cm long, with the depth intervals indicated the top of each image. The coloured arrows indicate matching positions (i.e., depth in core) in each x-radiograph. The calculated depth range for sediment deposited in the 1980s (^{210}Pb dating) is indicated.

Figure 3-8: Core P-56 (Tuapiro Estuary) - ages of sediment layers, sediment accumulation rates (SAR), and sediment properties. (a) Excess ^{210}Pb activity profiles with 95% confidence intervals shown. Time-averaged SAR (mm yr^{-1}, black text) derived from regression fit (r^2 = 0.87) to natural log-transformed excess ^{210}Pb data. Calculated age at the base of activity profile is shown in red text. Surface mixed layer (SML), where indicated inferred from ^{210}Pb$_{ex}$ (half-life = 22 yr) profiles; (b) Sediment dry bulk density profile (g cm^{-3}).

3.2   Sediment Cores: Waikareao Estuary

3.2.1   Core P-16

The x-radiographs of core P-16 show preserved traces of fine (i.e., millimetre-scale) vertical burrows in a surface sand layer extending to 11-cm depth that overlays a cockle-shell rich layer (Figure 3-9). Coarse sand size particles of varying density (i.e., white to black) can also be observed in the top-most 3 cm of the core. These sediment textures are consistent with winnowing of mud in surface mixed layer. There is also evidence of mixing of mud and sand within the shell-rich layer and general increase in mud content with increasing depth. Abundant cockle-shell valves occur in core basal sediment below ~58-cm depth. Somewhat peculiarly, dry bulk densities decrease with depth from 0.9 g cm^{-3} at the surface to 1.4 g cm^{-3} at 40 cm (Figure 3-10). The sediment in core P-16 is composed of muddy very-fine to fine sand (mean: 126–137 μm, D90: 198–220 μm) with a mud content of 8–18%. Mud content increases with depth from 8% in surficial sediment and 16–18% below 20-cm depth (Figure 3-11, Table 3-2). The laser particle sizer A-lens (0.6–300 μm) results show that the < 10 μm fraction (clay – very fine silt/fine silt) accounted for < 1.6% (mean: 1.1%) for that size range in the three core P-16 samples analysed. Consequently, the actual contribution of the < 10 μm fraction to the entire particle size distribution of the sediment matrix ($\leq$ 2000 μm, very-coarse sand) will be substantially lower. The $^{210}Pb_{ex}$ profile extends to 40-cm, although the regression fit for the SAR calculation terminates at 30-cm depth (Figure 3-10Figure 3-10). This is due to apparent uniform $^{210}Pb_{ex}$ activity in the 30–40-cm depth increment. The time-average ^{210}Pb SAR at this site is calculated to be 6.4 mm yr^{-1} (fit: r^2 = 0.24) over the last ~48 years for the uppermost 40.5 cm of sediment).

Figure 3-9:   Core P-16 (intertidal: Waikareao Estuary): 0-61.   The x-radiographs represent core sections up to 35-cm long, with the depth intervals indicated the top of each image. The coloured arrows indicate matching positions (i.e., depth in core) in each x-radiograph. The calculated depth range for sediment deposited in the 1980s (^{210}Pb dating) is indicated.

These bioturbated sediments do not preserve any evidence of muddy event deposits that could be attributed to high fluxes of fine-sediment loads associated with either the failure of the Ruahihi dam or Cyclone Bola during the 1980s.
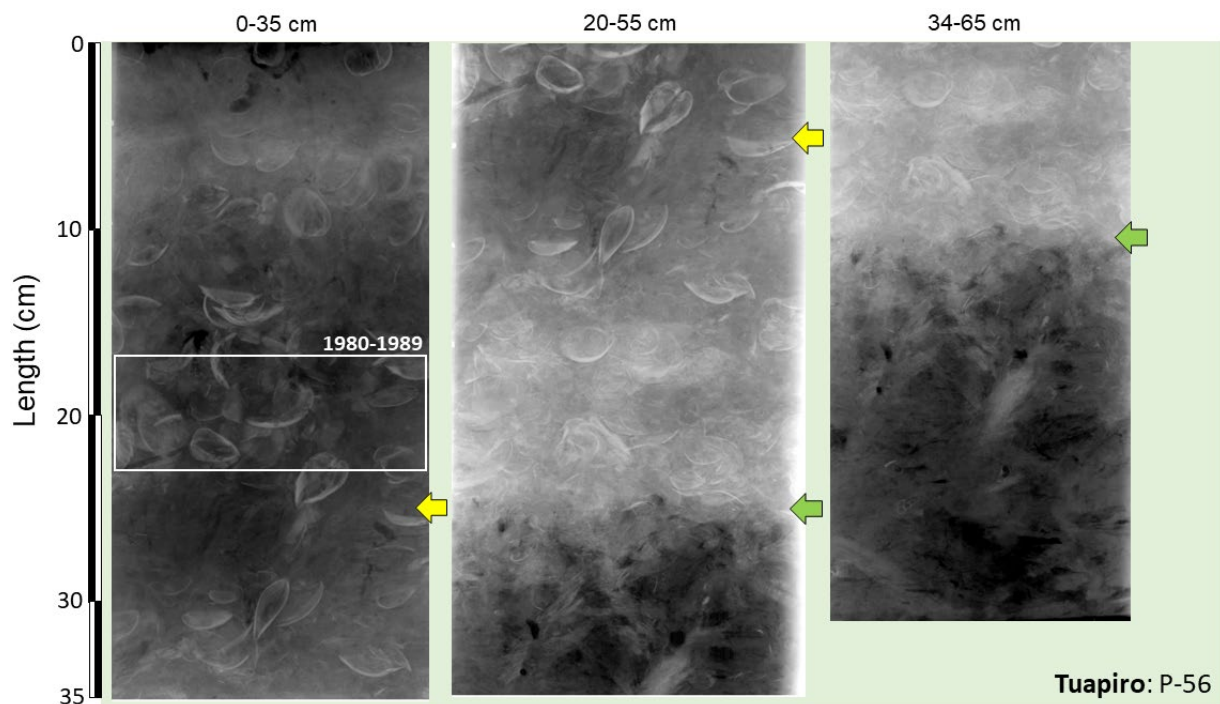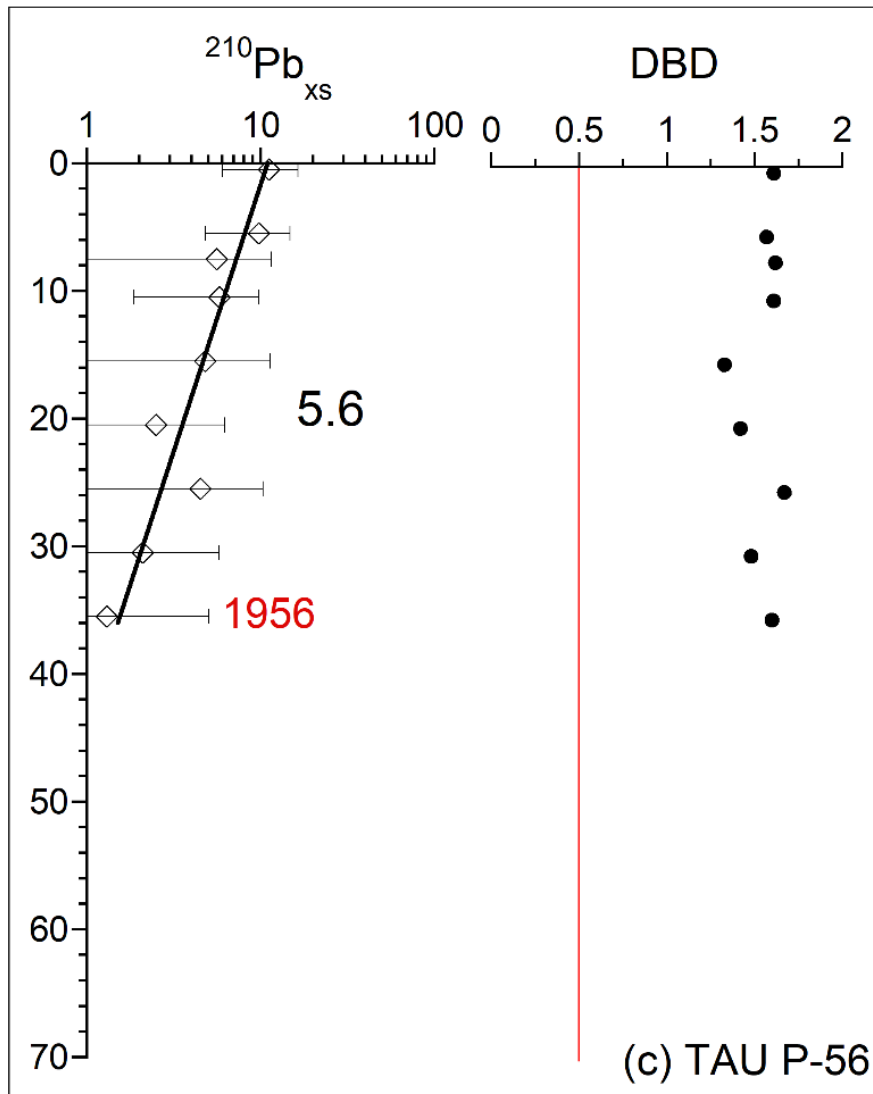

Figure 3-10: Core P-16 (Waikareao Estuary) - ages of sedient layers, sediment accumulation rates (SAR), and sediment properties. (a) Excess ^{210}Pb activity profiles with 95% confidence intervals shown. Time-averaged SAR (mm yr^{-1}, black text) derived from regression fit (r^2 = 0.24) to natural log-transformed excess ^{210}Pb data. Calculated ages of depth horizon (red text). Surface mixed layer (SML), where indicated inferred from [210]Pb$_{ex}$ (half-life = 22 yr) profiles; (b) Sediment dry bulk density profile (g cm^{-3}).
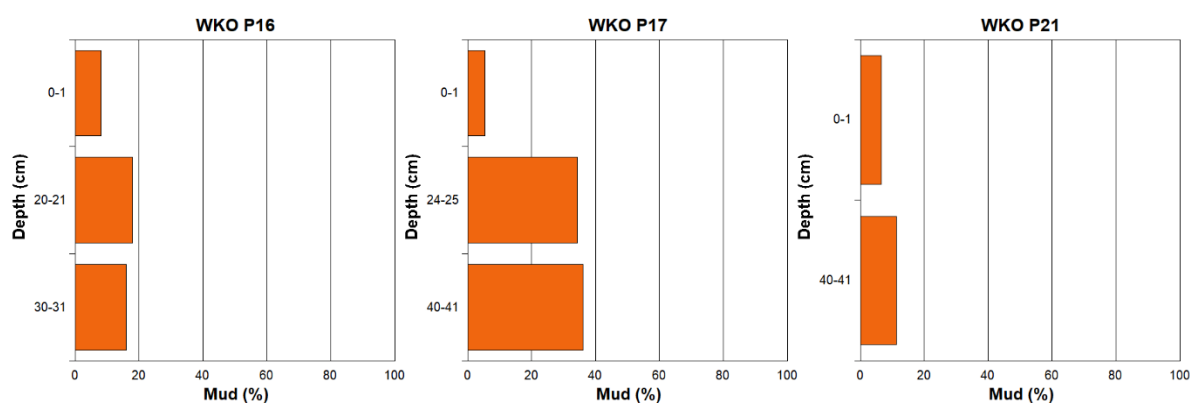
Figure 3-11: Mud content (% volume) for selected core samples, Waikareao Estuary. Particle size summary statistics are presented in Table 3-2. Note that the depth axis varies as time periods and/or particular units were targeted (surface sample, ~1988 (Bola) and base of excess Pb-210 profile), so the depth of samples varies depending on SAR.

3.2.2   Core P-17

X-radiographs for core-P-17 display a range of sediment units and structures. Sand-rich sediment (lighter grey in x-radiograph) occurs at the uppermost ~16-cm of the core with a gradational fining to more muddy sediment (i.e., darker grey) (Figure 3-12). Mixing between these two layers is indicated by abundant burrow traces, with sand-rich sediment from the upper layer infilling burrows penetrating into the underlaying mud. An abrupt transition to a cockle-shell rich sediment occurs at 50-cm depth. Dry bulk sediment densities vary between 1.2–1.4 g cm^{-3} and are highly uniform in the surface sand-rich layer (ρ_d = 1.4 g cm^{-3}). The ρ_d profile displays a parabolic behaviour through the mud unit below the upper sand layer, with a density minimum at ~30-cm depth (Figure 3-13). The sediment in core P-17 is composed of muddy very-fine to fine sand (mean: 85–190 μm, D90: 152–297 μm) with a mud content of 5–36%. Mud content increases with depth from 5% in surficial sediment (0–1 cm) to 34–36% below 24-cm (Figure 3-11,Table 3-2). The laser particle sizer A-lens (i.e., 0.6–300 μm) results show that the < 10 μm fraction (i.e., clay – very fine silt/fine silt) accounted for < 5.0% (mean: 3.26%) for that size range in the three core P-17 samples analysed. Consequently, the actual contribution of the < 10 μm fraction to the entire particle size distribution (≤ 2000 μm, very-coarse sand) will be lower. Time-average ^{210}Pb SAR at this site is 7.5 mm yr^{-1} (fit: r^2 = 0.97), over the last ~54 years (i.e., 1966–2020) and to 41-cm depth. No ^{210}Pb$_{ex}$ SML was observed (Figure 3-13).These bioturbated sediments do not preserve any evidence of muddy event deposits that could be attributed to high fluxes of fine-sediment loads associated with either the failure of the Ruahihi dam or Cyclone Bola during the 1980s.
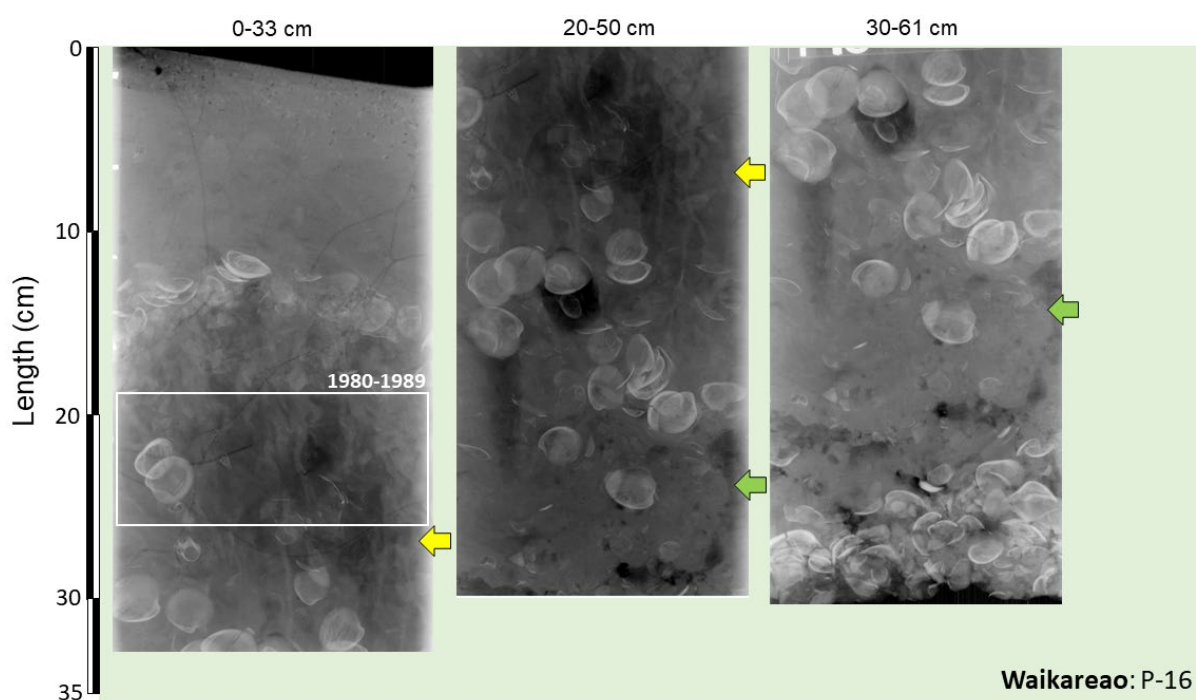
Figure 3-12:   Core P-17 (subtidal: Waikareao Estuary): 0-65 cm. The x-radiographs represent core sections up to 35-cm long, with the depth intervals indicated the top of each image. The coloured arrows indicate matching positions (i.e., depth in core) in each x-radiograph. The calculated depth range for sediment deposited in the 1980s (^{210}Pb dating) is indicated.
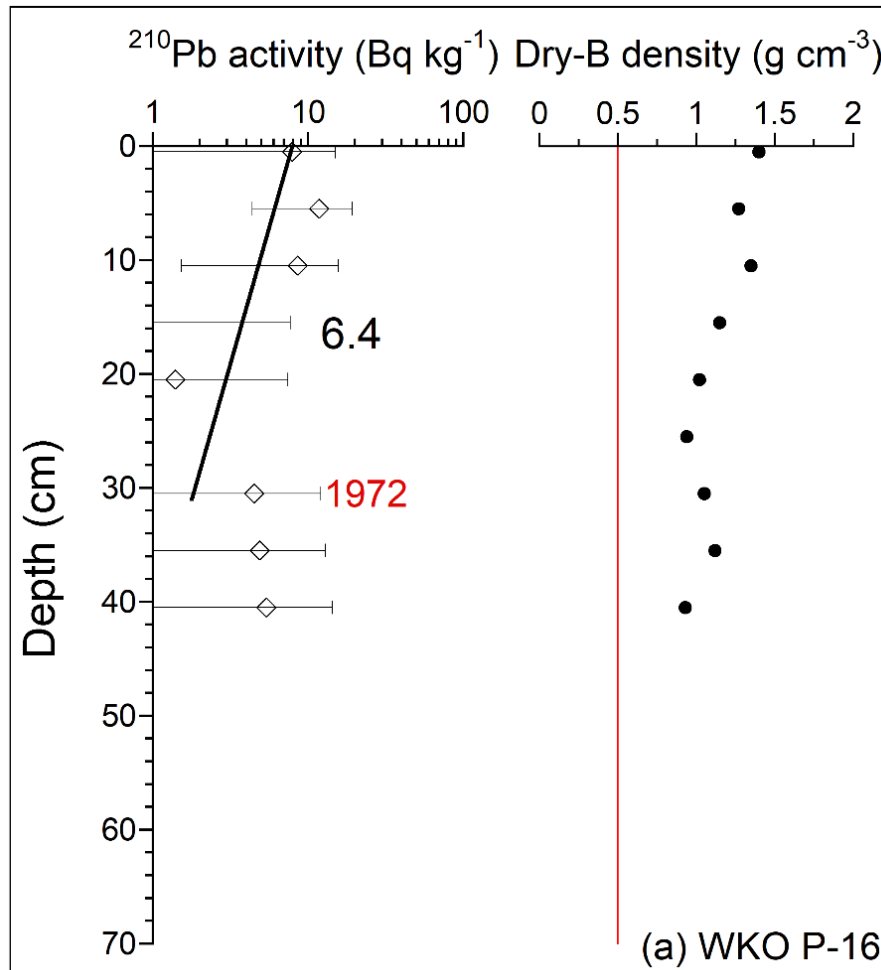
Figure 3-13: Core P-17 (Waikareao Estuary) - ages of sediment layers, sediment accumulation rates (SAR), and sediment properties. (a) Excess ^{210}Pb activity profiles with 95% confidence intervals shown. Time-averaged SAR (mm yr^{-1}, black text) derived from regression fit (r^2 = 0.97) to natural log-transformed excess ^{210}Pb data. Calculated age at the base of activity profile is shown in red text. Surface mixed layer (SML), where indicated inferred from ^{210}Pb$_{ex}$ (half-life = 22 yr) profiles; (b) Sediment dry bulk density profile (g cm^{-3}).

### 3.2.3   Core P-21

X-radiographs for sediment deposited at site P-21 display similarities with P-17. Sand-rich sediment (lighter grey in x-radiograph) occupies the top-most ~22-cm of the core with a gradation to more muddy sediment (i.e., darker grey) below that depth (Figure 3-14). Occasional cockle-shell valves occur in this layer. Again, mixing between these two layers is indicated by abundant mm-scale burrow traces. Dry bulk sediment densities in core P-21 vary between 1.1–1.5 g cm^{-3} and are relatively uniform (ρ_d ~1.5 g cm^{-3}) in the uppermost sand-rich layer to ~16 cm depth. The ρ_d gradually declines with depth through muddier sediment below the sand layer (Figure 3-15Figure 3-13). The sediment in core P-21 is composed of slightly-muddy very-fine to fine sand (mean: 116–160 μm, D90: 179–265 μm) with a mud content of 7–11% (Figure 3-11, Table 3-2). The laser particle sizer A-lens (i.e., 0.6–300 μm) results show that the < 10 μm fraction (i.e., clay – very fine silt/fine silt) accounted

for < 0.5% (mean: 0.0.32%) for that size range in the two core P-21 samples analysed. Consequently, the actual contribution of the < 10 μm fraction to the entire particle size distribution of the matrix ($\leq$ 2000 μm, very-coarse sand) will be substantially lower. The apparent ^{210}Pb SAR at this site has averaged 15.1 mm yr^{-1} (fit: r^2 = 0.46) over the last ~26 years (i.e., 1993–2020) and to 41-cm depth. No ^{210}Pb$_{ex}$ SML was observed. The depth range for sediment deposited in the 1980s could not be calculated for site P-21 as the maximum depth of the excess ^{210}Pb profile dates to the early-1990s.
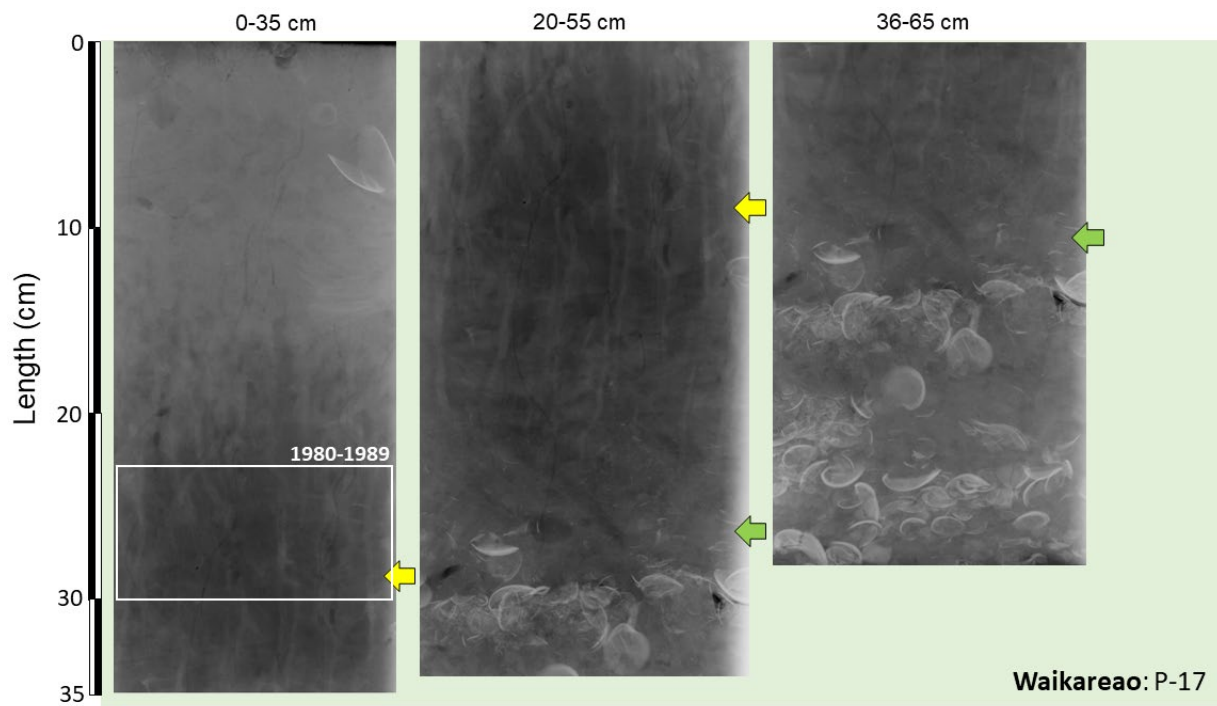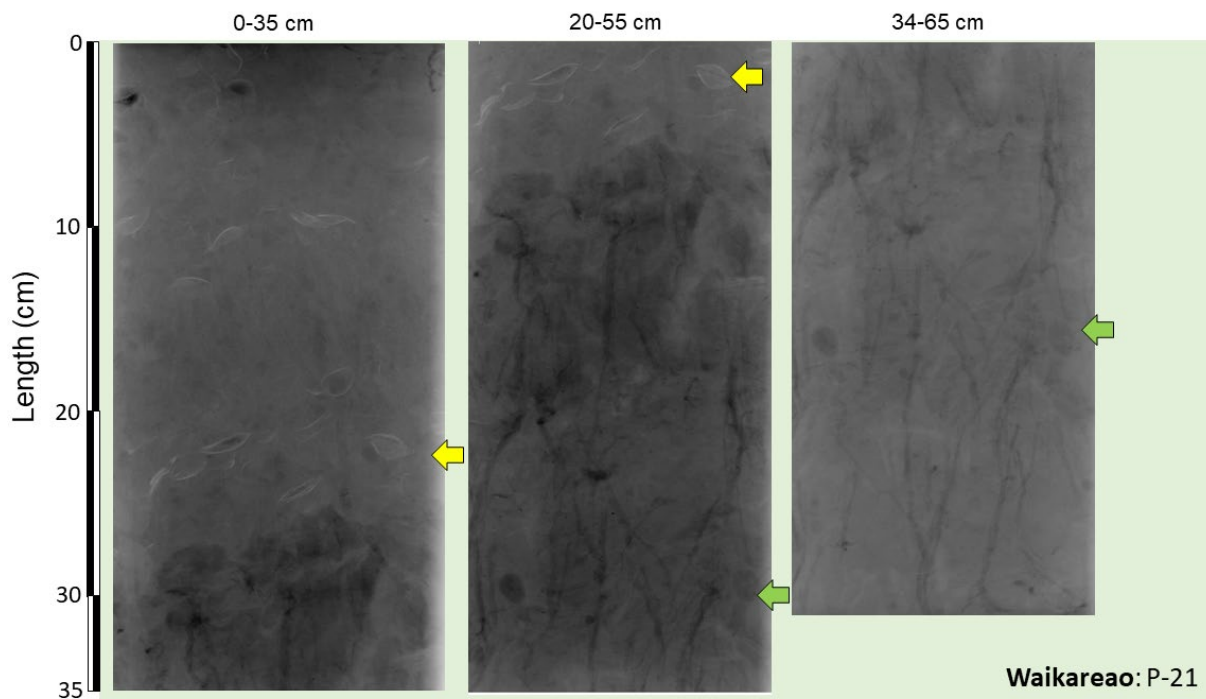

Figure 3-14:   Core P-21 (subtidal: Waikareao Estuary): 0-65 cm. The x-radiographs represent core sections up to 35-cm long, with the depth intervals indicated the top of each image. The coloured arrows indicate matching positions (i.e., depth in core) in each x-radiograph.
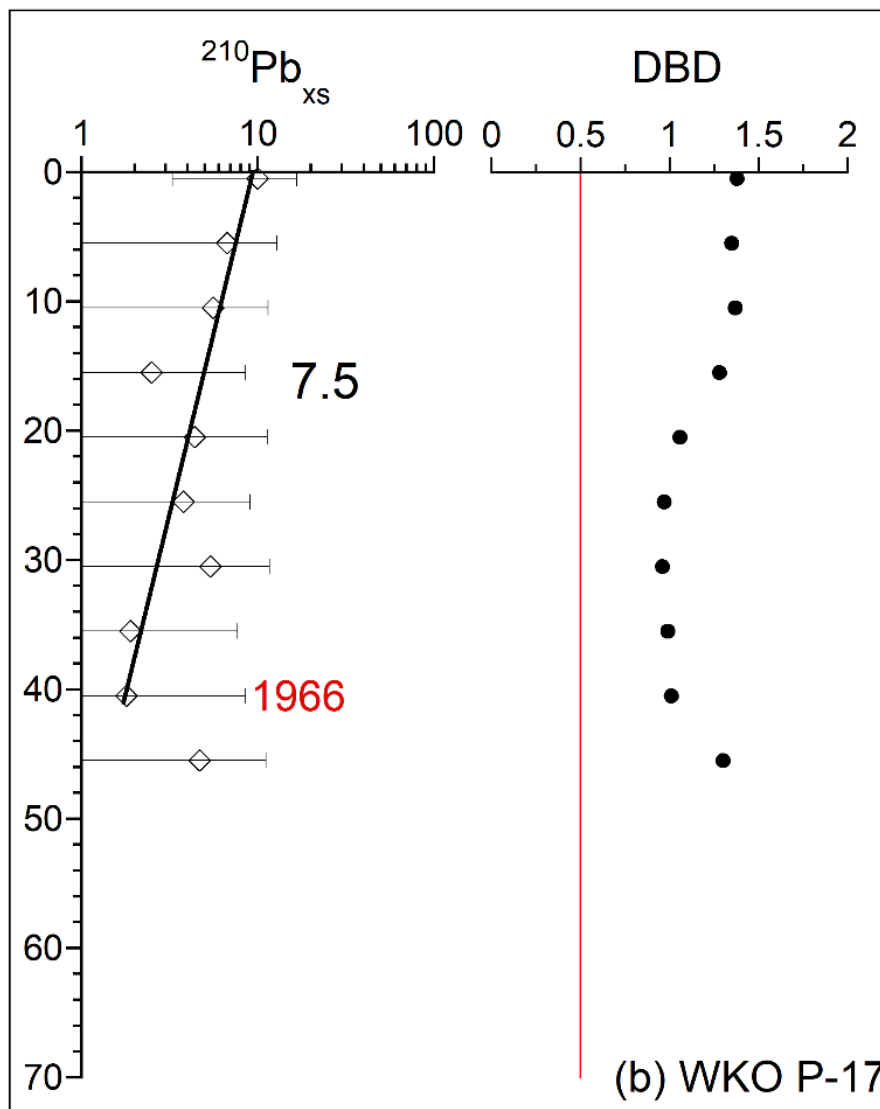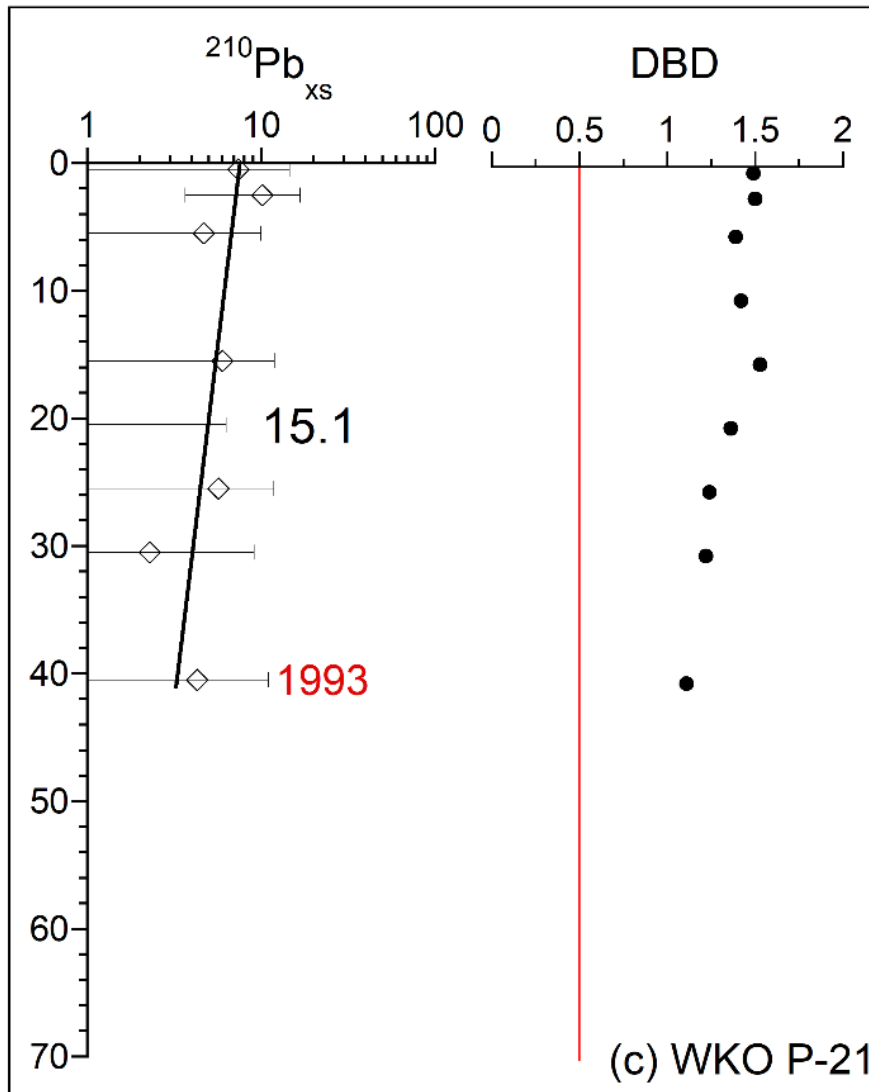
Figure 3-15: Core P-21 (Waikareao Estuary) - ages of sediment layers, sediment accumulation rates (SAR), and sediment properties. (a) Excess ^{210}Pb activity profiles with 95% confidence intervals shown. Time-averaged SAR (mm yr^{-1}, black text) derived from regression fit (r^2 = 0.46) to natural log-transformed excess ^{210}Pb data. Calculated age at the base of activity profile is shown in red text. Surface mixed layer (SML), where indicated inferred from ^{210}Pb$_{ex}$ (half-life = 22 yr) profiles; (b) Sediment dry bulk density profile (g cm^{-3}).

3.3 Sediment Cores: Waimapu Estuary

3.3.1 Core P-12

X-radiographs for core P-12 display a complex sediment fabric: large variations in sediment texture, multiple shell layers and apparent burrow traces mixing sediment between layers (Figure 3-16). Sand with mud and/or organic-rich sediment occupies the top-most ~20-cm of the core. In addition to cockle valves, this layer contains occasional large valves of the Oval Trough Clam (*Cyclomactra ovata*) and Large Wedge Shell (*Macomona liliana*) up to 4-cm in length. A contact with a ~2-cm thick cockle-shell lag occurs at the base of sand/mud layer at 21–22 cm depth (Figure 3-16). Cockle shell valves are abundant in the muddy-sands below the shell-lag layer. Dry bulk sediment densities in core P-54 vary between 1.05–1.7 g cm^{-3} but does not display a trend with depth (Figure 3-17). The sediment in core P-12 is composed of muddy very-fine to fine sand (mean: 78–152 μm, D90: 132–275 μm) with a

mud content of 12–39%. Mud content increases with depth, being 12% in the surficial sediment (0–1 cm) to 39% at 60–61-cm depth in core basal sediment (Figure 3-18,Table 3-2). The laser particle sizer A-lens (i.e., 0.6–300 μm) results show that the < 10 μm fraction (i.e., clay – very fine silt/fine silt) accounted for < 5.0% (mean: 2.6%) for that size range in the four core P-12 samples analysed. Consequently, the actual contribution of the < 10 μm fraction to the entire particle size distribution of the matrix (≤ 2000 μm, very-coarse sand) will be lower. The ^{210}Pb SAR at site P-12 has averaged 2.6 mm yr^{-1} (fit: r^2 = 0.86) over the last ~109 years (i.e., 1911–2020), within the upper 28 cm of sediment column. A ^{210}Pb$_{ex}$ SML extending to ~5-cm is apparent in the core (Figure 3-17).These bioturbated sediments do not preserve any evidence of muddy event deposits that could be attributed to high fluxes of fine-sediment loads associated with either the failure of the Ruahihi dam or Cyclone Bola during the 1980s.

Figure 3-16:   Core P-12 (subtidal Waimapu Estuary): 0-67 cm. The x-radiographs represent core sections up to 35-cm long, with the depth intervals indicated the top of each image. The coloured arrows indicate matching positions (i.e., depth in core) in each x-radiograph. The calculated depth range for sediment deposited in the 1980s (^{210}Pb dating) is indicated.

Radiocarbon dating of three cockle shell valves (*Austrovenus stutchburyi*) from three different individuals (59–63 cm depth) from the deep shell layer provided highly consistent results (Table 3-1). The 95% probability range of ^{14}C ages are very similar (i.e. 6,780–6,380 cal. yr B.P) and yielded a time-average SAR of 0.05 mm yr^{-1} below the excess ^{210}Pb layer (i.e., pre-1911).

Figure 3-17: Core P-12 (Waimapu Estuaries) - ages of sediment layers, sediment accumulation rates (SAR), and sediment properties. (a) Excess ^{210}Pb activity profiles with 95% confidence intervals shown. Time-averaged SAR (mm yr^{-1}, black text) derived from regression fit (r^2 = 0.86) to natural log-transformed excess ^{210}Pb data. Calculated age at the base of activity profile is shown in red text. Surface mixed layer (SML), where indicated inferred from ^{210}Pb$_{ex}$ (half-life = 22 yr) profiles; (b) Sediment dry bulk density profile (g cm^{-3}). Background SAR for ~6,500-year period (AMS ^{14}C dating of cockle shell valves) prior to the early-1900s shown.
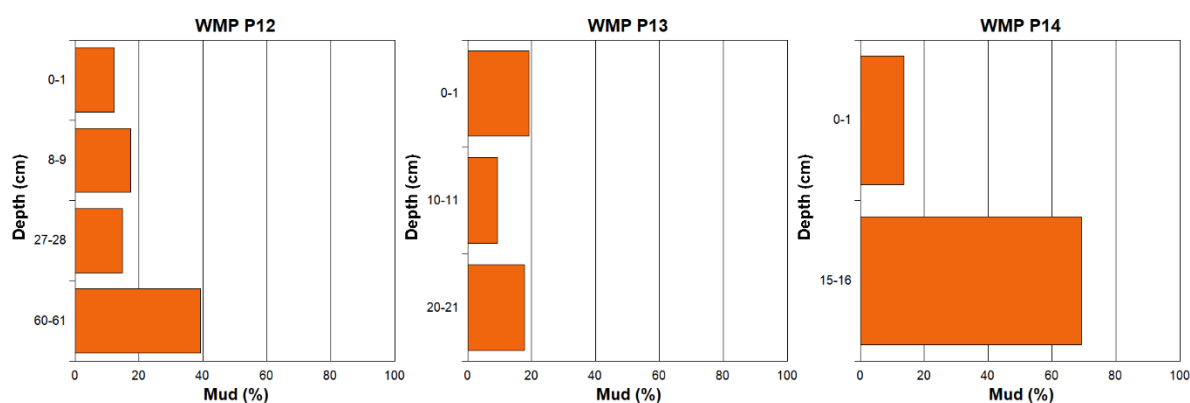
Figure 3-18: Mud content (% volume) for selected core samples, Waimapu Estuary. Particle size summary statistics are presented in Table 3-2. Note that the depth axis varies as time periods and/or particular units were targeted (surface sample, ~1988 (Bola) and base of excess Pb-210 profile), so the depth of samples varies depending on SAR.

3.3.2   Core P-13

The x-radiographs from cores P-13 and P-12 are similar, displaying a complex sediment fabric: large variations in sediment texture, multiple shell layers and apparent burrow traces mixing sediment between layers (Figure 3-19). Sand with mud and/or organic-rich sediment occupies the top ~18-cm of the core. This layer contains occasional cockle shell valves. A contact between a thick cockle-shell layer to 40-cm in a muddy-sand matrix occurs below the upper sand/mud layer. Muddy sand characterises the core below this depth. Dry bulk sediment densities vary between 0.7–1.5 g cm^{-3} and rapidly decrease from 1.3 g cm^{-3} below 18-cm depth (Figure 3-20). The sediment in core P-13 is composed of muddy very-fine to fine sand (mean: 108–153 μm, D90: 174–263 μm) with a mud content of 9–19%. Mud content is highest in the surficial (0-1-cm 19%) and at 20–21-cm depth (18%) (Figure 3-18,Table 3-2). The laser particle sizer A-lens (i.e., 0.6–300 μm) results show that the < 10 μm fraction (i.e., clay – very fine silt/fine silt) accounted for < 2.3% (mean: 1.4%) for that size range in the three core P-13 samples analysed. Consequently, the actual contribution of the < 10 μm fraction to the entire particle size distribution of the matrix (≤ 2000 μm, very-coarse sand) will be substantially lower. The ^{210}Pb SAR at this site has averaged 3.2 mm yr^{-1} (fit: r^2 = 0.83) over the last ~66 years (i.e., 1954–2020), in the upper 21 cm of the sediment column (Figure 3-20). A ^{210}Pb$_{ex}$ SML was indicated to ~4-cm depth, although this was not supported by the ρ_d profile, which declined in this layer. Excluding the top-most ^{210}Pb$_{ex}$ datapoint increased the SAR to 4.3 mm yr^{-1} but resulted in a substantially poorer regression fit (r^2 = 0.63).

These bioturbated sediments do not preserve any evidence of muddy event deposits that could be attributed to high fluxes of fine-sediment loads associated with either the failure of the Ruahihi dam or Cyclone Bola during the 1980s.
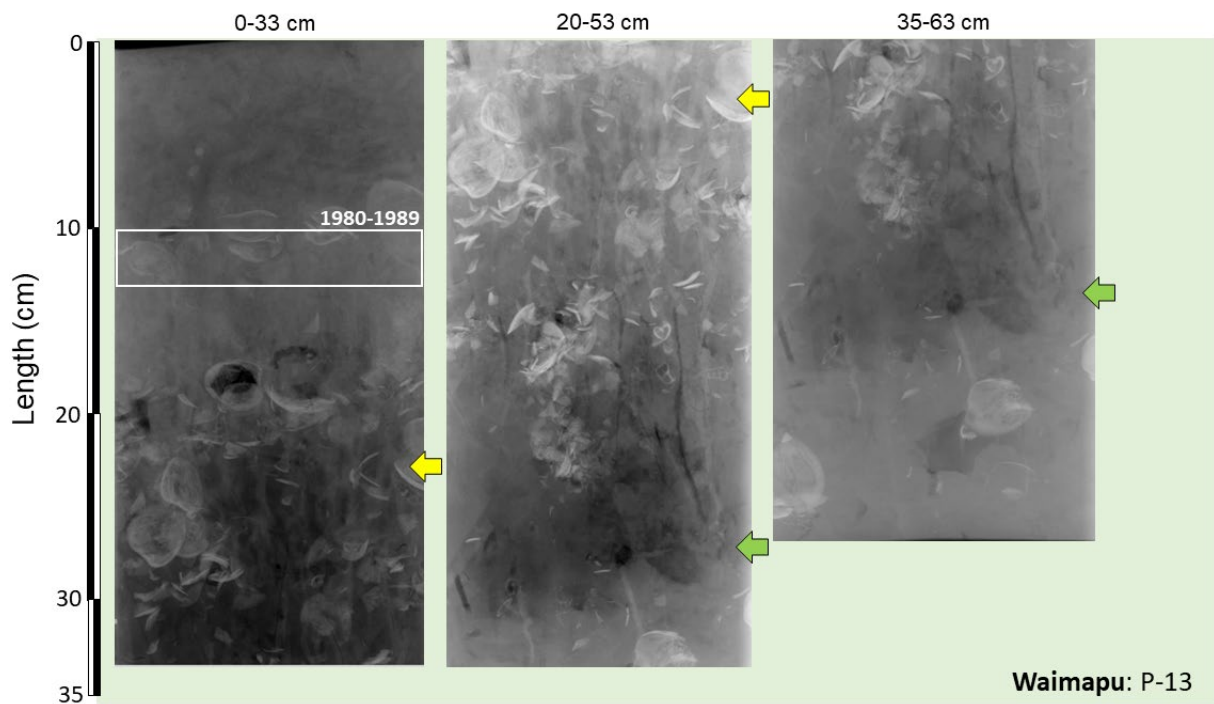
Figure 3-19: Core P-13 (subtidal: Waimapu Estuary): 0-63 cm. The x-radiographs represent core sections up to 35-cm long, with the depth intervals indicated the top of each image. The coloured arrows indicate matching positions (i.e., d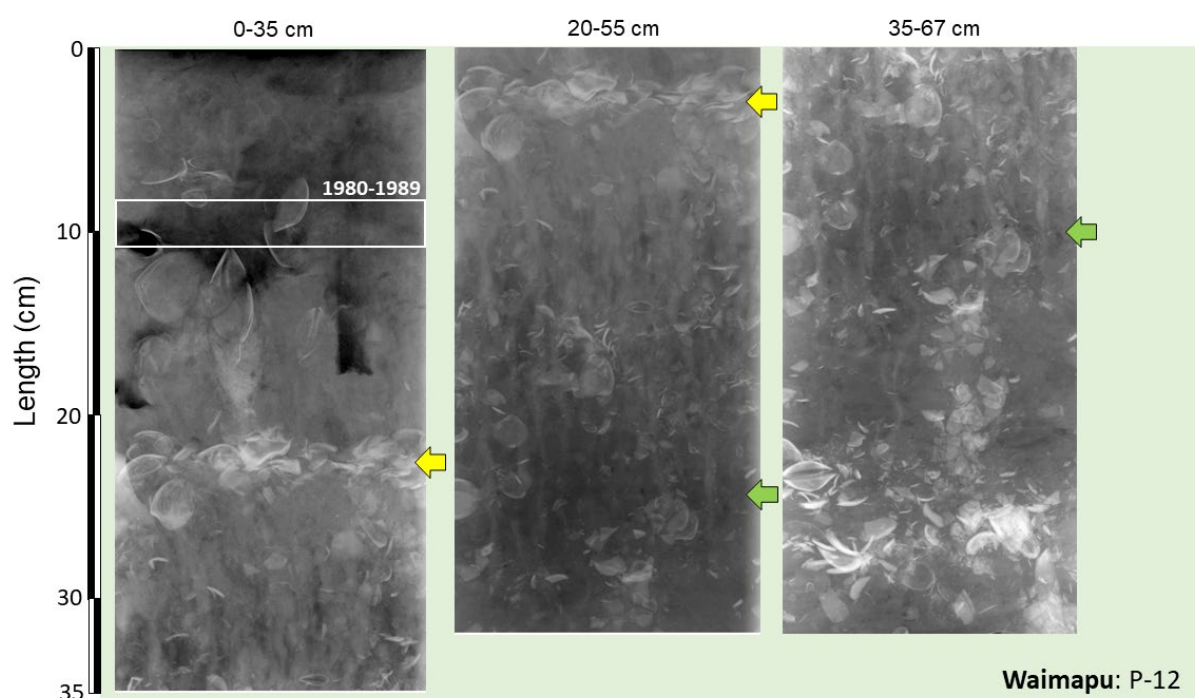epth in core) in each x-radiograph. The calculated depth range for sediment deposited in the 1980s (^{210}Pb dating) is indicated.
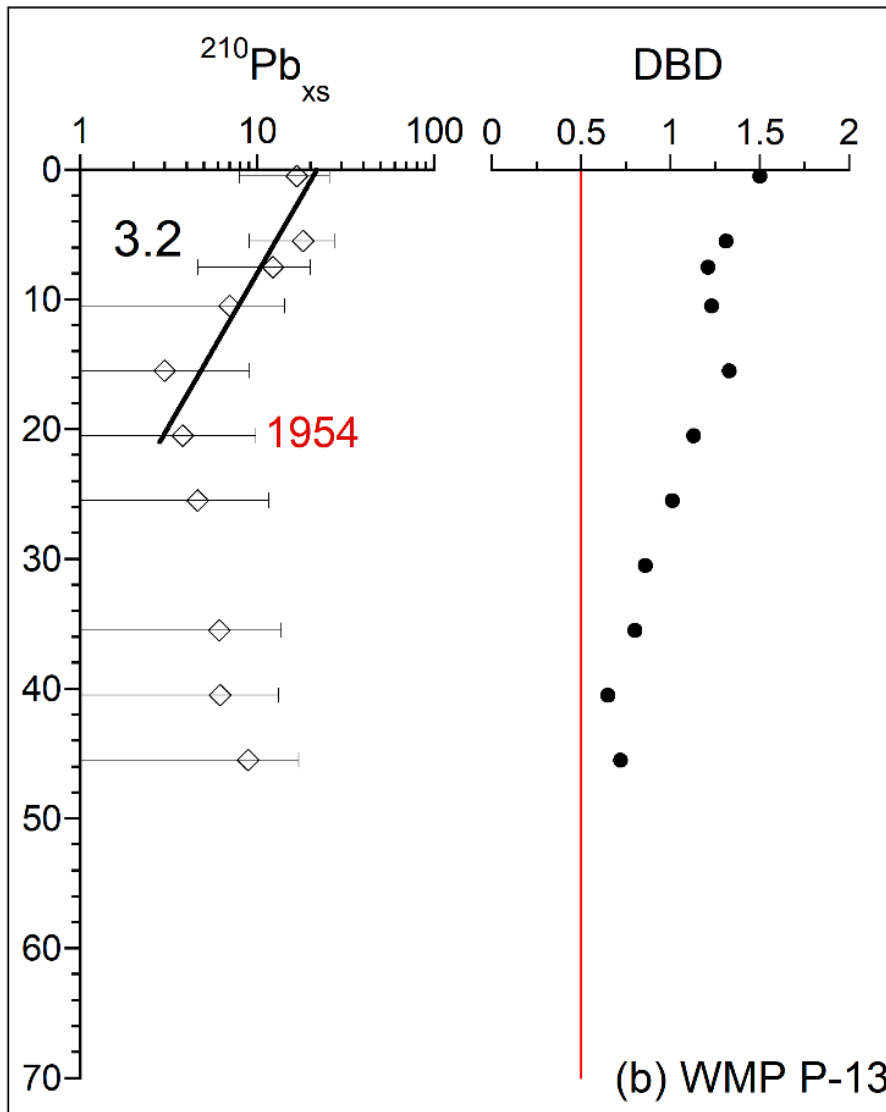
Figure 3-20: Core P-13 (Waimapu Estuary) - ages of sediment layers, sediment accumulation rates (SAR), sediment properties. (a) Excess ^{210}Pb activity profiles with 95% confidence intervals shown. Time-averaged SAR (mm yr^{-1}, black text) derived from regression fit (r^2 = 0.83) to natural log-transformed excess ^{210}Pb data. Calculated age at the base of activity profile is shown in red text. Surface mixed layer (SML), where indicated inferred from ^{210}Pb$_{ex}$ (half-life = 22 yr) profiles; (b) Sediment dry bulk density profile (g cm^{-3}).

3.3.3 Core P-14

X-radiographs of core-P14 show a range of sediment fabrics, with a surface layer of sand to ~9-cm capping sandy mud at depth. Occasional large cockle-shell valves and gastropods (screw shells) are dispersed throughout the core (Figure 3-21). Dry bulk densities (1.3 g cm^{-3}) are uniform in the top 6-cm of the core, then decline smoothly to 0.8 g cm^{-3} at 20-cm depth, then gradually increase to   1 g cm^{-3} at 50-cm depth. The sediment in core P-14 is composed of very-muddy very-fine sand (mean: 53–130 μm, D90: 86–228 μm) with a mud content of 14–69%. Mud content in the surficial sediment (0–1 cm) is 14% and 69% at 15–16-cm depth (Figure 3-18,Table 3-2). The laser particle sizer A-lens (i.e., 0.6–300 μm) results show that the < 10 μm fraction (i.e., clay – very fine silt/fine silt) accounted for < 9.8% (mean: 5.8%) for that size range in the two core P-14 samples analysed. The surficial (0-1 cm) sample contained < 2% in the < 10 μm fraction whereas this accounted for 9.8% of the sample at 15–16-cm depth. The actual contribution of the < 10 μm fraction to the entire particle size distribution (≤ 2000 μm, very-coarse sand) will be lower. The ^{210}Pb SAR at this site has averaged 6.2 mm yr^{-1} (fit: r^2 = 0.63) over the last ~26 years (i.e., 1994–2020), in the upper 16 cm of sediment column. A shallow ^{210}Pb$_{ex}$ SML (0–4-cm) is indicated by the ^{210}Pb$_{ex}$ and bulk density profiles (Figure 3-22). The depth range for sediment deposited in the 1980s could not be calculated for site P-14 as the maximum depth of the excess ^{210}Pb profile dates to the early-1990s.
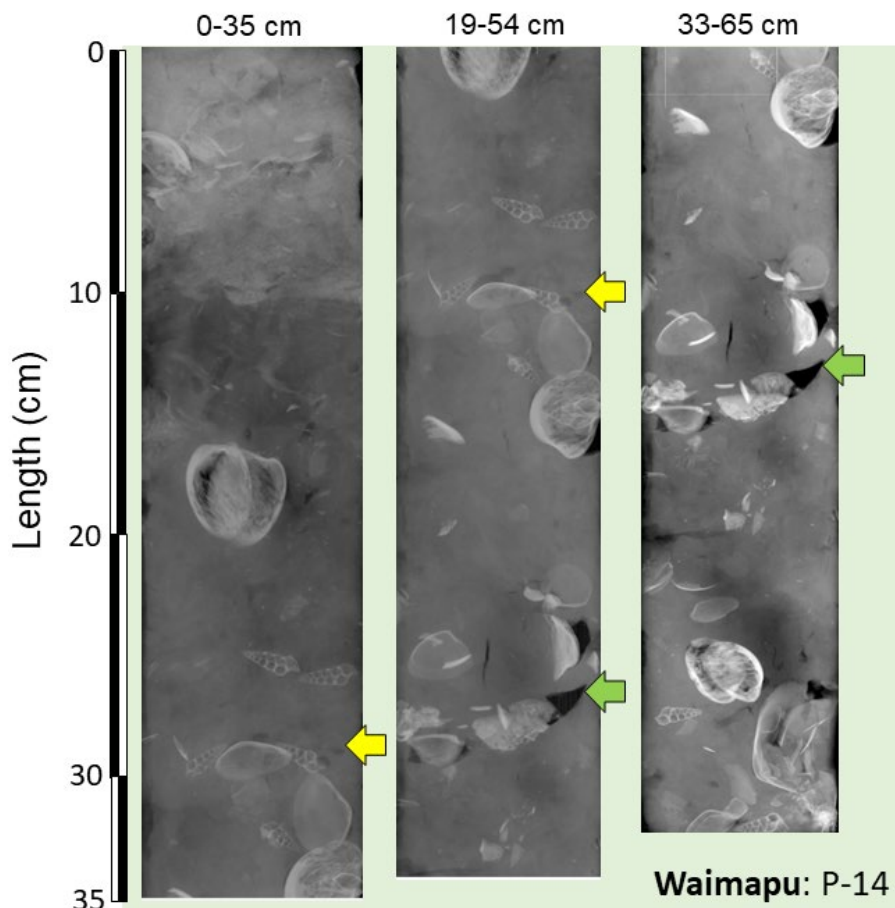
Figure 3-21:   Core P-14 (subtidal: Waikareao Estuary): 0-63 cm. The x-radiographs represent core sections up to 35-cm long, with the depth intervals indicated the top of each image. The coloured arrows indicate matching positions (i.e., depth in core) in each x-radiograph.
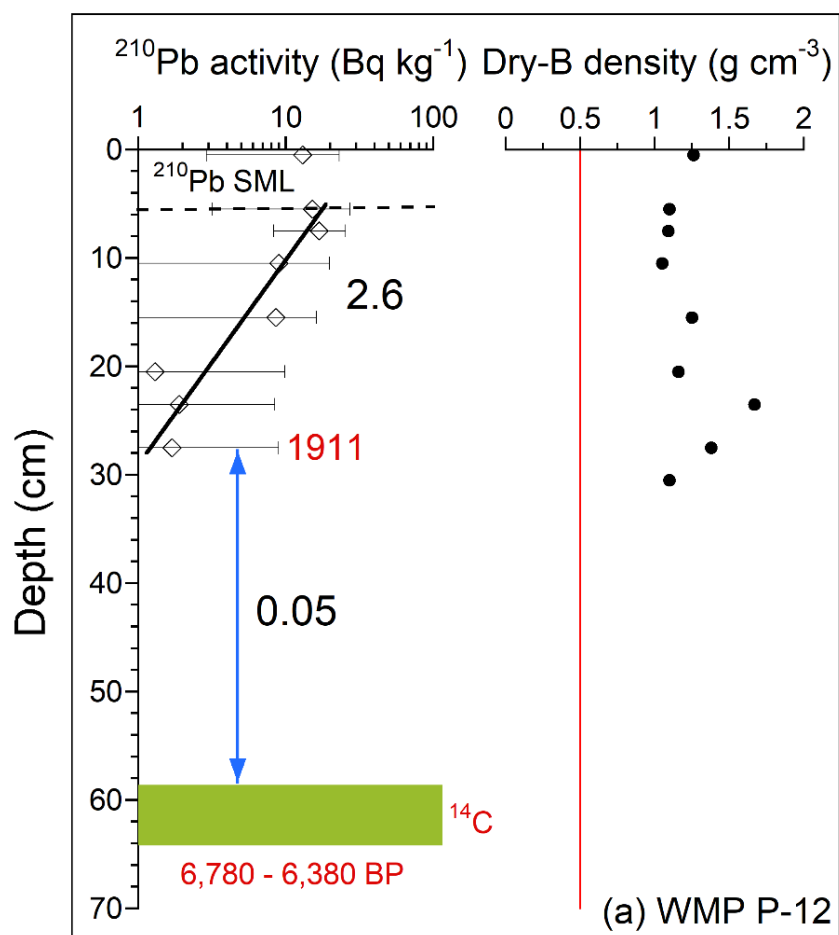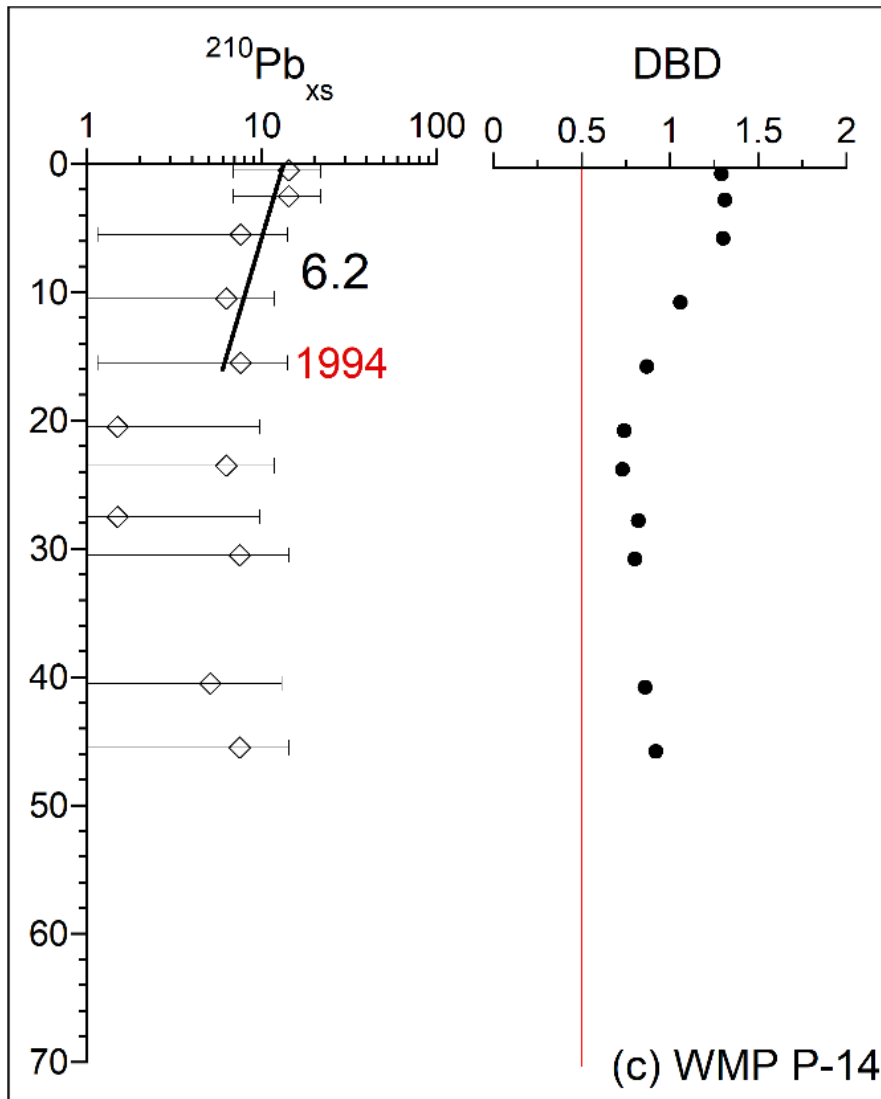
Figure 3-22: Core P-14 (Waimapu Estuary) - ages of sediment layers, sediment accumulation rates (SAR), and sediment properties. (a) Excess ^{210}Pb activity profiles with 95% confidence intervals shown. Time-averaged SAR (mm yr^{-1}, black text) derived from regression fit (r^2 = 0.63) to natural log-transformed excess ^{210}Pb data. Calculated age at the base of activity profile is shown in red text. Surface mixed layer (SML), where indicated inferred from ^{210}Pb$_{ex}$ (half-life = 22 yr) profiles; (b) Sediment dry bulk density profile (g cm^{-3}).

3.4 Particle-size summary statistics

The particle size statistics for each sediment core are summarised in Table 3-2. These data relate to the analysis of the sediment matrix (i.e., < 2000 μm fraction) and does not account for the modest to minor biogenic gravel fraction of preserved shell hash and whole valves captured in the cores.

Table 3-2: **Particle-size statistics summary.** Eyetech laser particle sizer B-lens data (range: 10–2000 mm) for cores collected at monitoring sites in Tuapiro, Waikareao and Waimapu Estuaries.

Estuary	Site	Depth (cm)	210Pb Year	Mean Size (μm)	Median (D50)	Standard Deviation	D90	Mud (<62.5 μm) (%)
Tuapiro	**TUA P54**	**0-1**	**2019**	**170.2**	**168.2**	**67.1**	**264.6**	**4.4**
Tuapiro	TUA P54	10-11	2000	175.9	146.1	121.4	278.6	4.3
Tuapiro	TUA P54	17-18	1988	142.2	131.0	60.5	224.0	6.0
Tuapiro	TUA P54	25-26	1971	119.7	116.0	46.8	181.1	9.9
Tuapiro	**TUA P55**	**0-1**	**2019**	**124.7**	**113.6**	**58.2**	**218.3**	**14.2**
Tuapiro	TUA P55	14-15	1988	122.9	120.6	49.4	202.0	11.1
Tuapiro	TUA P55	35-36	1940	113.0	113.6	48.3	185.7	16.9
Tuapiro	TUA P55	62-63	N/A	85.7	82.3	36.9	141.5	30.8
Tuapiro	**TUA P56**	**0-1**	**2019**	**150.7**	**137.0**	**64.2**	**256.9**	**5.1**
Tuapiro	TUA P56	17-18	1988	114.6	111.3	47.7	185.7	13.1
Tuapiro	TUA P56	35-36	1956	182.7	182.3	68.1	276.5	3.5
Waikareao	**WKO P16**	**0-1**	**2019**	**137.2**	**131.1**	**56.0**	**220.6**	**8.1**
Waikareao	WKO P16	20-21	1988	122.8	124.1	56.3	198.4	18.0
Waikareao	WKO P16	30-31	1972	126.5	119.5	60.6	218.3	16.0
Waikareao	**WKO P17**	**0-1**	**2019**	**190.1**	**171.8**	**114.2**	**297.3**	**5.4**
Waikareao	WKO P17	24-25	19888	90.0	85.7	45.1	152.0	34.4
Waikareao	WKO P17	40-41	1966	85.3	74.2	44.2	159.1	36.2
Waikareao	**WKO P21**	**0-1**	**2020**	**160.0**	**146.2**	**70.4**	**264.8**	**6.5**
Waikareao	WKO P21	40-41	1993	116.2	113.6	42.8	178.7	11.2
Waimapu	**WMP P12**	**0-1**	**2020**	**146.5**	**140.5**	**71.0**	**253.3**	**12.3**
Waimapu	WMP P12	8-9	1988	137.6	119.4	72.8	242.6	17.3
Waimapu	WMP P12	27-28	1911	151.6	139.2	81.5	275.2	14.9
Waimapu	WMP P12	60-61	N/A	77.8	75.3	35.6	132.2	39.2
Waimapu	**WMP P13**	**0-1**	**2019**	**108.1**	**106.7**	**46.1**	**174.1**	**19.1**
Waimapu	WMP P13	10-11	1988	152.7	141.6	72.3	262.6	9.4
Waimapu	WMP P13	20-21	1954	144.9	135.8	79.5	259.1	17.8
Waimapu	**WMP P14**	**0-1**	**2019**	**129.5**	**113.6**	**65.3**	**227.6**	**13.6**
Waimapu	WMP P14	15-16	1994	52.8	49.7	22.7	85.7	69.2

As described for the individual cores (sections above), the particle size data and x-radiographs do not indicate a clearly identifiable mud-rich deposit that could readily be attributable to the failure of the Ruahihi Power Station dam (1981) or Cyclone Bola (March 1988) event has been preserved in the cores.

4 Discussion

4.1 Sediment accumulation rates – spatial patterns

Mapping the apparent ^{210}Pb SAR measured in the sediment cores reflects differences in conditions and resulting sedimentation patterns in the three estuaries (Figure 4-1). The range of SAR measured in Tuapiro Estuary (i.e. 4.5–5.6 mm yr^{-1}) are relatively narrow, which suggests that physical conditions are relatively uniform across the intertidal flats. Key factors controlling local sediment accumulation rate include hydroperiod (i.e., duration of tidal submergence), sediment settling flux and resuspension (i.e., by tidal currents and wind waves) that controls net deposition.

By contrast, a large difference in ^{210}Pb SAR is observed in the Waikareao Estuary, between the bay west of Motuopae (Peach) Island (15 mm yr^{-1}) and core sites located in the main body of the estuary (i.e., 6.4 and 7.5 mm yr^{-1}). This two-fold difference in SAR most likely reflects difference in wind-wave exposure between the sites, with winnowing of fine sediment more pronounced at the southern sites. The Waimapu Estuary sites show a north to south decrease in SAR between the three cores sites from 6.2 to 2.6 mm yr^{-1} (Figure 4-1), so that sedimentation actually occurs at a lower rate near the catchment outlet.

These sedimentation patterns observed across these three estuaries reflect the sediment transport processes that characterise shallow fetch-limited estuaries. Wave-driven sediment resuspension, fine-sediment winnowing and transport in particular. In the western Bay of Plenty, the common occurrence of northerly sea breezes during the summer that penetrate inland (i.e., 20–30 km hr^{-1}, Chappell, 2013) seasonally influence wave climate and sediment resuspension in these fetch-limited and shallow intertidal estuaries. In these infilled intertidal systems, waves are controlled by daily tidal fluctuations in water levels. During the short window over several hours either side of high tide, small short-period waves generated by the wind become more energetic with down fetch distance (e.g., Swales et al., 2004), whereas the upwind lee-shore is sheltered.

This process of wave growth interacts with (bed) frictional dissipation of waves as the propagate across the intertidal flats. These small estuarine waves (typically less than 0.3 m high and 2–3 s. period), are highly effective at resuspending mud in shallow intertidal waters. This process of wind-wave growth generates the so-called "turbid fringe" in estuaries that migrates up and down the intertidal zone with the flooding and ebbing tides (Green and Coco, 2014). Once resuspended, these fine sediments are transported by wind-driven currents and ebb tides into channels. In turn these sediments are either exported to the sea or deposited in fringing mangrove and salt mash where quiescent conditions favour settling out of suspension and deposition. The low mud content of surficial sediment observed in the cores reflects this winnowing process of fine sediment by wind waves.
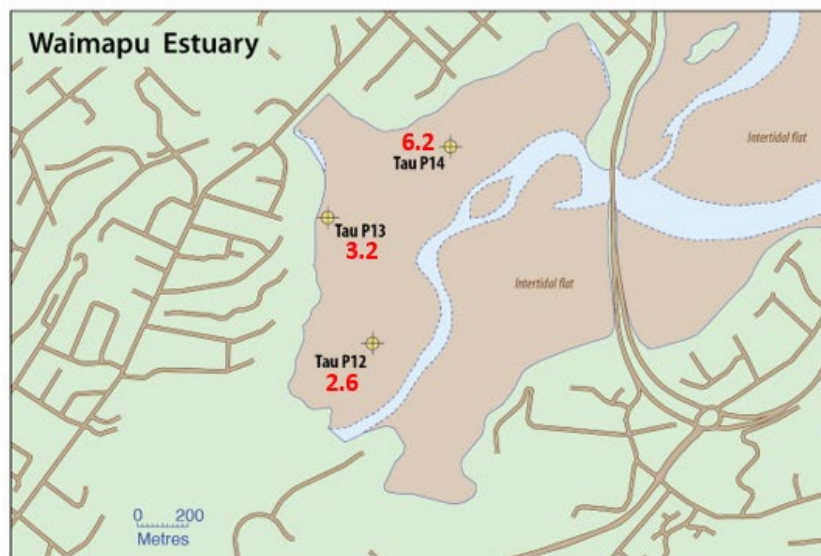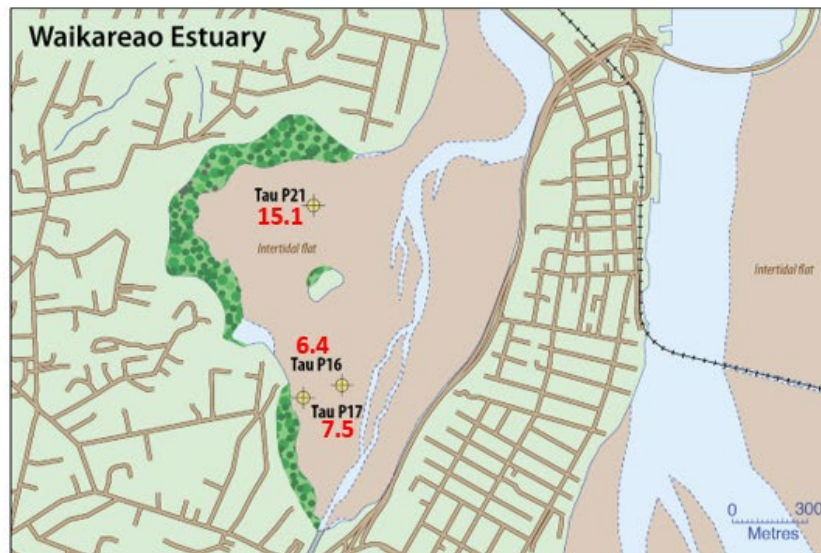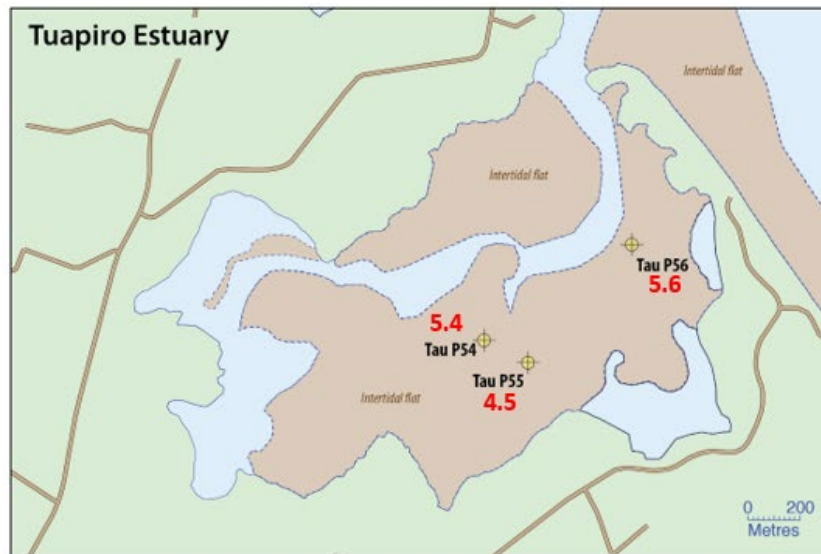
Figure 4-1: Spatial patterns in SAR in the Tuapiro, Waikareao and Waimapu Estuaries.

4.2   Changes in sediment accumulation rates

Lead-210 dating indicates that sediment accumulation rates (SAR) in Tuapiro, Waikareao and Waimapu Estuaries have averaged between **2.6–15.1 mm yr^{-1}** (overall average: 5.3 mm yr^{-1}) since the early-1900's. These ^{210}Pb SAR are similar to values obtained for several estuaries near Tauranga City (1.3–7.2 mm yr^{-1} over 70–90 years, Hancock et al., 2009). In Waikaraka Estuary, Stokes (2010) calculated a ^{210}Pb SAR of 2.3 mm yr^{-1} (1950–1990). The ^{10}Pb SAR measured in the present study are also of a similar order to modelled values for present-day land-use scenarios in the Waimapu (4.8 mm yr^{-1}) and Waikareao (2 mm yr^{-1}) Estuaries (Green, 2010).

The ^{210}Pb SAR measured in these Tauranga Harbour estuaries are **at least fifty-fold higher** than time-average SAR over the previous ~7,000 years (i.e., **0.05 mm yr^{-1}**) calculated from radiocarbon dating of cockle shell obtained from Tuapiro and Waimapu Estuary cores (Section 3). An **order of magnitude increase in SAR above background values** is more typical of NZ estuaries (e.g., Thrush et al., 2004; Hunt, 2019 and references therein). Stokes (2010) obtained a similar ^{14}C SAR of 0.1 mm yr^{-1} (cockle shell) for a core from Waikaraka Estuary (Tauranga Harbour). These background SAR values for the study estuaries are some of the lowest measured in a number of NZ estuaries (range: 0.04–1.2 mm yr^{-1}, Figure 4-2).

A limitation of the sediment core dating in the present study is the absence of ^{137}Cs that is typically used to validate the ^{210}Pb geochronology. This is not a typical situation in New Zealand estuaries where cores have analysed and suggest that a regional process has limited atmospheric deposition of ^{137}Cs. In general, ^{137}C dating can be problematic due to: (1) decreasing ^{137}C activity associated with radioactive decay (half-life = 30 yr); (2) uncertainty in what time horizon the maximum ^{137}Cs penetration depth in sediment cores represents. ^{137}Cs deposition in New Zealand was first detected in 1952, with peak deposition in 1963/1964 (Matthew, 1989). The 1963/64 ^{137}Cs peak is not commonly observed in NZ estuaries due to contributions of ^{137}Cs-labelled eroded soils. Instead, maximum ^{137}C depth is use as a marker/time horizon. It is also unlikely that ^{137}Cs deposited in the early 1950s is still detectable so that the maximum penetration depth measured in a core represents a time horizon sometime between 1952 and the 1963/64 peak. Despite the absence of ^{137}C in the Tauranga cores, there is general agreement with SAR estimates from other studies (2–4.8 mm yr-1 [Green, 2010], 1.3–7.2 [Hancock et al., 2009]).

Estuary-average ^{210}Pb SAR compiled from NIWA studies of some 30 New Zealand estuaries enables the sedimentation of these Tauranga Harbours estuaries to be considered in a wider context. These studies have primarily been undertaken for Regional Councils over the last ~20 years and includes data from 128 cores. These SAR have been measured using the same methods (^{210}Pb with ^{137}Cs validation). The estuary-average ^{210}Pb SAR values for the study estuaries are time-weighted values based on ^{210}Pb record length (range: 26–109 years). Waikareao core P-16 was excluded from the assessment due to the poor ^{210}Pb$_{ex}$ profile regression fit (i.e., r^2 = 0.24). This weighting procedure aims to reduce the influence of outliers. In the present study, the ^{210}Pb SAR Waikareao P-21 has a ^{210}Pb SAR of 15.1 mm yr^{-1} but over a short time period between 1993–2020.

The overall weighted-average SAR for the study estuaries is **5.2 mm yr^{-1}** (Figure 4-2) and 4.6 mm yr^{-1}, excluding core P-21. Excluding P-21 does not change the rank-order (i.e., highest) of these Tauranga Harbour estuaries in the comparison with other NZ estuaries. The 5.2 mm yr^{-1} estuary-average SAR is **at least five-fold higher** than measured on intertidal flats in Tauranga Harbour (1 mm yr^{-1} [3 cores sites] data: Hancock et al.,2009) and model predictions that indicate no long-term accumulation of fine sediment in the main body of Tauranga Harbour, south of Matahui Point (0 mm yr^{-1}, Figure 4.5

Green, 2010). Comparison with the NZ estuaries database shows that the estuary-average SAR in the **Tauranga estuaries of 5.2 mm yr⁻¹ is 2 mm yr⁻¹ higher than the average** rates in NZ estuaries (**3.2 mm yr⁻¹**) for which NIWA have available data.
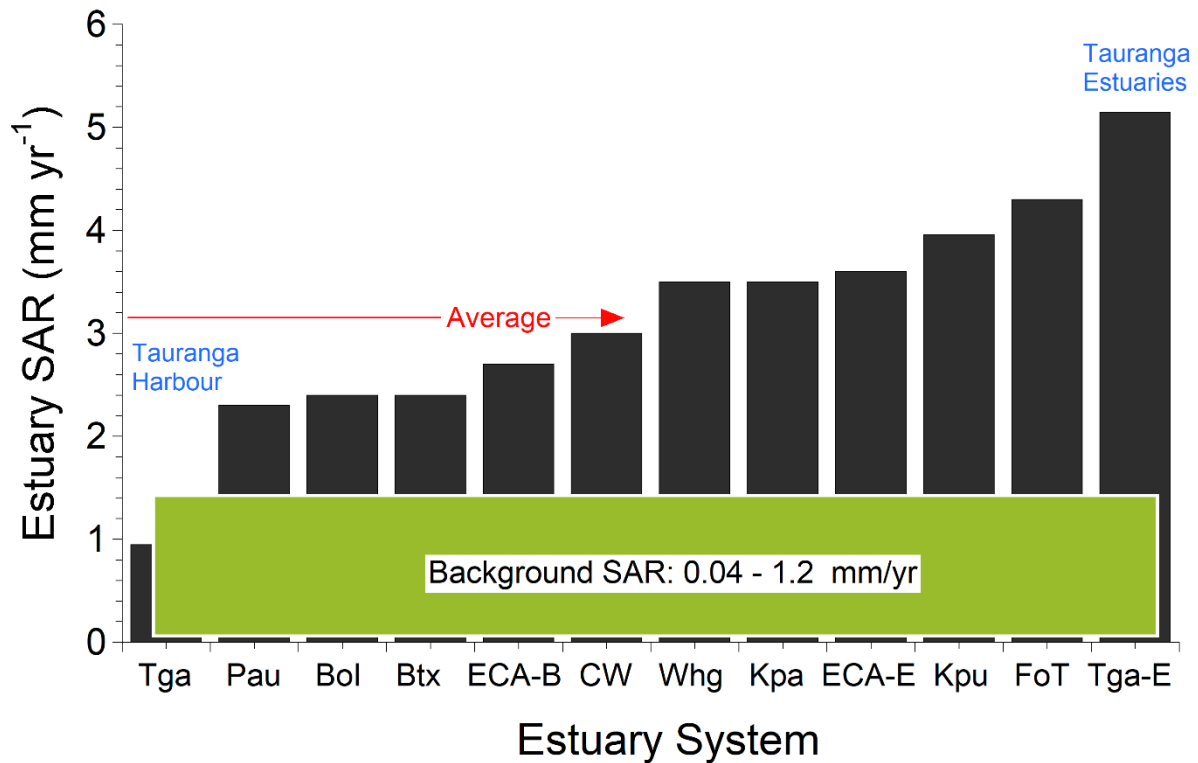
Figure 4-2:   Distribution of estuary-average sediment accumulation rates (SARe) in NZ estuaries over the last 26 to 130 years.   Lead-210 SAR values for individual cores weighted by record length (years) and averaged across core sites to calculate an estuary-average SAR value. The average SARe value across all estuaries included in this comparison is 3.2 ± 1.1 mm yr⁻¹ (±1 SD). Background SAR are based on radiocarbon (14C) dating of cockle shell preserved in cores and span the 2,000 –10,000 years prior to the early 1900s. Key: Tauranga Harbour (Tga), Pauatahanui (Pau), Bay of Islands (BoI), Beatrix Bay (Btx), Auckland East-Coast Embayments (ECA-B), Central Waitemata Harbour (CW), Whangarei (Whg), Kaipara (Kpa), Auckland East-Coast Estuaries (ECA-E), Kenepuru (Kpu), Firth of Thames (FoT) and Tauranga Estuaries (Tga-E). Source: NIWA studies.

4.3   Comparison with BoPRC sediment accretion data

Bay of Plenty Regional Council monitor sediment accretion at 65 intertidal sites in Tauranga Moana, including the study estuaries as one facet of the regions Estuarine Health Monitoring Programme. Sediment accretion rates at these sites have been measured approximately seasonally using buried plates since late-2013. Changes in the vertical position of the substrate relative to the buried plate are determined by multiple randomly located measurements of the depth to the plate using a pin gauge. In Tauranga Moana, sediment accretion monitoring was initiated in December 2013 and surveys were conducted 3–5 times per year until November 2020.

Short-term **sediment accretion** measurements such as those made with buried plates quantify variations in the vertical position of the intertidal flat substrate surface relative to a buried plate due to cycles of sediment deposition and erosion over characteristic time scales of months to years. By contrast, **sediment accumulation rates** (SAR) calculated from sediment cores integrate the long-term impact of cumulative short-term (annual-to-centennial or longer time scales) effects, such as erosion

and deposition cycles that occur at event or seasonal time scales. Comparison of these two types of measurements can provide insights into the processes controlling estuary sedimentation. Figure 4-3 presents the time-series data for each of the study estuaries.

The sediment accretion data display considerable variability at most sites and annual minima occur across seasons. This suggests that tidal-flat erosion and accretion is driven by storm events where wind and rainfall are enhanced, which may occur across the year. Between-survey changes in bed level vary considerably, from -14 to +13 mm (Tuapiro), -16 to +18 mm (Waikareao) and -13 to +16 mm (Waimapu). The time-series plots and these summary statistics indicate that the Waikareao Estuary is a particularly energetic system. Positive accretion trends occur at 7 of the 9 sites, although correlations are only significant at two sites (Tuapiro Estuary, r^2 = 0.65, 0.73, P < 0.001, Figure 4-3). Here, net sediment accretion rates are 2.3 and 3.1 mm yr^{-1}, which are ~50% of the long-term ^{210}Pb SAR values at these two sites. The high variability and low apparent accretion or even erosion at most sites suggest that there was no net sediment accretion at these intertidal sites over the seven-year measurement period. This interpretation is seemingly at odds with the SAR values determined by sediment core dating. This likely reflects winnowing of fine sediment from the intertidal substrate, driven by resuspension by waves together with flushing of suspended fine sediments by ebb-tide currents, such as occurs at intertidal flats in most estuaries (i.e., Green and Coco, 2014). In these sediment-infilled systems, long-term fine sediment accumulation will be limited to more quiescent and typically vegetated fringing coastal wetlands, the upper intertidal flat or exported to similar environments in the main body of the Harbour, or the coast.

Net sediment accumulation rates determined from core geochronology integrate cycles of sediment erosion and deposition over much longer time scales (i.e., 10–1000 yr). Sedimentation in an estuary is also an episodic process, with a large fraction of the catchment sediment load delivered by the high-magnitude-low frequency events (Hicks and Gomez, 2016). Long-term sedimentation records provided by cores are therefore more likely to sample the full range of conditions and events that occur over decadal time scales, than a short-term monitoring programme designed to provide SOE information. Sediment accretion monitoring does, however, have a number of benefits. These include: (1) ability to quantify annual sedimentation trends and the effects of discrete storm events that can link to ecological/ benthic health data for SOE reporting and; (2) evaluation of contemporary sedimentation trends than can span across event, seasonal and annual time scales.
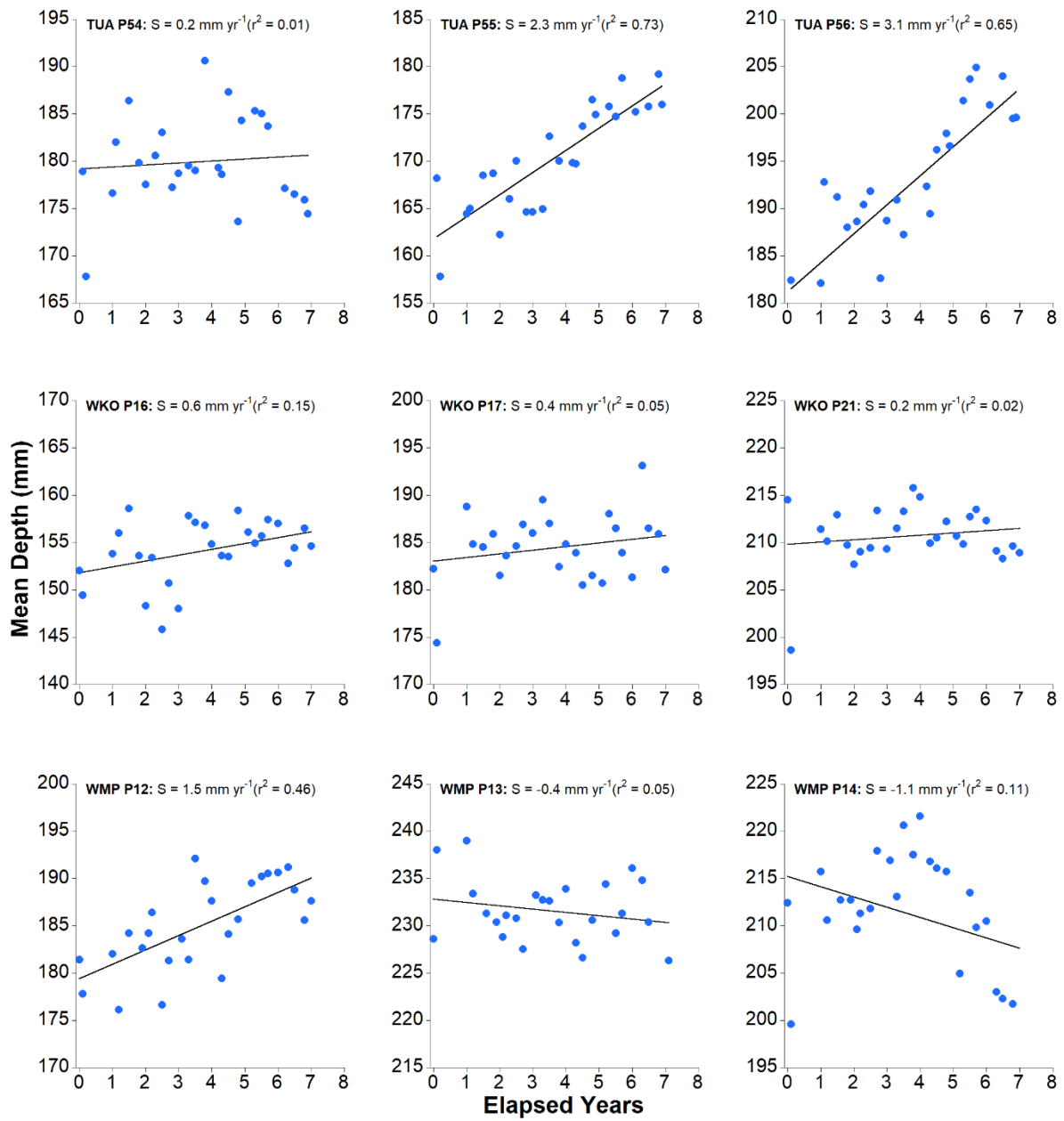
Figure 4-3: **BoPRC estuaries sediment accretion data (December 2013 – November 2020).** Top: Tuapiro Estuary, Middle: Waikareao Estuary, Bottom: Waimapu Estuary. Sediment accretion rates (S, mm yr^{-1}) and linear regression fits shown. Source: Mr Stephen Park (BoPRC Environmental Scientist).

5   Concluding comments

Irrespective of the present-day rate of sediment accumulation, the results of the present study show that these Tauranga Harbour estuaries have been severely impacted by sedimentation. This conclusion is supported by: (1) SAR that are substantially higher (over last ~30–100 yr) than measured in other estuaries for which there is comparable data; and (2) historical SAR that are 50-fold higher than background values, whereas an order of magnitude increase above background SAR is more typical for NZ estuaries.

These estuaries receive substantial quantities of fine suspended sediment from their catchments due to soil erosion: Tuapiro (~3,570 t yr^{-1}), Waikareao (~2,690 t yr^{-1}) and Waimapu (~7,090 t yr^{-1}, Hicks, 2019). A secondary source of fine sediment is that imported from other sub-catchments by tidal currents (Green, 2010). Fine sediment is one of the most damaging diffuse-source contaminants responsible for degrading the ecological health of New Zealand estuaries and coastal marine environments (Thrush et al., 2004, MacDiarmid, 2012). It is likely that a substantial fraction of the catchment fine sediment delivered to these highly infilled estuaries does not accumulate on intertidal flats in the long term due to resuspension and flushing by waves and tidal currents (i.e., Green and Coco, 2014). This reworked fine sediment will eventually accumulate in long term sinks, namely fringing coastal wetlands, or will be exported to the sea. The temporary nature of this deposition does not, however, avoid the chronic adverse effects of reduced water clarity on estuarine productivity, human amenity or cultural values, nor the chronic effects, mortality or loss of biodiversity in benthic ecosystems and kaimoana that is caused by repeating cycles of catchment soil erosion and fine-sediment delivery. Identifying the major sources of eroded soil that supply fine sediment to these study estuaries, can inform the integrated catchment-to-estuary management that will be required to restore freshwater and estuarine receiving environments.

6   Acknowledgements

7   References

Basher, L.R. (2013) Erosion processes and their control in New Zealand. *Ecosystem services in New Zealand–conditions and trends*, 2013: 363-374.

Bay of Plenty Regional Council (2012a) Kopurererua: Sub-catchment Action Plan 2012. https://cdn.boprc.govt.nz/media/424220/kopurereruasubcatchmentactionplan.pdf

Bay of Plenty Regional Council (2012b) Tuapiro: Sub-catchment Action Plan 2012. https://cdn.boprc.govt.nz/media/424226/tuapirosubcatchmentactionplan.pdf

Bay of Plenty Regional Council (2012c) Waimapu: Sub-catchment Action Plan 2012. https://cdn.boprc.govt.nz/media/424229/waimapusubcatchmentactionplan.pdf

Bentley, S.J., Shermet, A., Jaeger, J.M. (2006) Event sedimentation, bioturbation, and preserved sedimentary fabric: Field and model comparisons in three contrasting marine settings. *Continental Shelf Research*, 26: 2108-2124.

Bentley, S.J., Swales, A., Pyenson, B., Dawe, J. (2014) Sedimentation, bioturbation, and sedimentary fabric evolution on a modern mesotidal mudflat: A multi-tracer study of processes, rates, and scales. *Estuarine, Coastal and Shelf Science*, 141: 58-68.

Briggs, R.M., Hall, G.J., Harmsworth, G.R., Hollis, A.G., Houghton, B.F., Hughes, G.R., Morgan, M.D., Whitbread-Edwards, A.R. (1996) *Geology of the Tauranga area*. Hamilton, University of Waikato.

Burggraaf, S., Langdon, A.G., Wilkins, A.L. (1994) Organochlorine contaminants in sediments of the Tauranga Harbour, New Zealand. *New Zealand journal of marine and freshwater research*, 28(3): 291-298.

Cahoon, D.R., Turner, R.E. (1989) Accretion and canal impacts in a rapidly subsiding wetland: II. Feldspar marker horizon technique. *Estuaries,* 12: 260–268.

Callaway, J.C., Cahoon, D.R., Lynch, J.C. (2013) The surface elevation table–marker horizon method for measuring wetland accretion and elevation dynamics. In: DeLaune, R.D., Reddy, K.R., Richardson, C.J., Megonigal, J.P. (Eds.), *Methods in Biogeochemistry of Wetlands*. Book Series 10, Soil Science Society of America, Madison, WI, USA: 901–917, 53711-55801.

Chapman, V.J., Ronaldson, J.W. (1958) The mangrove and saltmarsh flats of the Auckland Isthmus. N. Z. *Department of Scientific and Industrial Research Bullentin,* 125: 79.

Christensen, E.R. (1982) A model of radionuclides in sediments influenced by mixing and compaction. *JGR Oceans,* 87 (C1): 566–57

Chappell, P.R. (2013) The climate and weather of Bay of Plenty. *NIWA Science and Technology Series* 62: 40.

Clark, K., Howarth, J., Litchfield, N., Cochran, U., Turnbull, J., Dowling, L., Howell, A., Berryman, K., Wolfe, F. (2019) Geological evidence for past large earthquakes and tsunamis along the Hikurangi subduction margin, New Zealand. *Marine Geology*, *412*: 139-172.

Conroy, E., Donald, M., Ellis, K. (2019) Tuaranga Moana Iwi Management Plan 2016-2026: A joint environmental plan for Ngāti Ranginui, Ngāi Te Rangi and Ngāti Pūkenga. https://atlas.boprc.govt.nz/api/v1/edms/document/A3249719/content

Crawshaw, J. (2020a) Personal Communication: Historical events that may have impacted sedimentation in Tauranga Harbour.

Crawshaw, J. (2020b). Personal Communication: Impacts of sedimentation on the shelfish beds in Waikareao and Waimapu estuaries.

Ellis, J., Clark, D., Hewitt, J., Taiapa, C., Sinner, J., Patterson, M., Hardy, D., Park, S., Gardner, B., Morrison, A., Culliford, D., Battershill, C., Hancock, N., Hale, L., Asher, R., Gower, F., Brown, E., McCallion, A. (2013) Ecological survey of Tauranga Harbour: Prepared for Manaaki Taha Moana. *Manaaki Taha Moana Research Report,* 13: 56.

French, J.R., Spencer, T. (1993) Dynamics of sedimentation in a tide-dominated backbarrier saltmarsh, Norfolk, UK. *Marine Geology,* 110: 315–33.

Green, M.O. (2010) Tauranga Harbour Sediment Study: Predictions of Harbour Sedimentation under Future Scenarios. *NIWA Client Report* HAM2009-078 for Bay of Plenty Regional Council, 63.

Green, M., Coco, G. (2014) Review of wave-driven sediment resuspension and transport in estuaries. *Reviews of Geophysics*, 52. 10.1002/2013RG000437

Hancock, N., Hume, T.M., Swales, A. (2009) Tauranga harbour sediment study: harbour bed sediments. *NIWA Client Report* HAM2008-123.

Handley, S., Gibbs, M., Swales, A., Olsen, G., Ovenden, R., Bradley, A. (2017) A 1,000 year history of seabed change in Pelorus Sound/Te Hoiere, Marlborough: Prepared for Marlborough District Council, Ministry of Primary Industries and the Marine Farming Association. *NIWA Client Report* 2016119NE. 10.13140/RG.2.2.32135.65443

Hicks, D.M., Hume, T.M. (1997) Determining sand volumes and bathymetric change on an ebb-tidal delta. *Journal of Coastal Research*: 407-416.

Hicks, D.M., Gomez, B. (2016) Sediment Transport. In: Kondolf, G.M., Piegay, H., (Eds). *Tools in Fluvial Geomorphology, Second Edition*. John Wiley and Sons: 324–356.

Hicks, M. (2019) Review and analysis of suspended sediment monitoring in the Tauranga Moana Catchment: Prepared for Bay of Plenty Regional Council. *NIWA Client Report* 2019183CH.

Hogg, A.G., Higham, T.F., Dahm, J. (1998) ^{14}C dating of modern marine and estuarine shellfish. *Radiocarbon*, 40(2): 975-984.

Hughes, A., Hoyle, J. (2014) The importance of bank erosion as a source of suspended sediment within the Kopurererua catchment: Prepared for Bay of Plenty Regional Council. *NIWA Client Report* HAM2014-064.

Hughes, A. (2016) Riparian management and stream bank erosion in New Zealand. *New Zealand Journal of Marine and Freshwater Research,* 50(2): 277–290.

Hume, T., McGlone, M. (1986) Sedimentation patterns and catchment use change recorded in the sediments of a shallow tidal creek, Lucas Creek, Upper Waitemata Harbour, New Zealand. *New Zealand journal of marine and freshwater research*, 20(4): 677-687.

Hume T.M., Hart, D. (2020) Coastal hydrosystem responses to sea level rise. In: Hendtlass, C., Morgan, D. and Neale, D. (eds.). *Coastal Systems and Sea Level Rise: what to Look for in the future*, New Zealand Coastal Society: 45–53, 68. https://www.coastalsociety.org.nz/assets/Publications/Special-Issues/SP4-Low-res-version.pdf

Hunt, S. (2019) *Summary of historic estuarine sedimentation measurements in the Waikato region and formulation of a historic baseline sedimentation rate*. Waikato Regional Council, Hamilton, N.Z. ISSN2230-4363.

Jantschik, R., Nyffeler, F., Donard, O. (1992) Marine particle size measurement with a stream-scanning laser system. *Marine Geology*, 106(3-4): 239-250.

King, D.J., Newnham, R.M., Gehrels, W.R., Clark, K.J. (2021) Late Holocene sea-level changesand vertical land movements in New Zealand. *New Zealand Journal of Geology and Geophysics,* 64(1): 21–36.

Lambeck, K., Rouby, H., Purcell, A., Sun, Y., Sambridge, M. (2014) Sea level and global ice volumes from the Last Glacial Maximum to the Holocene. *Proceedings of the National Academy of Sciences,* 111(43): 15297.

Lawton, R., Conroy, E. (2019) *Tauranga Moana: State of the environment report 2019*. Bay of Plenty Regional Council.

MacDiarmid, A., McKenzie, A., Sturman, J., Beaumont, J., Mikaloff-Fletcher, S., Dunne, J. (2012) Assessment of anthropogenic threats to New Zealand marine habitats. Wellington, New Zealand: Ministry of Agriculture and Forestry.

MacPherson, D., Fox, B.R., de Lange, W.P. (2017) Holocene evolution of the southern Tauranga Harbour. *New Zealand Journal of Geology and Geophysics*, 60(4): 392-409.

Matthews, K.M. (1989) Radioactive fallout in the South Pacific: a history. Part 1: Deposition in New Zealand. *Report* NRL1989/2, National Radiation Laboratory, Christchurch, New Zealand.

Miller, A.J. and Kuehl, S.A. (2010) Shelf sedimentation on a tectonically active margin: a modern sediment budget for Poverty continental shelf, New Zealand. *Marine Geology,* 270(1-4): 175–187.

Neubauer, S.C., Anderson, I.C., Constantine, J.A., Kuehl, S.A. (2002) Sediment deposition and accretion in a mid-Atlantic (USA) tidal freshwater marsh. *Estuarine Coastal and Shelf Science,* 54: 713–727.

Nolte, S., Koppenaal, E.C., Esselink, P., Dijkema, K.S., Schuerch, M., De Groot, A.V., Bakker, J.P., Temmerman, S. (2013) Measuring sedimentation in tidal marshes: a review on methods and their applicability in biogeomorphological studies. *Journal of Coastal Conservation,* 17: 301–325.

Parkinson, R.W., Delaune, R.D., White, J.R. (1994) Holocene sea level rise and the fate of mangrove forests within the wider Caribbean region. *Journal of Coastal Research* 10: 1077–1086.

Pasternack, G.B., Brush, G.S. (1998) Sedimentation cycles in a river-mouth tidal freshwater marsh. *Estuaries,* 21: 407–41

Parliamentary Commissioner for the Environment (2020) Managing our estuaries. https://www.pce.parliament.nz/publications/managing-our-estuaries

Petchey, F., Anderson, A., Zondervan, A., Ulm, S., Hogg, A. (2008) New marine ΔR values for the South Pacific subtropical gyre region. *Radiocarbon*, 50(3): 373-397.

Reed, D.J. (1989) Patterns of sediment deposition in subsiding coastal salt marshes, Terrebonne Bay, Louisiana: the role of winter storms. *Estuaries,* 12: 222–227.

Ritchie, J.C., McHenry, J.R. (1990) Application of radioactive fallout cesium-137 for measuring soil erosion and sediment accumulation rates and patterns: A review. *Journal of environmental quality*, 19(2): 215-233.

Rjikse, W., Guinto, D. (2010) *Soils of the Bay of Plenty volume 1: Western Bay of Plenty*. Bay of Plenty Regional Council, Whakatane.

Robbins, J.A., Edgington, D.N. (1975) Determination of recent sedimentation rates in Lake Michigan using Pb-210 and Cs-137. *Geochimica et Cosmochimica Acta*, 39(3): 285-304.

Sadler, P.M. (1981) Sediment-accumulation rates and the completeness of stratigraphic sections. *Journal of Geology,* 89: 569–58.

Sheffield, A., Healy, T., McGlone, M. (1995) Infilling rates of a steepland catchment estuary, Whangamata, New Zealand. *Journal of Coastal Research*: 1294-1308.

Smith, J.N. (2001). Why should we believe 210Pb geochronologies. *Journal of Environmental Radioactivity,* 55: 121–123.

Sommerfield, C., Nittrouer, C., Alexander, C. (1999) 7Be as a tracer of flood sedimentation on the northern California continental margin. *Continental Shelf Research*, 19(3): 335-361.

Sommerfield, C.K., (2006) On sediment accumulation rates and stratigraphic completeness: Lessons from Holocene ocean margins. *Continental Shelf Research*, 26(17-18): 2225-2240.

Stokes, D. (2010) *The physical and ecological impacts of mangrove expansion and mangrove removal: Tauranga Harbour, New Zealand*. Doctoral thesis, University of Waikato.

Stuiver, M., Polach, H.A. (1977) Discussion: Reporting of C-14 data. *Radiocarbon,* 19(3): 355–363.

Swales, A., Hume, T.M., Oldman, J.W., Green, M.O. (1997) Holocene sedimentation and recent human impacts on infilling in a drowned valley estuary. *Pacific Coasts and Ports' 97: Proceedings of the 13th Australasian Coastal and Ocean Engineering Conference and the 6th Australasian Port and Harbour Conference; Volume 2*.

Swales, A., Williamson, R.B., Van Dam, L.F., Stroud, M.J., McGlone, M.S. (2002a) Reconstruction of urban stormwater contamination of an estuary using catchment history and sediment profile dating. *Estuaries*, 25(1): 43-56.

Swales, A., Hume, T.M., McGlone, M.S., Pilvio, R., Ovenden, R., Zviguina, N., Hatton, S., Nicholls, P., Budd, R., Hewitt, J., Pickmere, S., Costley, K. (2002b) Evidence for the physical effects of catchment sediment runoff preserved in estuarine sediments: Phase II (field study). ARC Technical Publication 221. *NIWA Client Report* HAM2002-067.

Swales, A., MacDonald, I.T., Green, M.O. (2004) Influence of wave and sediment dynamics on cordgrass (Spartina anglica) growth and sediment accumulation on an exposed intertidal flat. *Estuaries*, 27(2): 225-243.

Swales, A., Rickard D., Craggs R.J., Morrison M., Lundquist C.J., Stott R., Fitzgerald J.J., Ahrens M.J., Davies-Colley R.J., Matheson F.E., Bell R.G., Hune A.C., Felsing M., Hewitt J.E., Ovenden R., Crump M.E., Smith M.A. (2011) *Ngā Waihotanga Iho – Estuary Monitoring Toolkit for Iwi. NIWA Information Series* 81. NIWA, Wellington. ISSN 1174-264X (Print), ISSN 2230-5548 (online).

Swales A., Bentley S.J., Lovelock C.E. (2015) Mangrove-forest evolution in a sediment-rich estuarine system: Opportunists or agents of geomorphic change? *Earth Surface Processes and Landforms,* 40: 1672–1687. doi: 10.1002/esp.3759.

Swales, A., Bell, R., Lohrer, D. (2020a) Estuaries and lowland brackish habitats. In: Hendtlass, C., Neale, D. (eds) *Coastal Systems and Sea Level Rise*. New Zealand Coastal Society Special Publication: 55–63.

Swales, A., Lovelock, C.E. (2020b) Comparison of sediment-plate methods to measure accretion rates in an estuarine mangrove forest (New Zealand). *Estuarine, Coastal and Shelf Science,* 236: https://doi.org/10.1016/j.ecss.2020.106642.

Thomas, S., Ridd, P.V. (2004) Review of methods to measure short time scale sediment accumulation. *Marine Geology,* 207: 95–114

Thrush, S., Hewitt, J., Cummings, V., Ellis, J., Hatton, C., Lohrer, A., Norkko, A. (2004) Muddy waters: elevating sediment input to coastal and estuarine habitats. *Frontiers in Ecology and the Environment*, 2(6): 299-306.

Townsend, M., Lohrer, A. (2015) ANZECC guidance for estuary sedimentation. *NIWA Client Report* HAM2015-096 prepared for Ministry for the Environment: 45.

Watson, E.B. (2008) Marsh expansion at Calaveras Point Marsh, south San Francisco bay, California. Estuarine Coastal and Shelf Science 78: 593–602.

Wilmshurst, J.M., Anderson, A.J., Higham, T.F., Worthy, T.H. (2008) Dating the late prehistoric dispersal of Polynesians to New Zealand using the commensal Pacific rat. *Proceedings of the National Academy of Sciences*, 105: 7676-7680.

Wise, S. (1977) The use of radionuclides ^{210}Pb and ^{137}Cs in estimating denudation rates and in soil e/rosion measurement. *Occasional Paper* (7).

Appendix A   Sediment core sites

Core Site	Date	Time	NZTM-East	NZTM-North	Comments
Tuapiro Estuary					
TUA P54	29/9/20	1200	1860287	5846207	Muddy upper layer (300mm) on top of sand. Very easy to penetrate and secure a good quality X-ray slide (2 x 100mm dia. cores collected).
TUA P55	29/9/20	1245	1860456	5846127	Muddiest site in estuary with upper layer (350-400mm) on top of sand. Easy to penetrate and secure a good quality X-ray slide (2 x 100mm dia. cores collected).
TUA P56	16/10/20	1400	1860851	5846587	Hard packed sand with several shell layers. Very difficult to penetrate. Secured a good quality X-ray slide.
Waikareao Estuary					
WKO P16	28/9/20	1140	1878054	5823917	Hard packed sand with a very hard-shell layer at 15-25cm below surface.
WKO P17	16/10/2020	1045	1877855	5823857	Soft mud on hard sand. Water still receding on arrival. Located on edge of mangrove area, frequently disturbed.
WKO P21	16/10/2020	1150	1877920	5824834	Hard packed sand. Soft penetration. Easy site to core.
Waimapu Estuary					
WMP P12	30/9/2021	1220	1878071	5820246	Muddy top layer on hard shell and soft mud beneath. Easy to penetrate and secure good quality X-ray slide (2 x 100mm dia. cores collected).
WMP P13	30/9/2021	1140	1877860	5820741	Small muddy top layer. Located Easy to penetrate and secure a good quality X-ray slide (2 x 100mm dia. cores collected).
WMP P14	30/9/2021	1310	1878338	5821047	Muddy upper layer (50mm) on top of sand up to 300mm deep. After 300mm hit soft mud - secured good quality X-ray slide (2 x 100mm dia. cores collected).

Figure A-1: **Tuapiro Estuary core site TUA P54.** Date of collection: 29 September 2020.

Figure A-2: **Tuapiro Estuary core site TUA P56.** Date of collection: 16 October 2020.

Figure A-3: **Waikareao Estuary core site WKO P16.** Date of collection: 28 September 2020.

Figure A-4: **Waikareao Estuary core site WKO P1.** Date of collection: 16 October 2020.

Figure A-5:   Waikareao Estuary core site WKO P21.   Date of collection: 16 October 2020.

Figure A-6:   Waimapu Estuary core site WMP P12.   Date of collection: 30 September 2020.

Figure A-7: **Waimapu Estuary core site WMP P13.** Date of collection: 30 September 2020.

Figure A-8: **Waimapu Estuary core site WMP P14.** Date of collection: 30 September 2020.

Appendix B   Sediment dating

Radionuclides as geological clocks

Radionuclides are unstable atoms that release excess energy in the form of radiation (i.e., gamma rays, alpha particles) in the process of radioactive decay. The radioactive-decay rate can be considered fixed for each type of radionuclide and it is this property that makes them very useful as geological clocks. The half-life ($t_{1/2}$) of a radionuclide is one measure of the radioactive decay rate and is defined as the period of time taken for the quantity of a substance to reduce by exactly half. Therefore, after two half-lives only 25% of the original quantity remains.

The $t_{1/2}$ value of radionuclides also defines the timescale over which they are useful for dating. For example, ^{210}Pb (naturally occurring radionuclide) has a half-life of 22 years and can be used to date sediments up to seven half-lives old or about 150 years. Dating by ^{210}Pb is based on the rate of decrease in unsupported or <u>excess</u> ^{210}Pb activity with depth in the sediment. Excess ^{210}Pb is produced in the atmosphere and is deposited continuously on the earth's surface, where it falls directly into the sea or on land. Like other radionuclides, ^{210}Pb is strongly attracted to fine sediment particles (e.g., clay and silt), which settle out of the water column and are deposited on the seabed. ^{210}Pb also falls directly on land and is attached to soil particles. When soils are eroded, they may eventually by carried into estuaries and the sea and provide another source of excess ^{210}Pb. As these fine sediments accumulate on the seabed and bury older sediments over time, the excess ^{210}Pb decays at a constant rate (i.e., the half-life). The rate of decline in excess ^{210}Pb activity with depth also depends on the local SAR. Slow declines in ^{210}Pb activity with depth indicate rapid sedimentation whereas rapid declines indicate that sedimentation is occurring more slowly. More details of ^{210}Pb dating are described below.

Although radionuclides can occur naturally, others are manufactured. Caesium-137 ($t_{1/2}$ = 30 yr) is an artificial radionuclide that is produced by the detonation of nuclear weapon or by nuclear reactors. In New Zealand, the fallout of caesium-137 associated with atmospheric nuclear weapons tests was first detected in 1953, with peak deposition occurring during the mid-1960s. Therefore, caesium-137 occurs in sediments deposited since the early 1950s. The feeding and burrowing activities of benthic animals (e.g., worms and shellfish) can complicate matters due to downward mixing of younger sediments into older sediments. Repeated reworking of seabed sediments by waves also mixes younger sediment down into older sediments. X-radiographs and short-lived radionuclides such as ^{7}Be ($t_{1/2}$ = 53 days) can provide information on sediment mixing processes.

^{210}Pb profiling and dating

^{210}Pb ($t_{1/2}$ = 22.3 yr) is a naturally occurring radionuclide that has been widely applied to dating recent sedimentation (last 150 years) in lakes, estuaries and the sea (Figure H-1). ^{210}Pb is an intermediate decay product in the uranium-238 (^{228}U) decay series and has a radioactive decay constant (*k*) of 0.03114 yr^{-1}. The intermediate parent radionuclide radium-226 (^{226}Ra, half-life 1622 years) yields the inert gas radon-222 (^{222}Rn, half-life 3.83 days), which decays through several short-lived radionuclides to produce ^{210}Pb. A proportion of the ^{222}Rn gas formed by ^{226}Ra decay in catchment soils diffuses into the atmosphere where it decays to form ^{210}Pb. This atmospheric ^{210}Pb is deposited at the earth surface by dry deposition or rainfall. The ^{210}Pb in estuarine sediments has two components: supported ^{210}Pb derived from *in situ* ^{222}Rn decay (i.e., within the sediment column) and an unsupported ^{210}Pb component derived from atmospheric fallout. This unsupported ^{210}Pb component of the total ^{210}Pb concentration in excess of the supported ^{210}Pb value is estimated from the ^{226}Ra assay (see below). Some of this atmospheric unsupported ^{210}Pb component is also

incorporated into catchment soils and is subsequently eroded and deposited in estuaries. Both the direct and indirect (i.e., soil inputs) atmospheric ^{210}Pb input to receiving environments, such as estuaries, is termed the unsupported or excess ^{210}Pb.

The activity profile of unsupported ^{210}Pb in sediment is the basis for ^{210}Pb dating. In the absence of atmospheric (unsupported) ^{210}Pb fallout, the ^{226}Ra and ^{210}Pb in estuary sediment would be in radioactive equilibrium, which results from the substantially longer ^{226}Ra half-life. Thus, the ^{210}Pb activity profile would be uniform with depth. However, what is typically observed is a reduction in ^{210}Pb activity with depth in the sediment column. This is due to the addition of unsupported ^{210}Pb directly or indirectly from the atmosphere that is deposited with sediment particles on the bed. This unsupported ^{210}Pb component decays with age (k = 0.03114 yr^{-1}) as it is buried through sedimentation. In the absence of sediment mixing, the unsupported ^{210}Pb activity decays exponentially with depth and time in the sediment column. The validity of ^{210}Pb dating rests on how accurately the ^{210}Pb delivery processes to the estuary are modelled, and in particular the rates of ^{210}Pb and sediment inputs (i.e., constant versus time variable).
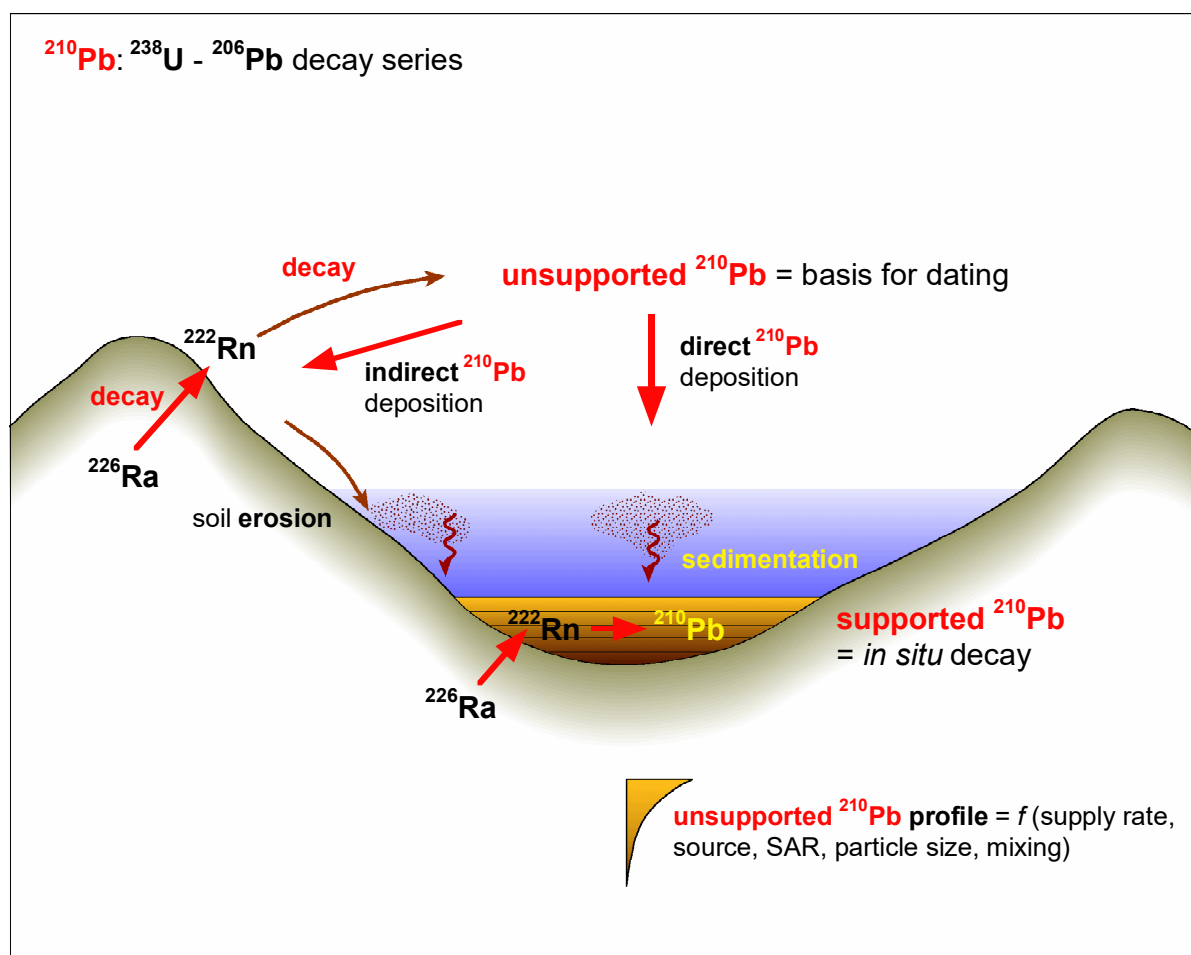

Figure B-1: ^{210}Pb pathways to estuarine sediments.

Sediment accumulation rates

Time-averaged SAR were calculated from the excess lead-210 ($^{210}Pb_{ex}$) activity vertical profiles. This assumes that the $^{210}Pb_{ex}$ profile is primarily a product of radioactive decay and sediment accumulation rate, rather than sediment mixing. The $^{210}Pb_{ex}$ activity at time zero (A_0, Bq kg^{-2}), declines exponentially with age (t):

$$A_t = A_0 e^{-kt} \tag{1}$$

Assuming that within a finite time period, sedimentation (S) is constant then $t = z/S$ can be substituted into Eq. 2 and by re-arrangement:

$$\frac{ln\left[\frac{A}{A_0}\right]}{z} = -k/S \tag{2}$$

Because $^{210}Pb_{ex}$ activity decays exponentially and assuming that sediment age increases with depth, a vertical profile of natural log(A) should yield a straight line of slope $b = -k/S$. Fitting a linear regression model to natural-log transformed $^{210}Pb_{ex}$ activity profile to calculate b. The SAR over the depth of the fitted data is given by:

$$S = -(k)/b \tag{3}$$

An advantage of the ^{210}Pb-dating method is that the SAR is based on the entire $^{210}Pb_{ex}$ profile rather than a single layer, as is the case for ^{137}Cs deposition peak or maximum penetration depth, or ^{14}C dating of a shell layer.

The uncertainty ($U_{2\sigma}$) of the $^{210}Pb_{ex}$ activities was calculated as:

$$U_{2\sigma} = \sqrt{(^{210}Pb_{2\sigma})^2 + (^{226}Ra_{2\sigma})^2} \tag{4}$$

where $^{210}Pb_{2\sigma}$ and $^{226}Ra_{2\sigma}$ are the two standard deviation uncertainties in the total ^{210}Pb and ^{226}Ra concentrations at the 95% confidence level. The main source of uncertainty in the measurement of radionuclide activities relates to the counting statistics (i.e., variability in the rate of radioactive decay). This source of uncertainty is reduced by increasing the sample size and the counting time.

Pre 20th century time-average SAR, over time scales of several hundred years, were estimated from the radiocarbon dates (^{14}C) obtained from pairs of shell samples collected below the maximum depth of excess ^{210}Pb in each core. The time averaged ^{14}C SAR (mm yr^{-1}) was calculated as:

$$S_B = (D_{Pb} - D_C)/T_{Pb210} - T_{C14} \tag{5}$$

Where D_{Pb} and D_C are respectively the depths (mm) below the top of each core of the maximum penetration of the $^{210}Pb_{ex}$ profile and mean AMS ^{14}C age of the dated shell samples. The matching ages of these layers (T_{Pb210}, T_{C14}) are estimates as years A.D., with the AMS 14C age (before present [BP = 1950]), adjusted to the year of core collection (2015). The S_B estimate integrate the effects of land disturbance and soil erosion by Māori and early Europeans over several hundred years as well as background SAR prior to human arrival.

Radiocarbon dating – sample details and results

Table B-1:   Summary of cockle shell samples submitted for radio carbon dating.   The Wk number is the sample identification for the University of Waikato Radiocarbon Dating Laboratory. Whether or not the cockle was preserved in an articulated state is indicated, however, only a single valve was prepared and submitted for analysis.

Core	Depth increment (cm)	Sample type	Articulated	Wk number
TUA P55	63-65 (Sample A)	Cockle shell valve (*Austrovenus stutchburyi*)	No	Wk-52640
TUA P55	63-65 (Sample B)	Cockle shell valve (*Austrovenus stutchburyi*)	No	Wk-52641
TUA P55	63-65 (Sample C)	Cockle shell valve (*Austrovenus stutchburyi*)	No	Wk-52642
WMP P12	59.5-63.5 (Sample A)	Cockle shell valve (*Austrovenus stutchburyi*)	Yes	Wk- 52643
WMP P12	63-64 (Sample B)	Cockle shell valve (*Austrovenus stutchburyi*)	No	Wk- 52644
WMP P12	58.5-61 (Sample C)	Cockle shell valve (*Austrovenus stutchburyi*)	Yes	Wk- 52645

Shell samples were acid-washed in 0.1 N hydrochloric acid, rinsed and dried prior to AMS analysis. The AMS dating results are expressed as calibrated radiocarbon ages in years before present (B.P., 1950 AD, Stuiver and Polach, 1977). Duplicate samples were analysed from the same depth interval in several cores to evaluate the likelihood of shell material being reworked from its original stratigraphic position. The UoW Radiocarbon Dating reports for the cockle shell samples are appended below.

THE UNIVERSITY OF
WAIKATO
Te Whare Wānanga o Waikato

Private Bag 3105
Hamilton,
New Zealand.
Ph +64 7 838 4278
email c14@waikato.ac.nz

Radiocarbon Dating Laboratory

Friday, 21 May 2021

Report on Radiocarbon Age Determination for Wk- 52640

Submitter	M Huirama
Submitter's Code	BOP20207_TUA-P55_63_65_Sample A
Site & Location	Core site TUA-P55, Tuapiro Estuary, Tauranga, New Zealand
Sample Material	Austrovenus stutchburyi
Physical Pretreatment	Surfaces cleaned. Washed in an ultrasonic bath. Tested for recrystallization: aragonite.
Chemical Pretreatment	Sample acid washed using 0.1N HCl, rinsed and dried.

$D^{14}C$	-570.5 ±	1.1 ‰
$F^{14}C\%$	42.9 ±	0.1 %
Result	**6790 ± 21 BP**	

(AMS measurement)

Comments
Please note: The Carbon-13 stable isotope value ($\delta^{13}C$) was measured on prepared graphite using the AMS spectrometer. The radiocarbon date has therefore been corrected for isotopic fractionation. However the AMS-measured $\delta^{13}C$ value can differ from the $\delta^{13}C$ of the original material and it is therefore not shown.

OxCal v4.4.4 Bronk Ramsey (2021) r.5; Marine data from Heaton et al (2020) Delta_R(-154,38)

Wk52640 R_Date(6790,21)
68.3% probability
7330 (68.3%) 7170BP
95.4% probability
7420 (95.4%) 7100BP
Agreement 100.2%

- Explanation of the calibrated Oxcal plots can be found at the Oxford Radiocarbon Accelerator Unit's calibration web pages (http://c14.arch.ox.ac.uk/embed.php?File=explanation.php)
- Result is *Conventional Age or Percent Modern Carbon (pMC)* following Stuiver and Polach, 1977, Radiocarbon 19, 355-363. This is based on the Libby half-life of 5568 yr with correction for isotopic fractionation applied. This age is normally quoted in publications and must include the appropriate error term and Wk number.
- Quoted errors are 1 standard deviation due to counting statistics multiplied by an experimentally determined Laboratory Error Multiplier.
- The isotopic fractionation, $\delta^{13}C$, is expressed as ‰ wrt PDB and is measured on sample CO_2.
- $F^{14}C\%$ is also known as *Percent Modern Carbon (pMC)*.

THE UNIVERSITY OF WAIKATO
Te Whare Wānanga o Waikato

Private Bag 3105
Hamilton,
New Zealand.
Ph +64 7 838 4278
email c14@waikato.ac.nz

Radiocarbon Dating Laboratory

Friday, 21 May 2021

Report on Radiocarbon Age Determination for Wk- 52641

Submitter	M Huirama
Submitter's Code	BOP20207_TUA-P55_63_65_Sample B
Site & Location	Core site TUA-P55, Tuapiro Estuary, Tauranga, New Zealand
Sample Material	Austrovenus stutchburyi
Physical Pretreatment	Surfaces cleaned. Washed in an ultrasonic bath. Tested for recrystallization: aragonite.
Chemical Pretreatment	Sample acid washed using 0.1N HCl, rinsed and dried.

$D^{14}C$	-568.2 ± 1.1 ‰
$F^{14}C\%$	43.2 ± 0.1 %
Result	**6747 ± 21 BP**

(AMS measurement)

Comments
Please note: The Carbon-13 stable isotope value ($\delta^{13}C$) was measured on prepared graphite using the AMS spectrometer. The radiocarbon date has therefore been corrected for isotopic fractionation. However the AMS-measured $\delta^{13}C$ value can differ from the $\delta^{13}C$ of the original material and it is therefore not shown.

OxCal v4.4.4 Bronk Ramsey (2021); r:5; Marine data from Heaton et al (2020) Delta R[-154,38]

Wk52641 R_Date(6747,21)
68.3% probability
7310 (68.3%) 7140BP
95.4% probability
7390 (95.4%) 7040BP
Agreement 100.3%

- Explanation of the calibrated Oxcal plots can be found at the Oxford Radiocarbon Accelerator Unit's calibration web pages (http://c14.arch.ox.ac.uk/embed.php?File=explanation.php)
- Result is *Conventional Age or Percent Modern Carbon (pMC)* following Stuiver and Polach, 1977, Radiocarbon 19, 355-363. This is based on the Libby half-life of 5568 yr with correction for isotopic fractionation applied. This age is normally quoted in publications and must include the appropriate error term and Wk number.
- Quoted errors are 1 standard deviation due to counting statistics multiplied by an experimentally determined Laboratory Error Multiplier.
- The isotopic fractionation, $\delta^{13}C$, is expressed as ‰ wrt PDB and is measured on sample CO_2.
- $F^{14}C\%$ is also known as *Percent Modern Carbon (pMC)*.

THE UNIVERSITY OF
WAIKATO
Te Whare Wānanga o Waikato

Private Bag 3105
Hamilton,
New Zealand.
Ph +64 7 838 4278
email c14@waikato.ac.nz

Radiocarbon Dating Laboratory

Friday, 21 May 2021

Report on Radiocarbon Age Determination for Wk- 52642
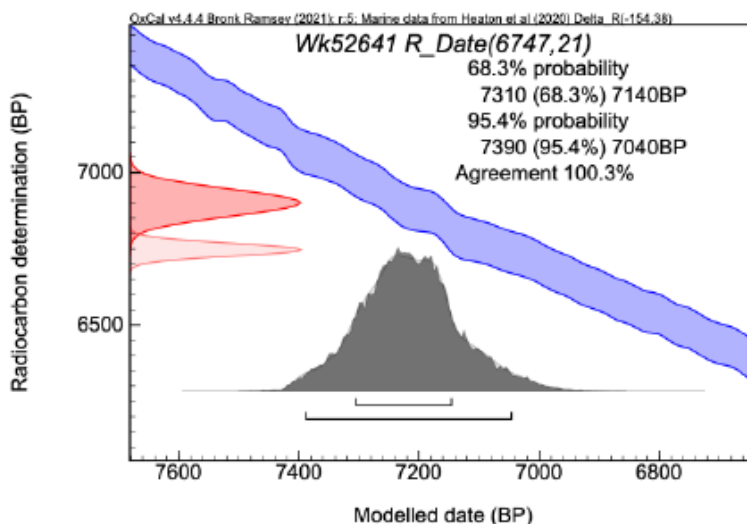
Submitter	M Huirama
Submitter's Code	BOP20207_TUA-P55_63_65_Sample C
Site & Location	Core site TUA-P55, Tuapiro Estuary, Tauranga, New Zealand
Sample Material	Austrovenus stutchburyi
Physical Pretreatment	Surfaces cleaned. Washed in an ultrasonic bath. Tested for recrystallization: aragonite.
Chemical Pretreatment	Sample acid washed using 0.1N HCl, rinsed and dried.

$D^{14}C$	-569.3 ± 1.1 ‰
$F^{14}C\%$	43.1 ± 0.1 %
Result	**6767 ± 21 BP**

(AMS measurement)

Comments
Please note: The Carbon-13 stable isotope value ($\delta^{13}C$) was measured on prepared graphite using the AMS spectrometer. The radiocarbon date has therefore been corrected for isotopic fractionation. However the AMS-measured $\delta^{13}C$ value can differ from the $\delta^{13}C$ of the original material and it is therefore not shown.

OxCal v4.4.4 Bronk Ramsey (2021); r:5; Marine data from Heaton et al (2020) Delta_R(-154,38)

Wk52642 R_Date(6767,21)
68.3% probability
7320 (68.3%) 7150BP
95.4% probability
7410 (95.4%) 7060BP
Agreement 99.9%

- Explanation of the calibrated Oxcal plots can be found at the Oxford Radiocarbon Accelerator Unit's calibration web pages (http://c14.arch.ox.ac.uk/embed.php?File=explanation.php)

- Result is *Conventional Age or Percent Modern Carbon (pMC)* following Stuiver and Polach, 1977, Radiocarbon 19, 355-363. This is based on the Libby half-life of 5568 yr with correction for isotopic fractionation applied. This age is normally quoted in publications and must include the appropriate error term and Wk number.

- Quoted errors are 1 standard deviation due to counting statistics multiplied by an experimentally determined Laboratory Error Multiplier.

- The isotopic fractionation, $\delta^{13}C$, is expressed as ‰ wrt PDB and is measured on sample CO_2.

- $F^{14}C\%$ is also known as *Percent Modern Carbon (pMC)*.

THE UNIVERSITY OF

WAIKATO
Te Whare Wānanga o Waikato

Radiocarbon Dating Laboratory

Friday, 21 May 2021

Report on Radiocarbon Age Determination for Wk- 52643

Submitter	M Huirama
Submitter's Code	BOP20207_WMP-P12_59-5_63-5_Sample A
Site & Location	Core site WMP P12, Waimapu Estuary, Tauranga, New Zealand
Sample Material	Austrovenus stutchburyi
Physical Pretreatment	Surfaces cleaned. Washed in an ultrasonic bath. Tested for recrystallization: aragonite.
Chemical Pretreatment	Sample acid washed using 0.1N HCl, rinsed and dried.

$D^{14}C$ -535.6 ± 1.2 ‰
$F^{14}C\%$ 46.4 ± 0.1 %
Result   **6161 ± 21 BP**

(AMS measurement)

Comments
Please note: The Carbon-13 stable isotope value ($\delta^{13}C$) was measured on prepared graphite using the AMS spectrometer. The radiocarbon date has therefore been corrected for isotopic fractionation. However the AMS-measured $\delta^{13}C$ value can differ from the $\delta^{13}C$ of the original material and it is therefore not shown.

OxCal v4.4.4 Bronk Ramsey (2021); r.5; Marine data from Heaton et al (2020) Delta R(-154,38)

Wk52643 R_Date(6161,21)
68.3% probability
6650 (68.3%) 6470BP
95.4% probability
6740 (95.4%) 6380BP
Agreement 99.9%

- Explanation of the calibrated Oxcal plots can be found at the Oxford Radiocarbon Accelerator Unit's calibration web pages (http://c14.arch.ox.ac.uk/embed.php?File=explanation.php)
- Result is *Conventional Age or Percent Modern Carbon (pMC)* following Stuiver and Polach, 1977, Radiocarbon 19, 355-363. This is based on the Libby half-life of 5568 yr with correction for isotopic fractionation applied. This age is normally quoted in publications and must include the appropriate error term and Wk number.
- Quoted errors are 1 standard deviation due to counting statistics multiplied by an experimentally determined Laboratory Error Multiplier.
- The isotopic fractionation, $\delta^{13}C$, is expressed as ‰ wrt PDB and is measured on sample CO_2.
- $F^{14}C\%$ is also known as *Percent Modern Carbon (pMC)*.

THE UNIVERSITY OF
WAIKATO
Te Whare Wānanga o Waikato

Radiocarbon Dating Laboratory

Report on Radiocarbon Age Determination for Wk- 52644

Submitter	M Huirama
Submitter's Code	BOP20207_WMP-P12_63-64_Sample B
Site & Location	Core site WMP P12, Waimapu Estuary, Tauranga, New Zealand
Sample Material	Austrovenus stutchburyi
Physical Pretreatment	Surfaces cleaned. Washed in an ultrasonic bath. Tested for recrystallization: aragonite.
Chemical Pretreatment	Sample acid washed using 0.1N HCl, rinsed and dried.

$\delta^{13}C$ -0.1 ± 0.3 ‰   (CRDS)
$D^{14}C$ -537.8 ± 1.1 ‰
$F^{14}C\%$ 46.2 ± 0.1 %

Result   **6200 ± 20 BP**

(AMS measurement)

Comments

OxCal v4.4.4 Bronk Ramsey (2021); r:5; Marine data from Heaton et al (2020) Delta_R(-154.38)

Wk52644 R_Date(6200,20)
68.3% probability
6690 (68.3%) 6500BP
95.4% probability
6780 (95.4%) 6420BP
Agreement 100.0%

- Explanation of the calibrated Oxcal plots can be found at the Oxford Radiocarbon Accelerator Unit's calibration web pages (http://c14.arch.ox.ac.uk/embed.php?File=explanation.php)
- Result is *Conventional Age or Percent Modern Carbon (pMC)* following Stuiver and Polach, 1977, Radiocarbon 19, 355-363. This is based on the Libby half-life of 5568 yr with correction for isotopic fractionation applied. This age is normally quoted in publications and must include the appropriate error term and Wk number.
- Quoted errors are 1 standard deviation due to counting statistics multiplied by an experimentally determined Laboratory Error Multiplier.
- The isotopic fractionation, $\delta^{13}C$, is expressed as ‰ wrt PDB and is measured on sample CO_2.
- $F^{14}C\%$ is also known as *Percent Modern Carbon (pMC)*.

THE UNIVERSITY OF WAIKATO
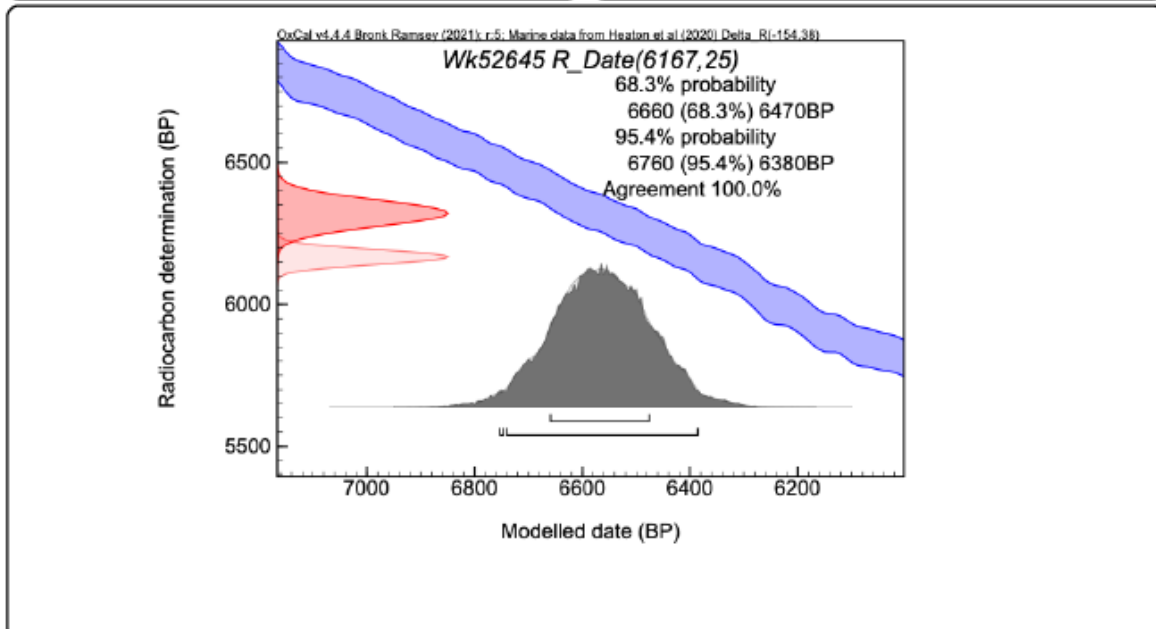## Te Whare Wānanga o Waikato

Radiocarbon Dating Laboratory

Friday, 21 May 2021

Report on Radiocarbon Age Determination for Wk- 52645

Submitter	M Huirama
Submitter's Code	BOP20207_WMP-P12_58-5_61Sample C
Site & Location	Core site WMP P12, Waimapu Estuary, Tauranga, New Zealand
Sample Material	Austrovenus stutchburyi
Physical Pretreatment	Surfaces cleaned. Washed in an ultrasonic bath. Tested for recrystallization: aragonite.
Chemical Pretreatment	Sample acid washed using 0.1N HCl, rinsed and dried.

$D^{14}C$ -535.9 ± 1.4 ‰
$F^{14}C\%$ 46.4 ± 0.1 %
Result   **6167 ± 25 BP**

(AMS measurement)

Comments
Please note: The Carbon-13 stable isotope value ($\delta^{13}C$) was measured on prepared graphite using the AMS spectrometer. The radiocarbon date has therefore been corrected for isotopic fractionation. However the AMS-measured $\delta^{13}C$ value can differ from the $\delta^{13}C$ of the original material and it is therefore not shown.

OxCal v4.4.4 Bronk Ramsey (2021); r:5; Marine data from Heaton et al (2020) Delta_R(-154,38)

Wk52645 R_Date(6167,25)
68.3% probability
6660 (68.3%) 6470BP
95.4% probability
6760 (95.4%) 6380BP
Agreement 100.0%

- Explanation of the calibrated Oxcal plots can be found at the Oxford Radiocarbon Accelerator Unit's calibration web pages (http://c14.arch.ox.ac.uk/embed.php?File=explanation.php)
- Result is *Conventional Age or Percent Modern Carbon (pMC)* following Stuiver and Polach, 1977, Radiocarbon 19, 355-363. This is based on the Libby half-life of 5568 yr with correction for isotopic fractionation applied. This age is normally quoted in publications and must include the appropriate error term and Wk number.
- Quoted errors are 1 standard deviation due to counting statistics multiplied by an experimentally determined Laboratory Error Multiplier.
- The isotopic fractionation, $\delta^{13}C$, is expressed as ‰ wrt PDB and is measured on sample CO_2.
- $F^{14}C\%$ is also known as *Percent Modern Carbon (pMC)*.